Environmental and Convective Influences on Tropical Cyclone Development vs. Non-development

by
Patrick A. Lunney

William M. Gray, P.I.

Department of Atmospheric Science
Colorado State University
Fort Collins, Colorado

NSF-ATM-8419116
AF-N00014-87-K-0203

Colorado State University

Department of Atmospheric Science

Paper No. 436

ENVIRONMENTAL AND CONVECTIVE INFLUENCES ON TROPICAL CYCLONE DEVELOPMENT VS. NON-DEVELOPMENT

By
Patrick A. Lunney

Department of Atmospheric Science
Colorado State University
Fort Collins, CO 80523

December, 1988

Atmospheric Science Paper No. 436

ABSTRACT

To study the physical processes associated with early-stage tropical cyclone development vs. non-development, composite and individual case analyses were made of US Air Force northwestern Pacific 950 mb (~1500 feet) aircraft "investigative" reconnaissance flights into tropical disturbances. Analysis of a 7-year period provided about 100 cases of development vs. 100 cases of non-development. Significantly higher radial inflow was observed in the inner-core of developing cases as compared to non-developing cases. Only minimal tangential winds and sea-level pressure differences were observed between developing and non-developing cases. Many formation cases had strong "packets" of radial momentum surges to inner-core radii at selective azimuthal locations. These wind surges were related to satellite-observed concentrations of deep convection near the inner-core of the developing disturbances and appeared to be environmentally induced.

Another factor influencing tropical cyclone genesis was the strength of a disturbance's upper-tropospheric (250 mb) relative wind "blowthrough" or ventilation. The direction of the 250 mb relative wind to the tropical disturbance's moving center was found to have a major influence on the location of the disturbance's meso-scale vortex (1-2° in diameter) or Low-Level Circulation Center (LLCC) in relation to the center of the parent cloud cluster convection. A fundamental characteristic of developing disturbances was their ability to generate more LLCCs than non-developing disturbances. Thus, an analysis of both wind "blowthrough" and low-level (~ 950 mb or 1500 feet) surge events in individual cases gives much assistance in distinguishing those systems which develop into named tropical cyclones from those which do not. Probability of formation is much higher for those disturbances with high wind surge and low upper-tropospheric "blowthrough" in comparison with those cases of low wind surge and high upper-level "blowthrough".

TABLE OF CONTENTS

LIST OF SYMBOLS AND ACRONYMS

LIST OF ACRONYMS

AFGWC = Air Force Global Weather Central, Offutt AFB, NE

ARWO = Aerial Reconnaissance Weather Officer

ATCR = Annual Tropical Cyclone Report (after 1979)

ATR = Annual Typhoon Report

BCE = Basic Convective Element

BMRC = Bureau of Meteorology Research Center

BT = blowthrough

CDO = Central Defense Overcast

CSU = Colorado State University

DMSP = Defense Meteorological Satellite Program

D1 = Early-stage Developing disturbances (MSLP $\geq$ 1003 mb)

ECMWF = European Centre for Medium Range Weather Forecasts

GMS = Geostationary Meteorological Satellite

GMT = Greenwich Mean Time

GOES = Geostationary Operational Environmental Satellite

Invest = Investigative reconnaissance flight

JTWC = Joint Typhoon Warning Center

LLCC = Low-Level Circulation Center

LT = Local Time

MOT = Motion, or storm-relative coordinate system

MSLP = Minimum Sea Level Pressure

NAT = Natural coordinate system, measured winds used without regard to cyclone motion.

NON-DEV = NON-DEVELOPING disturbances with no closed circulation or maximum surface winds never exceeded 25 knots.

NSIDC = National Snow and Ice Data Center

SST = Sea Surface Temperature

USAF = United States Air Force

54th WRS = 54th Weather Reconnaissance Squadron

LIST OF SYMBOLS

kt = knots

mb = millibar

ms^{-1} = meters per second

r = radius

V_R = radial wind

$V_R \, x \, V_T$ = relative angular momentum (or momentum surge)

V_T = tangential wind

Chapter 1

INTRODUCTION

Our understanding and forecasting of early-stage tropical cyclone development is inadequate. It has been difficult to document with observations how the early-stage tropical cyclone evolves. Particularly difficult to document are the processes occurring in the vicinity of the much smaller scale (1-2° latitude diameter) wind vortices which form within or on the side of the larger scale (3-6° latitude diameter) cyclonic circulation. Individual case and composite rawinsonde analyses are inadequate on this smaller space and time scale.

No other country but the United States has conducted tropical cyclone reconnaissance. Reconnaissance flights are rarely flown on early-stage Atlantic tropical cyclones due to their usual locations far out to sea. By contrast, early-stage reconnaissance data have been available for many years in the northwest Pacific from investigative or "invest" flights by Guam-based Air Force reconnaissance aircraft. Up until August 1987 the 54th Weather Reconnaissance Squadron (54th WRS) has routinely flown into tropical disturbances which appeared to show a potential for named-storm development. Approximately half (about 25 per year) of these invest flights are made into disturbances which later develop into named storms. Great amounts of money have been expended on taking these measurements. Little or no research has so far been conducted with this "invest" flight data. As Gray notes (in the foreword to the CSU report by Weatherford, 1985):

> "So far this flight information has been used almost exclusively in an operational sense to track the centers of these disturbances and storms and to measure how intense they are. Almost no research has been accomplished on this most extensive, unique, and valuable flight information."

This investigative (or "invest") flight data offer a unique opportunity to better document the characteristics of the early-stage developing tropical disturbances and compare these characteristics with those of the non-developing disturbances.

1.1 Characteristics of Flight Missions

The length of the average "invest" flight is about ten hours (four to five hours of the mission involve taking observations, the rest of the time is enroute travel). Typical missions cover about 2500-3000 nautical miles (4000-4800 km). Most flights are made at an absolute altitude of 1500 feet ($\sim$ 450 m) where, in addition to Doppler wind measurements, surface wind speed and direction can be estimated from sea state. The purpose of these flights is to determine if weak tropical systems have developed a small closed vortex circulation and if so, record the location and intensity of this closed circulation and its associated maximum wind and central pressure. About half of these early-stage invest flights find a well established Low-Level Circulation Center (LLCC) of 1-2° diameter. The majority of those systems displaying a LLCC go on to become named storms. Having a LLCC does not guarantee named-storm development however. About 20 percent of non-developing disturbances also displayed prominent low-level circulation centers. A major finding of this research is the documentation of such small, low-level circulation centers and the specification of their typical size and strength.

Another goal of this research is directed towards determining how the low-level wind and pressure fields of the disturbances which develop into named storms are different from disturbances that do not.

All of the observations used in this study are from northwest Pacific reconnaissance missions during the years 1977-1984. Henderson (1978) described the characteristics of the WC-130 aircraft and instrumentation used on these missions.

These invest flights differ from the "fix" flights in the NW Pacific in that fix missions are flown to pinpoint the already known location of an existing storm center. Weatherford (1985) describes the standard flight pattern flown on fix mission flights which usually are at 700 mb.

The flight missions in this study were almost exclusively flown at 1500 feet ($\sim$ 450 m altitude) and were made at the direction of Joint Typhoon Warning Center (JTWC). Figure 1.1 depicts an actual flight track flown into a cloud cluster that JTWC believed might develop into a named cyclone. JTWC provides an estimated center position and the Aerial Reconnaissance Weather Officer (ARWO) must use the winds he observes along the route, along with the estimated circulation location, to guide him to the actual circulation center if one exists. If this can be done, the system is closed off and its location and intensity noted.

Enough observations are taken to either locate the LLCC or to satisfy the ARWO and JTWC that no closed circulation exists. The aircraft will then return to base. If the circulation center has been located, then technically all flights thereafter are considered "fix" missions. The data set of this study includes both invest and fix missions at low levels ($\sim$ 950 mb) into systems which are in their early stage of development or do not develop at all.

There is no standard flight pattern and the number of observations needed to fix a low-level center can vary, as illustrated in Fig. 1.2 and Fig. 1.3.

1.2 Other Data Sources

This study was designed to complement the work of Lee (1986), Middlebrooke and Gray (1987) and Middlebrooke (1988). Along with extensive use of the low-level invest flight data, a number of other data sources were used to help in the task of distinguishing a tropical disturbance that will develop into a named storm from a disturbance that will not.

Other data sources used to augment invest mission information were:

1. Darwin 850 mb and 250 mb hand-analyzed maps of the Australia Bureau of Meteorology,

2. European Centre for Medium-Range Weather Forecasts (ECMWF) 850 mb and 200 mb objective tropical belt analyses,

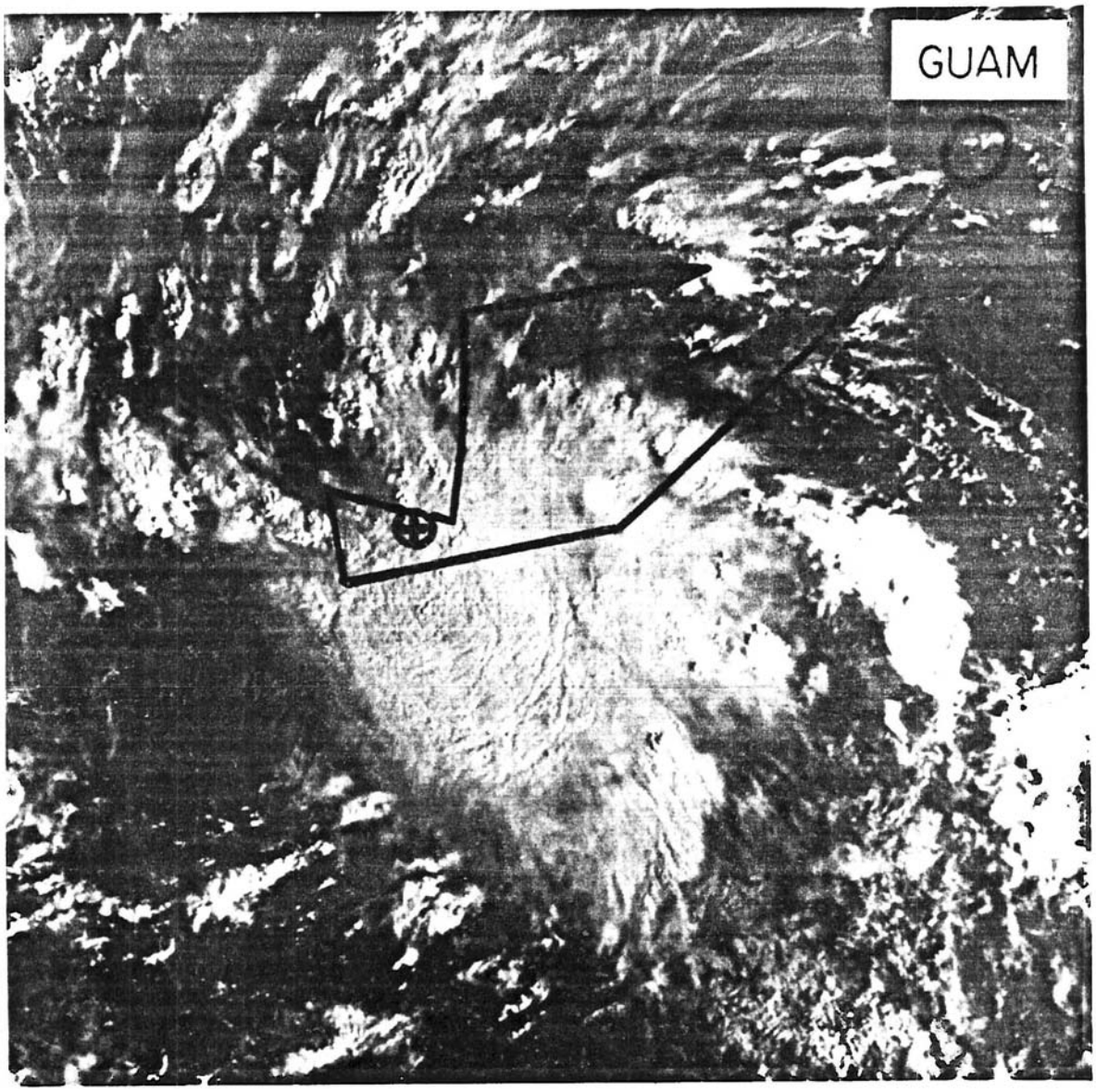

Figure 1.1: Sample of a DMSP visible image of the early developing stage of tropical cyclone Orchid, 16-17 Nov 1983. The flight track on the image is the actual path followed by the aircraft during the 4.5 hour mission. The ⊗ marks the low-level center as determined by the ARWO. ($V_{max} \sim 12\ ms^{-1}$).

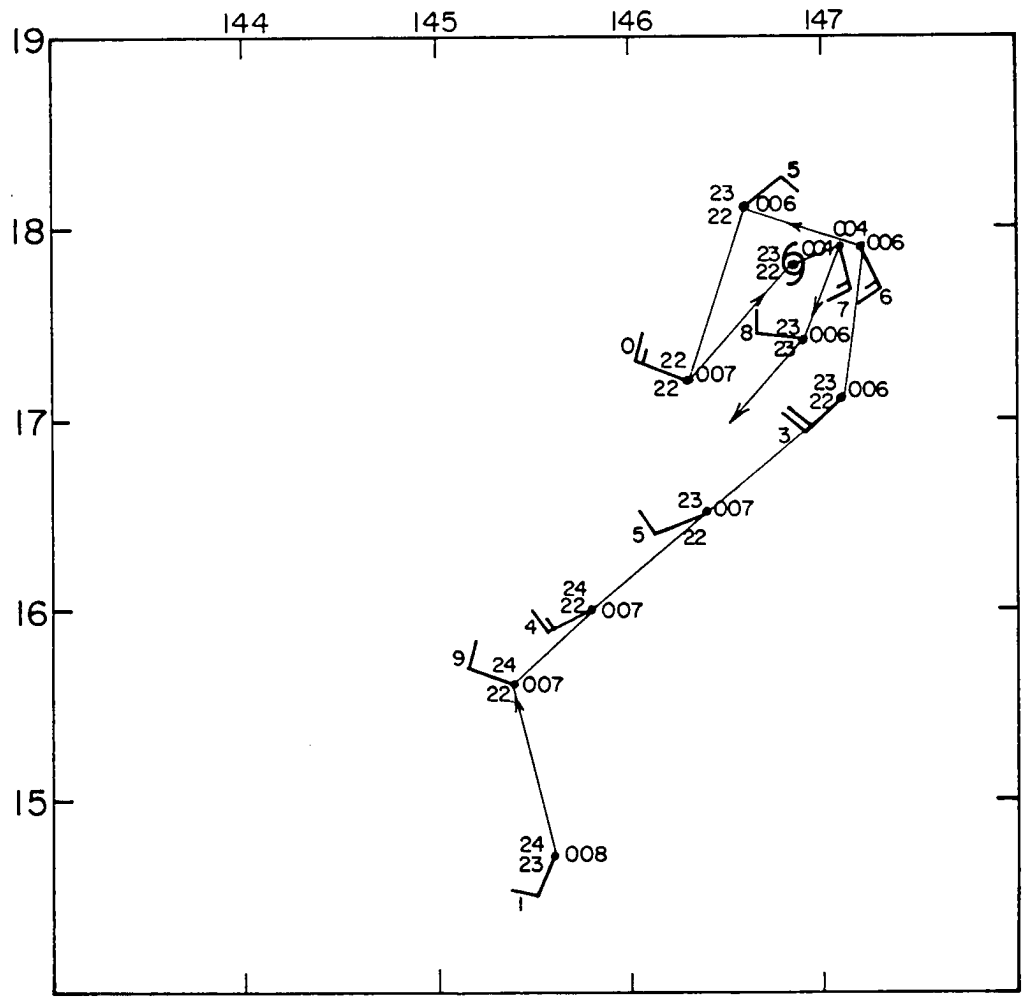

Figure 1.2: Depiction of an invest flight (450 m altitude $\sim$ 950 mb) that required 10 observations to "close-off" a Low-Level Circulation Center (LLCC). Data of future named storm Cary 6 July 1984 is shown. Minimum Sea Level Pressure (MSLP) 1004 mb. Each observation shows pressure (to nearest mb), temperature, dewpoint, and wind at flight level.

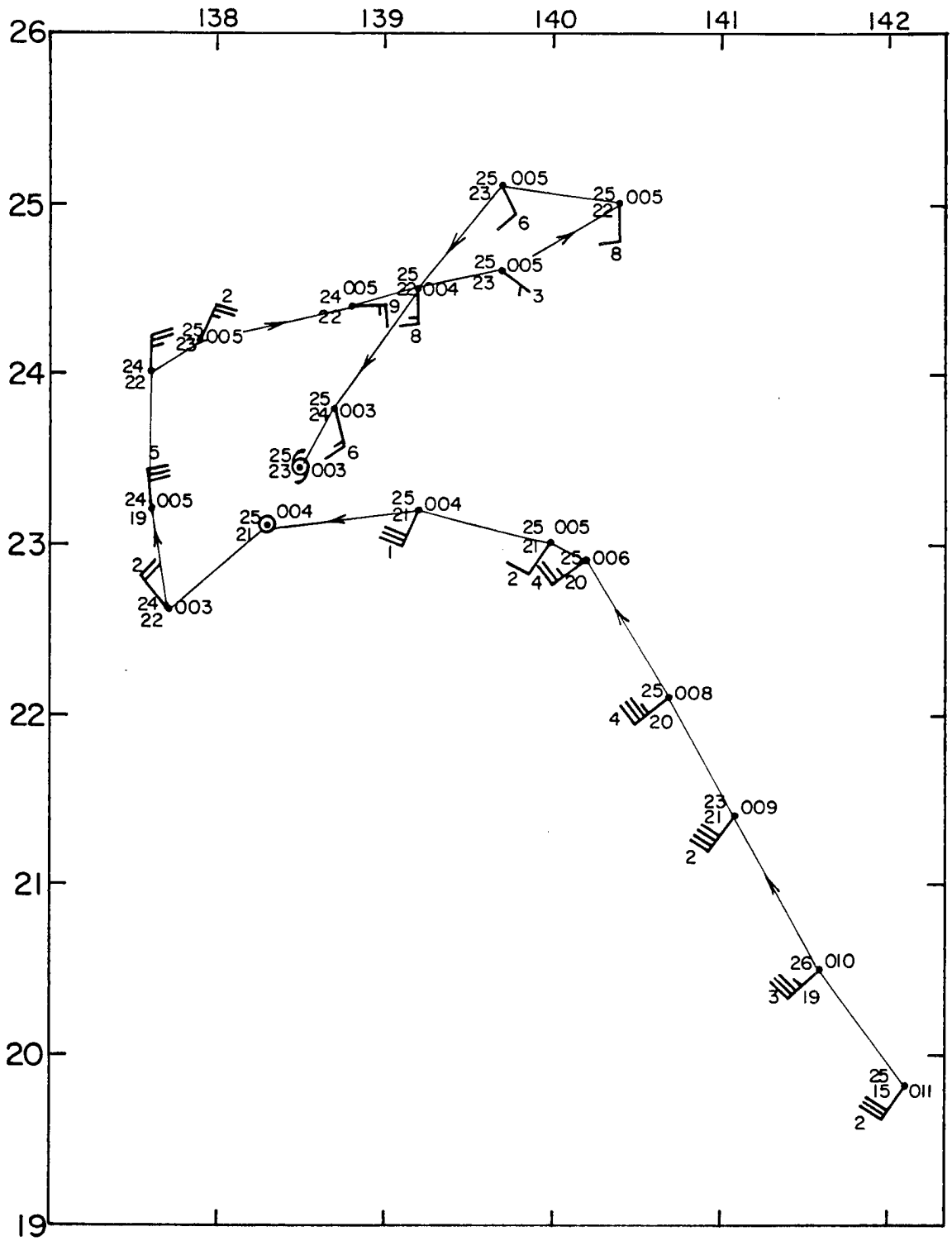

Figure 1.3: Depiction of an invest flight that required 20 observations to "close-off" a circulation center at low levels. Future named storm Dom 22 August 1983. MSLP 1003 mb.

3. High resolution polar-orbiting US Defense Meteorological Satellite Program (DMSP) satellite imagery, and

4. Japanese Geostationary Meteorological Satellite (GMS) imagery.

One hundred and thirty-four time periods of the 250 mb/200 mb analyses and Japanese GMS images for developing systems were compared to the same data for 148 prominent non-developing systems.

A portion of this study involved a determination of the effect of upper-tropospheric ventilation or "blowthrough" on disturbance development as previously discussed by (Gray, 1968, 1975), Lopez (1968), Zehr (1976), and others. Upper-tropospheric wind "blowthrough" can act to inhibit the maintenance of the cyclone's deep tropospheric structure. This acts to reduce the higher upper-level temperature anomaly and thus the cyclonic pressure and wind field. Upper-level wind "blowthrough" or ventilation prevents the accumulation of a deep layer of cyclonic momentum and concomitant warm air needed for deep tropical cyclone vortex establishment and maintenance. Synoptic wind fields were thus analyzed to detect any systematic differences in upper-level wind "blowthrough" or ventilation between developing and non-developing disturbances.

Arnold (1977) and others have pointed out that a higher concentration of deep convection near a disturbance center is favorable for its development. Accurate early-stage low-level center information provided by these invest flights also allows for better documentation of the relationship of the low-level circulation center to the cloud cluster's overall deep convection. It will be shown that this relationship is influenced by a combination of the disturbance's prevailing upper tropospheric wind patterns and the location and intensity of low-level wind surges.

Middlebrooke and Gray (op.cit.) and Middlebrooke (1988) have recently presented the only other invest flight information on the differences and similarities of NW Pacific developing and non-developing disturbances. The only significant difference they found between these two classes of systems was the greater 0-1.5° radius inflow at 1500 feet (see Fig. 1.4) in the developing as compared with the non-developing cases. This observation

was a major factor in focusing this research on further analysis of the early-stage disturbance's inner-core convection patterns. This involves an investigation of how the low-level wind inflow into the disturbance cases brings about such inner-core deep convection differences. These inflow patterns often manifest themselves through specially-induced outer radius, environmentally-induced surge actions.

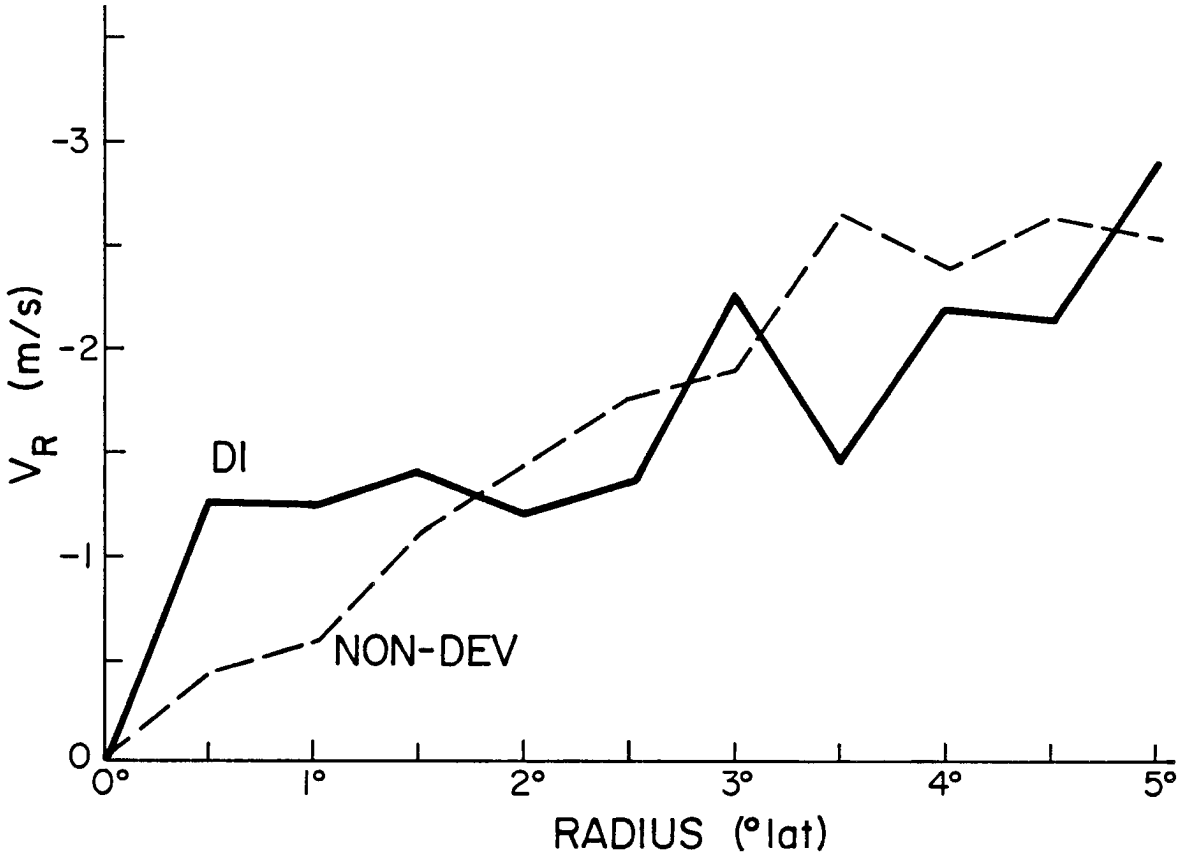

Figure 1.4: Comparison of the outward distribution of radial wind relative to the moving center (MOT system, ms^{-1}) at 1500 feet altitude ($\sim$ 450 m) for early-stage developing (D1) and non-developing systems. Negative values denote inflow. From Middlebrooke and Gray, 1987.

This research is directed towards producing a better understanding of those multiple conditions which combine to distinguish a tropical cloud cluster that will develop into a tropical storm from one that will not.

Chapter 2

CHARACTERISTICS OF INVEST FLIGHTS AND DATA REDUCTION PROCEDURES

Figure 2.1 indicates how concentrated the low-level invest observations are to the tropical disturbance centers. Never before has such an extensive data set been compiled on the inner radii of tropical disturbances of the weak early-stage developing disturbance and of other very prominent disturbances which are very close to developing but do not. These invest data provide valuable supplementary information beyond that available from rawinsonde composite analysis (Zehr, 1976; Erickson, 1977; McBride, 1979; Gray, 1981; Lee, 1986) of early-stage developing and non-developing disturbances. Rawinsonde data are scarce within 1-2° of disturbances.

2.1 The Invest Flight Data Set

M. Middlebrooke (1988) and Middlebrooke and Gray (1987) processed all available (1977-1984) low-level (< 1500 feet absolute altitude) invest flight missions into northwest Pacific tropical disturbances(Middlebrooke and Gray, 1987). Data were obtained from the National Climatic Center in Asheville, NC. It is this data set of which the author makes maximum use.

The instrumentally-sensed meteorological parameters on the invest flights included flight-level measures of:

1. wind direction and speed - from Doppler measurements. (This is often augmented by readings of the sea state). Invest flights are made primarily during daylight hours,

2. D-value - which is extrapolated to the surface to give sea-level pressure information,

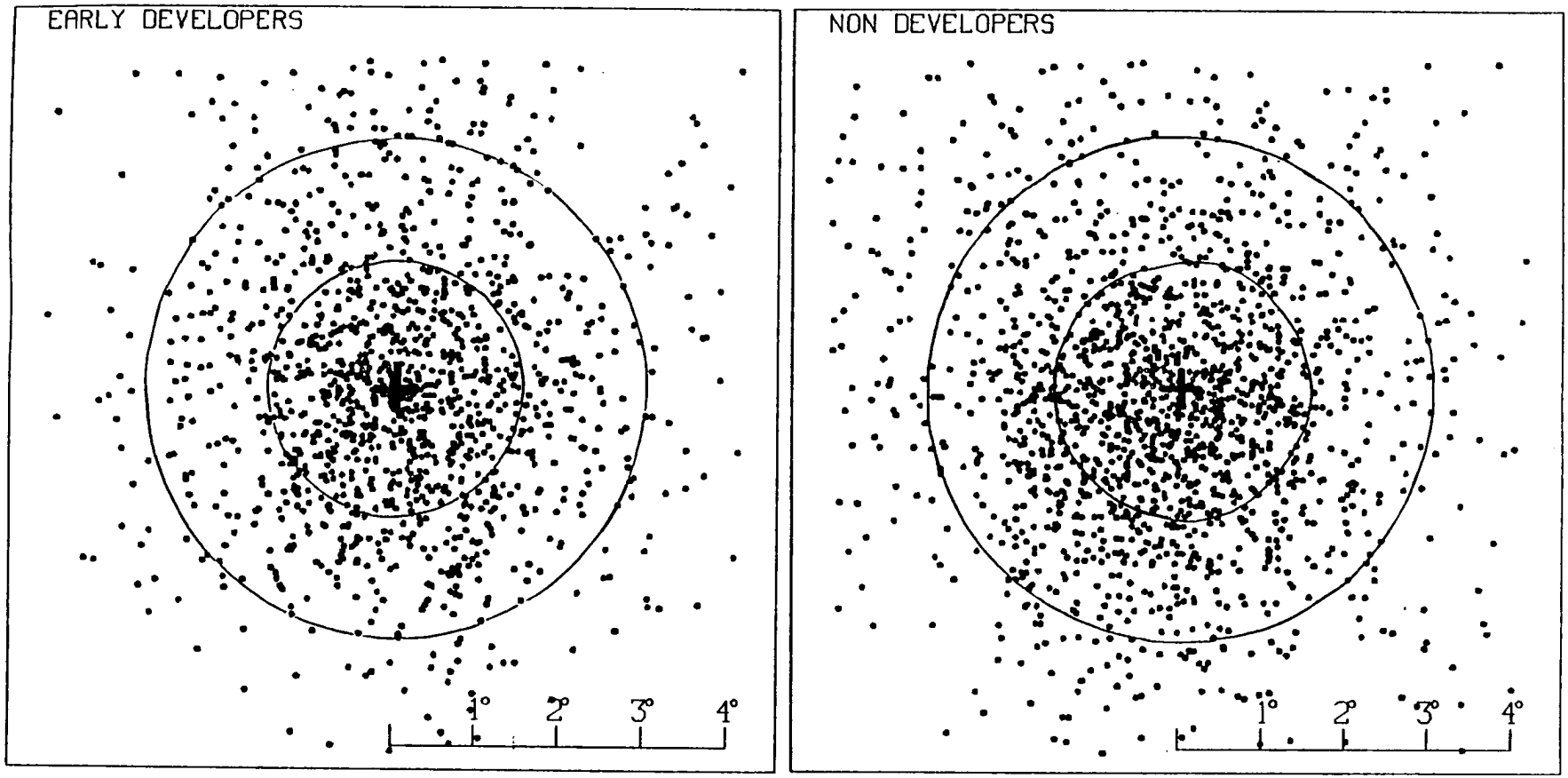

Figure 2.1: Representation of the location of individual invest flight observations for early-stage developers (D1) and non-developers (NON-DEV) for the years 1977-1984. Observation totals are 1409 for D1 class, 1342 for NON-DEV class. Circles at 1.5° and 3° latitude radius.

3. temperature,

4. dew point, and

5. SST measured from onboard radiometer.

Measurements are taken approximately every 15 minutes of flight time. The parameters of most interest for this study are wind direction (to the nearest ten degrees azimuth), wind speed (to the nearest knot), and surface pressure (mb). The position of each observation is reported to the nearest one-tenth of a degree of latitude and longitude. All surface pressure data are diurnally corrected. Observation time is to the nearest minute.

In order to determine the composite position of each observation in a mission, it is necessary to know where the center of the system is at any given time during the mission. If the mission contains a clearly defined center fix, center location is obviously an easy task. Otherwise, a center position has to be derived for the mission. To do this, several supplementary information sources were used. In many cases, even though a circulation center fix was not made, the observed winds gave a strong indication of where the center should be. This was enough to locate the center. In other cases where observations could not readily locate a center, or where the center was outside the area where observations were taken, centers were estimated using JTWC Best Tracks which are published yearly in their Annual Tropical Cyclone Report. After a cyclone has completed its life cycle, JTWC determines 6-hourly positions for the cyclone's surface center for its entire lifetime. These Best Track positions are derived from all sources of data which include an analysis of reconnaissance information, positions measured by satellite, land-based radar fixes, and synoptic surface observations. Indicated at each 00Z ($\sim$ 10 LT), 06Z ($\sim$ 16 LT), 12Z ($\sim$ 22 LT), or 18Z ($\sim$04 LT) position time on the Best Track are the storm's maximum sustained surface winds and the speed at which the center was moving. While these Best Tracks do not always correspond exactly with aircraft center fixes, they are still very useful for locating centers and determining the direction and speed of the centers. This Best Track information has been used extensively in other CSU project tropical cyclone genesis research, for instance, Lee (1986).

If a JTWC Best Track was not available, which was the case for most non-developing disturbances, the invest flight information in combination with the tropical surface analysis charts from both the National Weather Service and the forecast office at Darwin, Australia, and satellite information were used to specify a best possible center position. In many cases, the streamline analysis clearly indicated a position center, at least on a synoptic scale. If no cyclone was analyzed on the chart, surface observations in the region, in combination with the aircraft observations and satellite information, were often sufficient to confidently locate a center position.

It should be emphasized here that no center location was accepted unless it agreed closely with the aircraft data. If, after consulting all available sources, a reasonable center-position could not be specified that would be compatible with the aircraft data, the mission was rejected for compositing purposes. Thus, by using aircraft data, JTWC Best Tracks, and tropical surface charts, centers suitable for compositing were derived for all the invest missions which are to be studied. While many of these derived centers probably do represent actual closed circulations, there is no doubt that many cases occurred in which a complete closed circulation did not exist. In these cases, the derived center is better described as the center of action about which the observed winds appear to be organized or are organizing. Figure 2.2 shows a typical invest mission in which the circulation center had to be derived. In this case it is not clear that a closed circulation exists. The circled + indicates the derived center. The working assumption was that even in cases where a tightly-closed circulation may not have existed, the derived center is still suitable for individual case and composite analysis.

The centers determined by the above procedures were used not only to locate the observations with respect to the center, but also to define the movement of the system during the time period covered by each invest mission. Enough center positions and times were derived for each system so that its movement was well approximated during the time of each mission by moving the system at constant velocity between each pair of center positions. Thus, the position of the center was calculated for the time of any observation by

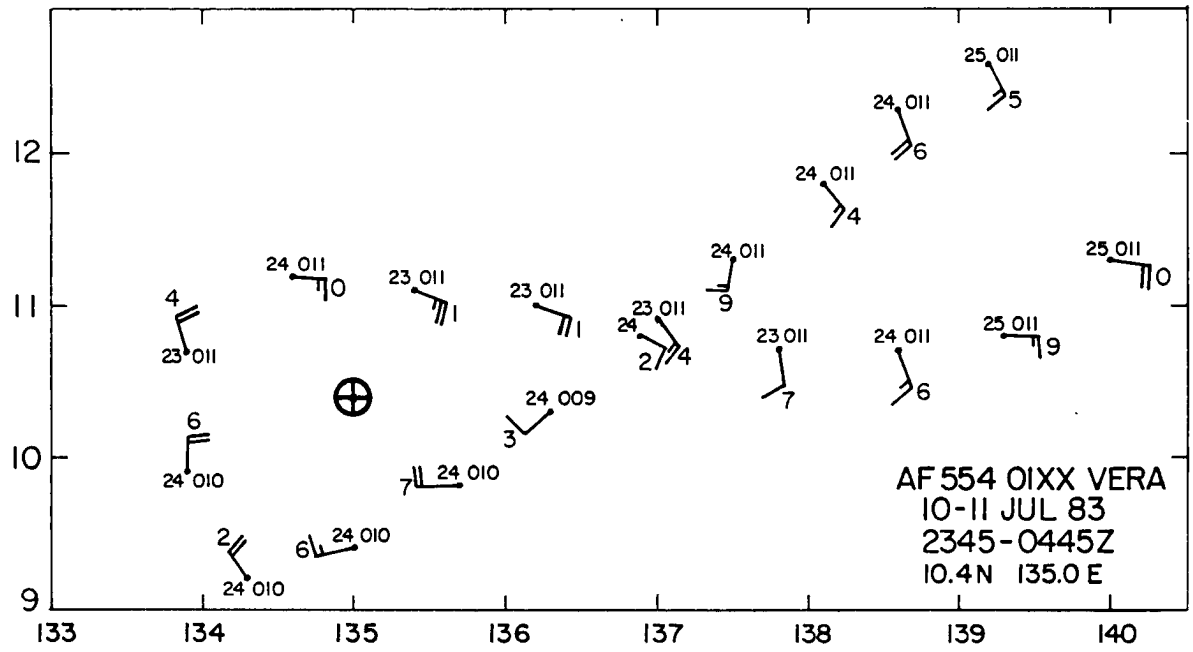

Figure 2.2: Sample invest flight in which a low-level circulation center could not be precisely located. Instead, the derived center was determined through use of synoptic analyses, satellite and aircraft data. The derived center is marked with a circled plus.

linearly interpolating between the center positions before and after the observation time. The center's velocity was easily found by simply dividing the distance vector between the two positions by the elapsed time. Once the disturbance's data were checked for accuracy and consistency, all the observations were entered into computer files for later analysis. Data were reduced so that each invest observation included:

DISTURBANCE NAME

MISSION NUMBER (for that disturbance)

STORM NUMBER (for that year)

YEAR, MONTH, DAY

TIME (GMT)

LATITUDE OF CENTER (accurate to 0.1°)

LONGITUDE OF CENTER (accurate to 0.1°)

PRESSURE (nearest mb - diurnally corrected)

TEMPERATURE (nearest °C)

DEWPOINT (nearest °C)

WIND DIRECTION (nearest 10 °)

WIND VELOCITY (nearest knot)

DISTANCE FROM CENTER

BEARING FROM CENTER (nearest °)

STORM SPEED OF MOVEMENT (nearest 0.1 ms^{-1})

STORM DIRECTION OF MOVEMENT (nearest °)

2.2 Stratifying the Invest Flight Data

After the laborious data reduction and preparation involved with processing the flight data, stratification of the data was made into two classes: Early-stage developing and non-developing cases. Middlebrooke's paper (1988) contains other stratifications. The stratifications selected for this analysis are comprised of the following two classes of developing and non-developing systems (from Middlebrooke and Gray, 1987):

Early-stage Developers (D1). All missions in this stratification were flown on systems with diurnally corrected Minimum Sea Level Pressure (MSLP) equal to or greater than 1003 mb. The system may or may not have had a closed circulation. Most of the missions in the D1 file were flown within 24 hours of the time the disturbance acquired a closed circulation. Maximum winds were usually 25 kts (12 ms^{-1}) or less.

NON-DEV. Renamed from Middlebrooke's Non-GEN designation. All missions flown on systems that either never developed a closed circulation, or if they did the maximum surface wind never exceeded 25 kts (or 12 ms^{-1}).

As shown in Table 2.1, these two classes of systems are approximately equal in intensity (from Middlebrooke and Gray, 1987).

Table 2.1: Various characteristics of the early-stage developing and non-developing classes for 1977-1984.

	Ave. Lat.	Ave. Long.	Number of Obs.	Number of Flt. Missions	Speed of Movement	Ave. MSLP (mb)	Ave. Max. Wind ms^{-1}
D1	12N	141E	1409	100	10.6	$\sim$ 1005	12-15
NON-DEV	14N	141E	1342	111	8.7	$\sim$ 1003	10-12

Information from individual cases is described in Chapters 3 through 6. The years of 1980-1984 were primarily used because of the simultaneous availability of GMS imagery and Darwin maps from 1980-1984.

2.3 Open vs. Closed Circulation Centers

Although there were centers specified for all D1 and NON-DEV systems, it is important to denote the percentage of actual tightly closed low-level circulation centers (or LLCCs) which were located by the ARWO during the invest mission in comparison with the missions when LLCCs were not found and centers had to be derived as open centers.

Table 2.2 summarizes the number of closed vs. open flight missions on D1 and NON-DEV disturbances. Note the large number of closed centers in the developing class as evident from the nearly 3 to 1 ratio in closed centers in the D1/NON-DEV comparison. The number of closed Low-Level Circulations Centers (or LLCC) in developers compared to non-developers indicates that the existence of small-scale vortices may be important in initiating the development processes.

2.4 Compositing the Invest Flight Data

Determination of the relative location of each observation to the actual or derived disturbance center was done through use of a compositing grid similar to that used by Lee (1986). The grid (see Fig. 2.3) for the invest data, however, is divided in 11 belts, each belt being only 30 n mi wide. Azimuthally the grid is divided into octants with the center of octant 1 pointing north. Winds are ignored in the 0.25° radius center circle but

pressures are averaged in the center ring and assigned to the center point. The center points of the remaining belts are at radii of 0.5°, 1.0°, 1.5°, etc. out to 5° radius for belt 11. All box centers are then in the middle of each octant and 0.5° (56 km or 30 n mi) radius separates each radial belt.

Each invest mission was thus made comparable to the later aircraft-fixed missions. Bearing and distance information could be determined for each invest observation. Each observation could be assigned to a particular grid box. All parameters to be composited were averaged and assigned to the center point of the grid box in which they lay.

The positioning of low-level centers is greatly improved over the method used in previous studies. Arnold (1977), McBride and Zehr (1981), and Lee (1986) used the center of the disturbance's cloud cluster convection as the best estimate of the low-level center when other information was not available. As will be discussed in Chapter 4, however, at early development stages, disturbances rarely have their LLCC in the center of their deep convection. The reconnaissance-derived or located low-level centers are much more reliable.

2.5 Middlebrooke's Earlier Invest Study Findings

Figure 2.4 shows Middlebrooke and Gray's composite radial profiles of tangential wind for D1 and NON-DEV cases. It was surprising that the tangential wind profile out to 3-4° of both classes was about the same. This is different from previous composite

Table 2.2: Number of invest flights which measured closed LLCCs vs. open (or derived) centers for D1 and NON-DEV disturbances.

	CLOSED LLCC	OPEN OR DERIVED CENTER
Early Developing (D1) 100 missions	47 (47%)	53 (53%)
Non-developing (NON-DEV) 76 missions	13 (17%)	63 (83%)
Ratio: D1/NON-DEV	(2.8/1)	(.64/1)
Maps for a number of NON-DEV missions were missing. This reduced the NON-DEV count from 111 to 76.		

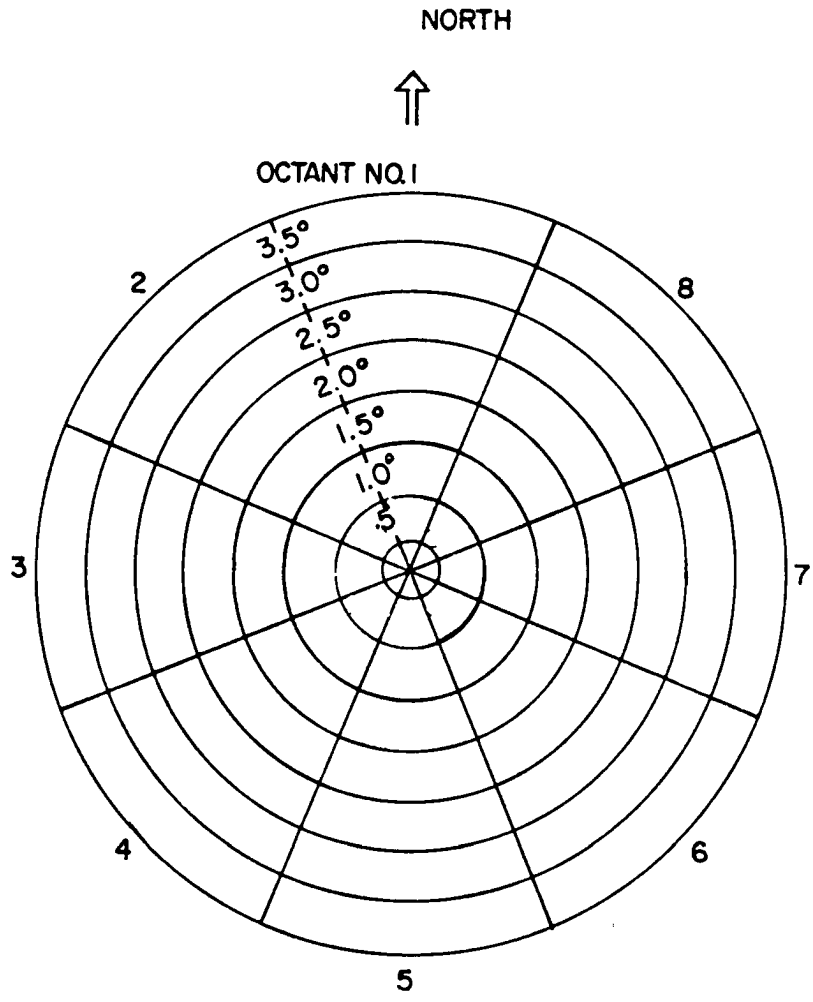

Figure 2.3: Sample of the 88 box grid used to composite the invest flight data. Belt 1 is 0-15 n mi (0-.25°) and each belt thereafter is 30 n mi (.5°) in radial distance. The center of octant 1 points north.

rawinsonde observations which showed (McBride and Zehr, 1981; Lee, 1986; and other similar research) that the outer 3-7° radius tangential wind of developing systems to be distinctly higher than that of non-developing systems. It is felt that the lack of invest flight tangential wind differences are a result of the special JTWC selection of invest flights. JTWC forecasters do not task flights into systems they believe do not have a very good potential for named storm development. Invest flights into systems very near the development stage are thus considered to be somewhat different than the average non-developing tropical disturbance or cloud cluster system upon which previous extensive rawinsonde composite analysis has been performed.

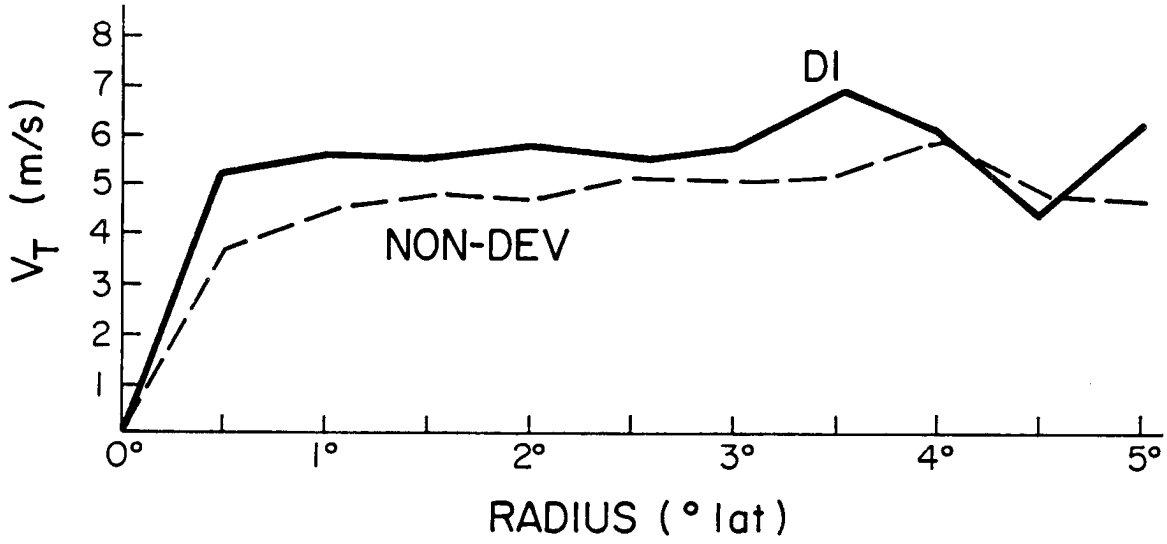

Figure 2.4: Comparison of the radial distribution of the composited tangential wind relative to the moving center (ms^{-1}) for developing and non-developing tropical disturbances. (From Middlebrooke and Gray, 1987.)

Figure 2.5 shows Middlebrooke and Gray's radial distribution of pressure profile. Note that the early stage developing systems (D1) had somewhat higher pressure than the non-developing disturbances. Development did not occur from a broad area of initial low pressure. Thus, sea-level pressure does not significantly distinguish development from non-development. These observations may indicate that wind rather than low pressure is more important in the initial development process.

Figure 1.4 depicts the only major difference which Middlebrooke and Gray found between early-stage developing (D1) and the non-developing systems - namely the strength of the inward-directed radial wind inside 1.5° radius. D1 systems have nearly twice as strong radial inflow at all inner-core radii as do NON-DEV systems. This difference cannot be due to positioning error because data indicate the average lowest pressure (as indicated in Fig. 2.5) was very close to the NON-DEV systems central position. The presence of similar tangential wind fields also precludes the idea that positioning errors account for these large differences in inner-core radial wind.

It is obvious from these radial wind differences that the D1 systems must have a greater concentration of deep convection near their centers compared with the NON-DEV

systems. A major question which arises is how the developing systems are better able to concentrate their deep convection at inner radii despite their having very similar tangential wind and pressure fields? This is a question this research attempts to pursue.

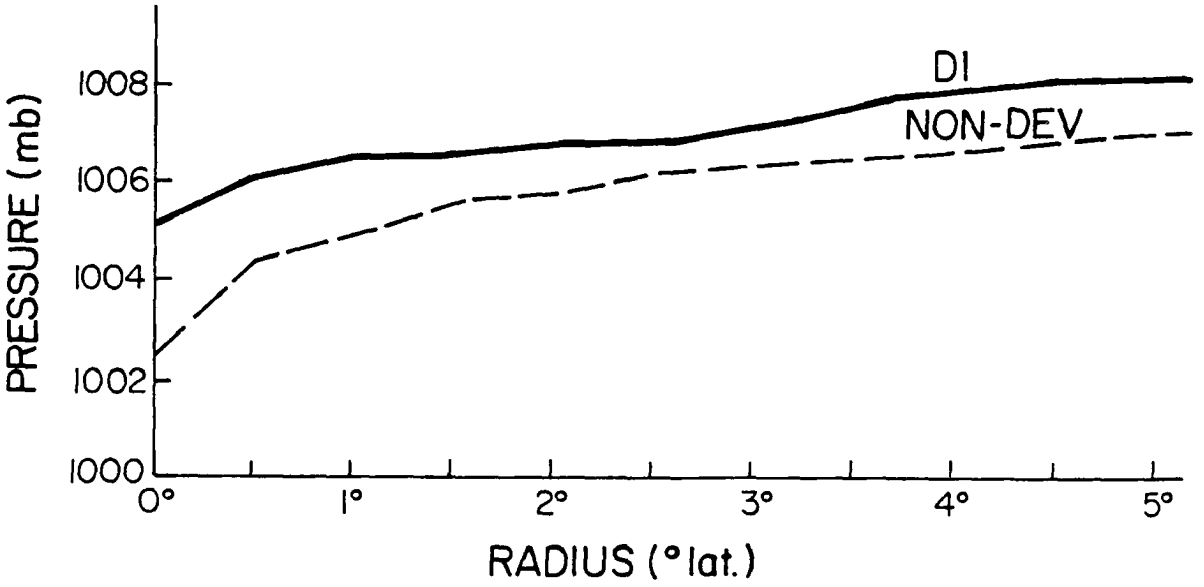

Figure 2.5: Comparison of the radial distribution of composite sea-level pressure (corrected for diurnal variation) for the early-stage developing and non-developing systems. (From Middlebrooke and Gray, 1987.)

Chapter 3

UPPER-TROPOSPHERIC BLOWTHROUGH (OR VENTILATION)

Upper-level winds across the disturbance might possibly be a key factor in helping to distinguish developing vs. non-developing disturbances. Perhaps non-developing systems have an upper-level wind blowthrough or ventilation which inhibits the concentration and maintenance of the deep convection evident near the centers of the typical developing systems.

Calculations of upper-tropospheric ventilation or blowthrough were thus made from the available upper-level synoptic charts in order to determine if this was a salient feature.

3.1 Upper-Tropospheric (250 mb/200 mb) Winds

The primary source of data for the blowthrough calculations was the Darwin 250 mb analyses. These analyses were supplied on microfilm courtesy of G. Holland, Bureau of Meteorology, Melbourne, Australia (BMRC). For each disturbance that had an invest flight and was determined to be an early-stage developer (MSLP > 1003 mb) or non-developer, the analyses were copied from microfilm. Generally, the 0000 GMT and 1200 GMT analyses were copied for each day the disturbance was classified as "early". Figure 3.1 shows a typical Darwin analysis of the 250 mb wind pattern.

Once all relevant maps were compiled, analysis was undertaken by placing a 6° radius acetate overlay on the wind chart (Fig. 3.2). Winds were selected at the eight primary compass points and at the center. These winds as well as the storm name and time were recorded on a sheet similar to Fig. 3.3. Wind direction was estimated to the nearest 10° and wind speed to the nearest 5 kts.

Figure 3.1: Example of the Australian Bureau of Meteorology, Darwin 250 mb analysis used for upper-tropospheric flow calculations in this study. Data depicted on this figure are from rawinsonde, satellite, and aircraft observations.

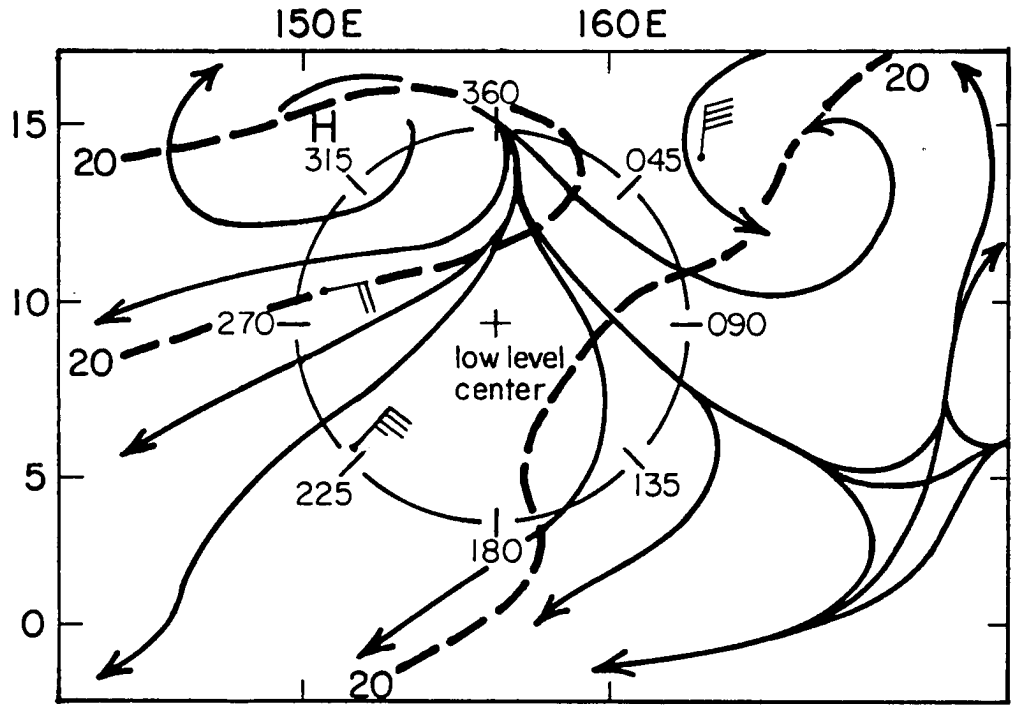

Figure 3.2: Example of a streamline analysis and the six degree radius overlay used to extract windspeed and direction from the analysis at the center and eight perimeter points (wind speed in knots).

It became apparent that the data were quite sparse at times and more information was needed. The addition of the European Centre for Medium Range Weather Forecasts (ECMWF) daily tropical belt 200 mb objective analysis helped fill in the "holes" in the Darwin maps and assisted in adjusting the Darwin analysis. The ECMWF analysis has a 1.875 degree grid spacing which far exceeded the data resolution requirements of this research. Figure 3.4 shows a typical ECMWF 200 mb analysis and the six degree radius circle around which wind calculations were made.

The positioning of the acetate overlay was dictated by the disturbance center information provided from the invest flight data. When the flight mission time failed to correspond to the analysis time, (this occurred most often at 1200 GMT—9 to 10 PM local time during nighttime hours), the position was adjusted through use of the JTWC ATCR best-track position and interpolation between known aircraft center fixes. This generally was not a problem for the 0000 GMT (or 9-10 AM local time) daylight analyses.

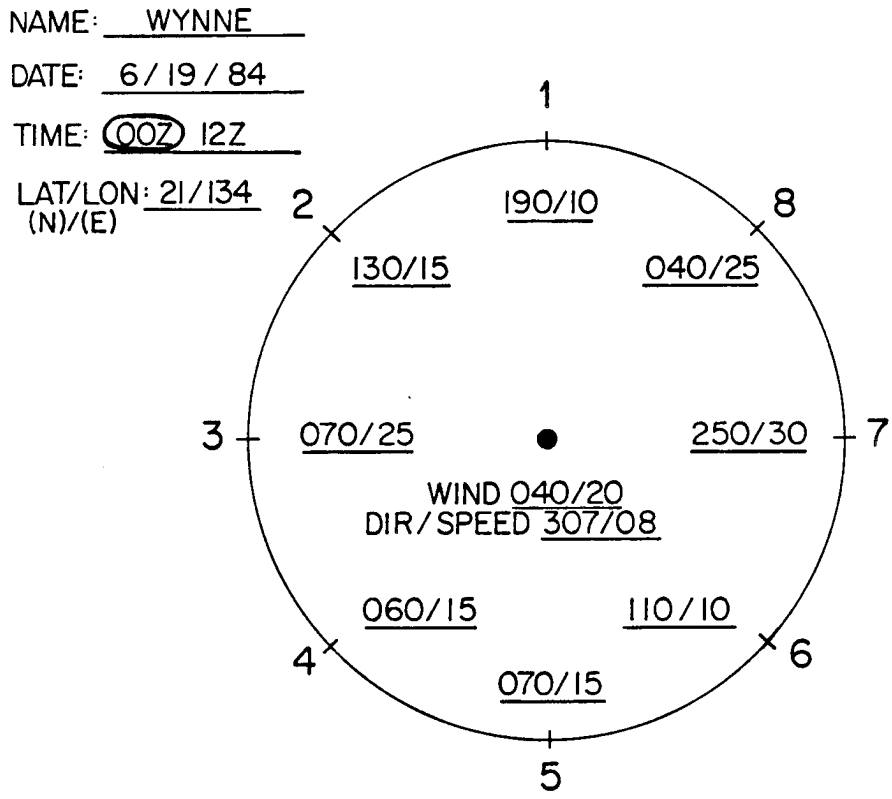

Figure 3.3: Recording sheet used for extracting wind data. The name of the D1/NON-DEV disturbance, date, time, location, wind speed and direction (within 5 knots, 10 degrees) at the center and eight perimeter points, and storm movement (direction and speed) were all entered on this form.

After checking each extracted wind value, center position, and disturbance intensity class, this wind information was entered into a file on the computer system.

3.2 Analysis of Upper-Tropospheric Wind Data

Section 3.1 detailed the process by which the upper-level wind data was extracted from the Darwin and ECMWF analyses. Data was entered into computer files in the following format:

- CASE NUMBER—flight mission number, corresponds to a 0000 GMT or 1200 GMT map time period for the particular early-stage disturbance on which invest flights were made.

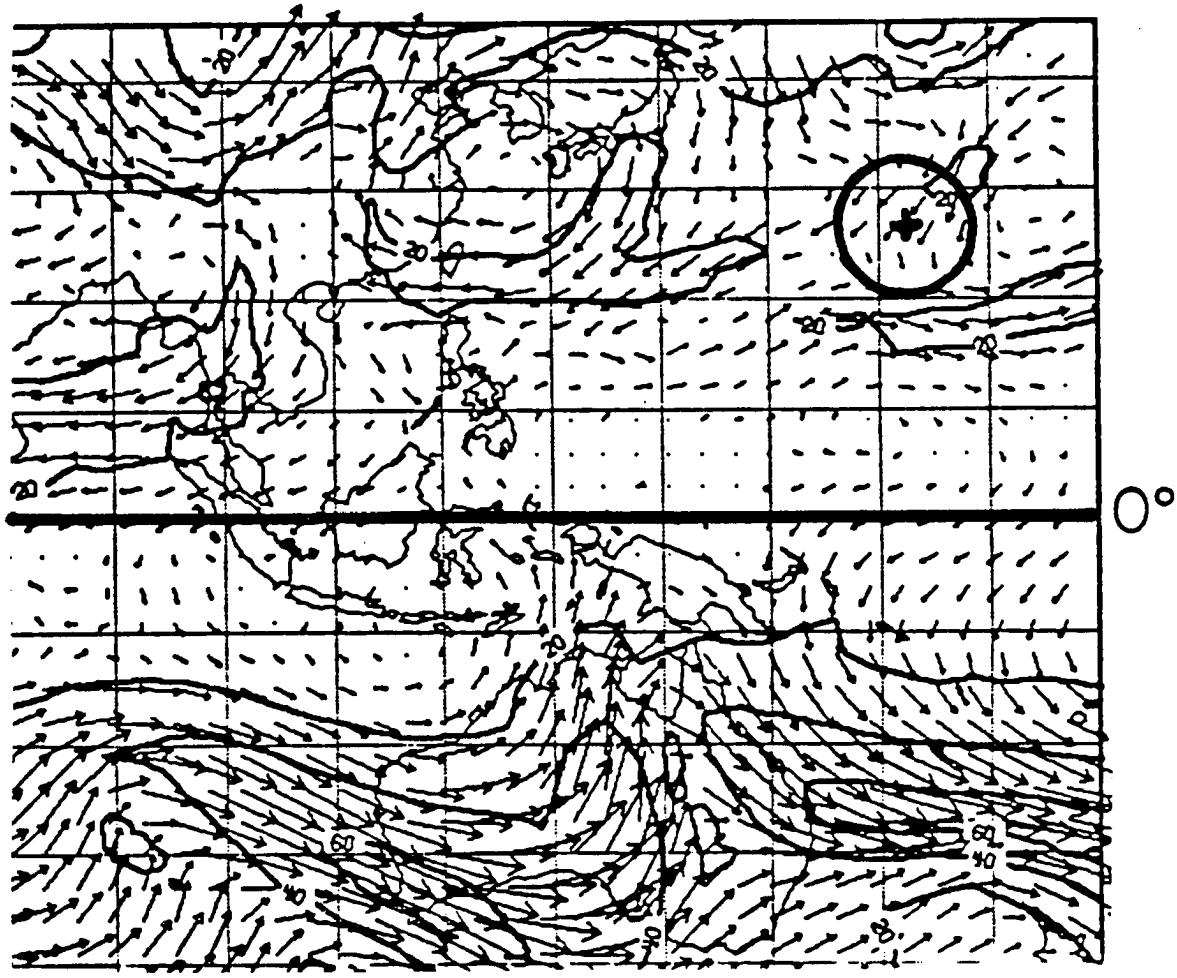

Figure 3.4: A sample of the 200 mb JTWC tropical belt objective analysis used to supplement the Darwin 250 mb analysis. Circle in upper right is for six degrees radius from center marked "+". Wind speeds in ms^{-1}.

- NAME—the identifier given to the disturbance. For developers, the name used is that given to the disturbance when it reaches tropical storm strength. For non-developers, simply: ND83-1, for example, the classification, year, and mission number.
- STORM NUMBER—the sequential assignment for that year.
- YEAR, MONTH, DAY
- HOUR—0000Z or 1200Z Darwin analysis.
- LATITUDE—(to the nearest degree)
- LONGITUDE—(to the nearest degree)
- DISTURBANCE DIRECTION OF MOVEMENT—(to one degree)
- DISTURBANCE SPEED OF MOVEMENT—(to one knot)
- CENTER AND OCTANT EXTRACTED WIND (9 ENTRIES)—Center plus eight octants (to 10 degrees, 5 knots)
- STAGE OF DEVELOPMENT—EARLY (MSLP $\geq$ 1003 mb), MIDDLE (1002 $\geq$ MSLP $\geq$ 997 mb), or NON-DEVELOPER

Disturbance blowthrough (or ventilation) at 250 mb is determined at 6° radius and along with the disturbance center wind estimate is interpolated to 3° radius. Zonal and meridional blowthrough components are separately calculated in order to individually determine east-west and north-south blowthrough components.

Before computing wind blowthrough, the extracted winds were first separated into 250 mb zonal (u) and meridional (v) components. The divergence in the u and v direction was then calculated. As illustrated in Fig. 3.5, for the u-direction computations, only the winds in octants 2-4 and 6-8 were used. Octant 3 and 7 winds were weighted twice and the remaining winds once. This was done so that for zonal blowthrough, extra weighting would be put on the winds directly east and west of the disturbance center. Similar

processes were carried out in the meridional direction where weighting favored meridional flow through octants 1 and 5. Figure 3.5 gives a sample calculations of u-divergence, v-divergence, mean divergence and u-blowthrough, v-blowthrough, and total blowthrough.

The left side of Fig. 3.5 shows sample zonal divergence and blowthrough calculations. The divergence calculation is carried out by adding the u-components of the wind in the boxes on each side. Considering the sign of all u-components and twice the value of the center u-components (octant 3 and 7), values for A and B are obtained. The total u-divergence (23.2) is calculated by taking the difference between A and B. In this case, A has general easterly flow, while B has general westerly flow, the total u-divergence is positive since both A and B indicate outflow. The v-DIV (-3.5) shows convergence since the northerly flow in D is greater than the northerly flow at C

The blowthrough (U_{BT}, V_{BT}) calculations are accomplished using the A and B values. U_{BT} is 2.1, V_{BT} is -16.1. The total blowthrough is the vector sum of the u and v blowthrough or 16.2.

Table 3.1 shows the results of all the calculations that were performed on the 250 mb wind data. Section 1 of this table shows the mean of all wind values for the composited D1 cases. Calculations were made in both the NATural (NAT) coordinate system (winds used in calculations without regard to motion) and the MOTion (MOT) coordinate system (motion vector subtracted from all winds). Section 1 shows the mean u- and v- components, mean radial and tangential winds, and mean direction and speed of all winds at 3° and 6° radius.

Section 2 of the table summarizes all of the divergence and blowthrough calculations.

Section 3 is a breakdown of composite wind speed and direction for each octant at the 3° and 6° radii and at the center.

Blowthrough (or ventilation) calculations were made for all individual and composited early-stage and middle-stage developing and non- developing systems. Calculations were made at both 6° radius and interpolated to 3° radius using the center wind and perimeter wind information.

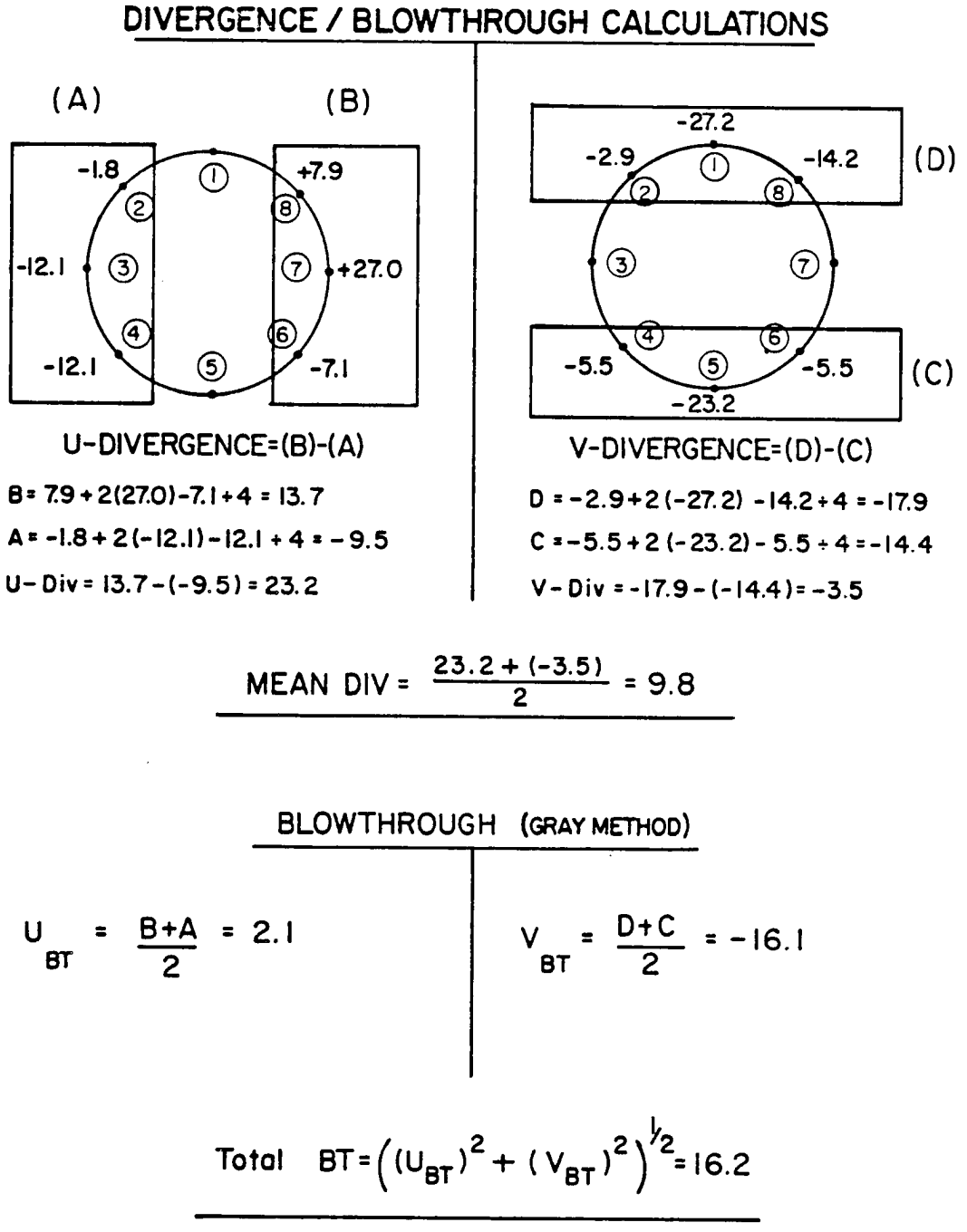

Figure 3.5: Illustration of how the divergence and blowthrough calculations were carried out for the 250 mb wind data extracted from the synoptic charts and separated into u and v components. (Values expressed in knots).

Calculations were made of mean wind vectors, mean wind speed of all octants, mean radial and tangential winds, storm speed and movement as well as the blowthrough and divergence calculations as shown in Table 3.1. These calculations provided information with which to compare any systematic upper-tropospheric wind differences between the disturbances that developed in comparison with those which do not.

3.3 Observational Findings—Upper-Tropospheric Wind Analysis

Calculations of 250 mb wind blowthrough (or ventilation) in the NAT and MOT systems at 3° and 6° radius showed general consistency for both the developing and non-developing classes. See Table 3.2. The MOT coordinate ventilation was then used throughout.

As is shown in Table 3.2, there was little difference in the composites of upper-tropospheric blowthrough for the developing and non-developing classes. Zehr (1976) showed similar results at the 250 mb level in his rawinsonde composite analysis. The reasoning behind this lack of average blowthrough difference stems from the fact that the non-developing systems were a very special class of disturbances very close to the point of cyclone development. Middlebrooke and Gray (1987) emphasized this point. Since JTWC only tasked reconnaissance flights on highly suspicious areas of deep and organized convection in very favorable synoptic environments, the NON-DEV disturbances must be considered to be a very special class of non-developing systems.

The fact that about half the invest flights were into systems which later became a named cyclone attest to this special class of systems with high potential for formation. Only 10-20% or so of the typical meso-scale cloud clusters in this region develop into name storms. Figures 3.6 and 3.7 further verify that there are no systematic wind blowthrough differences in these special class of developing and non-developing systems.

The 250 mb minus 850 mb zero zonal shear line, deemed important by Gray (1968) and substantiated by others, appears to be present near the disturbance center in both developing and non-developing cases. Note that wind velocities are stronger on the northern edge of the developers (possibly more Tropical Upper-Tropospheric Trough (TUTT) inter-

Table 3.1: Example of tabular display of calculations that were performed on the 250 mb wind data for all early-stage developers (D1) and non-developing cases. See text for explanation of calculations. (Wind values in knots).

EARLY STAGE DEVELOPERS. NO OBS: 134 STORM SPD: 9.30 STORM DIR: 286.31
MEAN OF COMPONENTS

Section 1

	NAT 3 DEG		NAT 6 DEG	
	U =	-7.3	U =	-6.1
	V =	1.7	V =	-.6
	VR =	1.3	VR =	2.6
	VT =	-3.1	VT =	-6.2
	DIR =	103.0	DIR =	84.6
	SPD =	7.5	SPD =	6.1
	MOT 3 DEG		MOT 6 DEG	
	U =	1.1	U =	2.3
	V =	-1.4	V =	-3.7
	VR =	1.3	VR =	2.6
	VT =	-3.1	VT =	-6.2
	DIR =	321.9	DIR =	327.9
	SPD =	1.8	SPD =	4.4

GRAY VENTILATION METHOD

Section 2

	GRAY VEN - NAT 3 DEG		GRAY VEN - NAT 6 DEG	
	U DIV =	1.8	U DIV =	4.1
	V DIV =	2.2	V DIV =	4.4
	MEAN DIV =	2.0	MEAN DIV =	4.2
	U BLOTHRU =	-7.4	U BLOTHRU =	-6.5
	V BLOTHRU =	1.8	V BLOTHRU =	-.4
	TOT BLOTHRU =	11.6	TOT BLOTHRU =	10.1
	GRAY VEN - MOT 3 DEG		GRAY VEN - MOT 6 DEG	
	U DIV =	2.2	U DIV =	4.4
	V DIV =	2.2	V DIV =	4.4
	MEAN DIV =	2.2	MEAN DIV =	4.4
	U BLOTHRU =	.9	U BLOTHRU =	1.8
	V BLOTHRU =	-1.3	V BLOTHRU =	-3.5
	TOT BLOTHRU =	9.8	TOT BLOTHRU =	10.0

Section 3.

OCT	NAT 3 DEG DDD/VV		NAT 6 DEG DDD/VV	
1	167. /	4.	243. /	7.
2	128. /	5.	167. /	2.
3	109. /	9.	99. /	9.
4	97. /	12.	85. /	16.
5	95. /	11.	80. /	15.
6	97. /	11.	82. /	13.
7	101. /	6.	63. /	5.
8	156. /	3.	262. /	6.
C	119. /	9.	119. /	9.

OCT	MOT 3 DEG DDD/VV		MOT 6 DEG DDD/VV	
1	265. /	8.	270. /	15.
2	268. /	4.	277. /	8.
3	318. /	0.	359. /	2.
4	65. /	4.	58. /	9.
5	54. /	4.	49. /	8.
6	51. /	3.	44. /	7.
7	309. /	3.	320. /	7.
8	274. /	7.	279. /	14.
C	197. /	1.	197. /	1.

Table 3.2: Values for upper-tropospheric blowthrough in both the MOT and NAT coordinate systems at 3° and 6° radius (ms^{-1}).

	BLOWTHROUGH			
	6°MOT	6°NAT	3°MOT	3°NAT
Early-Developing (134 cases)	5.0	5.0	4.9	5.8
Non-Developing (148 cases)	5.2	6.2	5.5	6.7

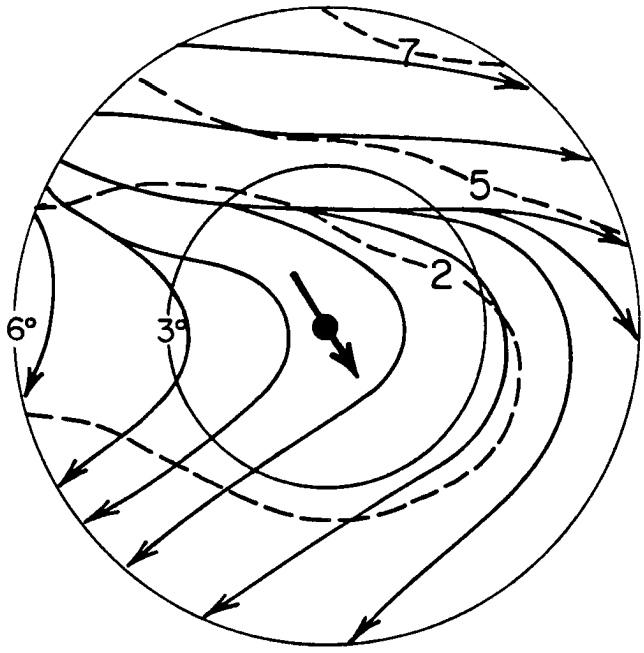

Figure 3.6: The composite upper-tropospheric flow pattern relative to the center of moving disturbance (MOT system) derived from averaging the center, 3° radius and 6° radius winds for early-stage developing disturbances (134 cases). Wind speeds in ms^{-1}. Center arrow indicates mean wind direction for all winds in this stratification.

action) while there are somewhat stronger winds on the south side of the non-developers (evidence of stronger easterly shear in non-developing disturbances).

Table 3.3 gives a breakdown in the number of D1 and NON-DEV cases that experienced high or low wind blowthrough at 6° radius. As the average 250 mb blowthrough value was about 5 ms^{-1} in both developing and non-developing cases, a blowthrough greater than 5 ms^{-1} was designated a high blowthrough case. A value below 5 ms^{-1} was designated low blowthrough.

Table 3.3: Number of high blowthrough/low blowthrough cases (MOT coordinates) for the two classes of D1 and NON-DEV systems.

	HIGH BLOWTHROUGH ($> 5\ ms^{-1}$)	LOW BLOWTHROUGH ($< 5\ ms^{-1}$)
Early-Developing (134 cases)	79 (59%)	55 (41%)
Non-Developing (148 cases)	77 (52%)	71 (48%)

All of the 250 mb wind cases in this study were at both 0000 GMT and 1200 GMT time periods. However, the flight times were all daytime missions near 00-06 GMT (10 LT-16 LT) in most cases. Although 250 mb divergence values can be different between 00Z and 12Z, ventilation values were not different.

Combining all cases of developing and non-developing systems gave an idea of how high or low the blowthrough was on the average. The average of the high blowthrough values was 14 knots (7.2 ms^{-1}) for the combined set while the average of the combined low blowthrough set was 6.5 knots (3.3 ms^{-1}). This gives more than a two to one difference between high and low blowthrough cases. In general, there were higher wind speeds on the southern edge of the disturbance in the high blowthrough cases, much like that in the non-developing case composite.

3.4 Comparison of NAT and MOT Wind Flow Fields

In the Natural coordinate system (NAT), winds are composited without regard to the motion of the disturbance. In the motion (MOT) coordinate system, the motion of the disturbance is subtracted from each wind value. The motion for the developing systems (D1) in the 1980-84 cases was found to be toward 286 degrees at 9.3 knots (4.8 ms^{-1}) while the motion for non-developers was 291 degrees at 8.4 knots (4.3 ms^{-1}). In NAT coordinates there is a weak easterly flow across developers and non-developers alike. In the MOT system, 6° radius wind flow through the disturbance from the NW (D1) and NE (NON- DEV). Table 3.4 summarizes the mean flow for both developers and non-developers in the NAT and MOT systems.

Table 3.4: Mean direction (in °) and speed (in ms^{-1}) for each class of disturbance (MOT and NAT coordinates). Values were obtained by taking average u and v component at each point around the respective radius and recombining into vector form (for the years 1980-1984).

	6°MOT	6°NAT	3°MOT	3°NAT
Early-Developing (134 cases)	328/2.2	085/3.0	322/0.9	103/3.8
Non-Developing (148 cases)	014/2.2	084/4.2	026/1.4	096/4.3

Notice from Table 3.4 the existence of an easterly component to the flow in both the NAT and MOT systems for non-developers. This again may point to the existence of inhibiting, excessively strong easterly shear in the non-developing cases. In general, the blowthrough is small in both developing and non-developing cases in the MOT system.

3.5 Contribution to Total Blowthrough by u-, v-components

Zonal (u) and meridional (v) ventilation comparisons have been calculated in the MOT system at 6 degrees. U-blowthrough in MOT coordinates for developing and non-developing systems show the only difference: 1.8 for D1 vs -1.0 for NON-DEV. This

corresponds to the mean wind values (Table 3.4) where it was shown that developing cases exhibited greater westerly flow (positive u) while non-developing cases showed more easterly flow (negative u). V-blowthrough dominated over u-blowthrough in both classes of disturbances. Meridional composite blowthrough values for both classes were nearly the same (-3.5 for D1, and -4.4 for NON-DEV).

Summary. These only very small average differences in upper-tropospheric wind blowthrough between these special class of developing and non-developing systems does not negate the importance of upper-level blowthrough as an inhibiting influence on individual case TC developing. As will be shown in the following chapters, individual case disturbances with low blowthrough require less influence by other favorable parameters for development. By contrast disturbances with higher upper-level blowthrough require more influence by other favorable parameters before development can occur.

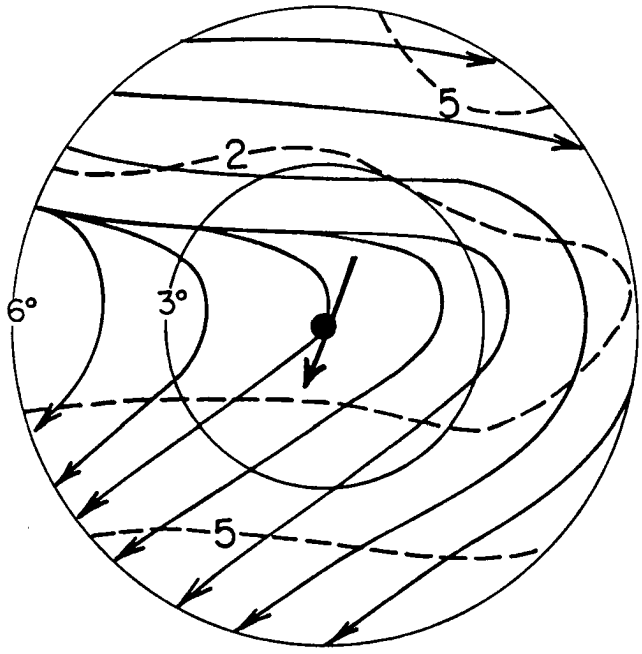

Figure 3.7: Same as for Fig. 3.6, but for non-developing disturbances (148 cases).

Chapter 4

DEEP CONVECTION/LOW-LEVEL CENTER RELATIONSHIP AS REVEALED BY SATELLITE DATA

Japanese Geostationary Meteorological Satellite (GMS) imagery and Defense Meteorological Satellite Program (DMSP) satellite information were used in combination to determine if there were any systematic relationships between the Low-Level Circulation Centers (LLCC) which the invest flights detected and the overall amount and location of deep convection occurring within the disturbance's cloud cluster system. Defense Meterological Satellite Program (DMSP) imagery was also used to study the concentration of deep convection near the center of the developing and non-developing disturbances. Also investigated was the possible relationship between the LLCC and cloud cluster convection as influenced by the upper tropospheric wind fields.

4.1 Japanese Geostationary Meteorological Satellite (GMS) Data Set

To study these relationships Japanese GMS imagery was extensively used. Imagery times were closely matched to flight times. The 2100 GMT ($\sim$ 06 LT), 0000 GMT ($\sim$ 09 LT), 0300 GMT ($\sim$ 12 LT) and 0600 GMT (15 LT) were closely associated in time with the invest flights.

Japanese GMS satellite imagery was supplied on microfilm by the Australian BMRC. Figure 4.1 shows a typical GMS visible satellite imagery with the grid overlay which was used. Reasonable identification of the deep convective areas is possible using this GMS visible imagery. The resolution of the raw GMS visual imagery is 1 km, but becomes degraded on microfilm and paper copies.

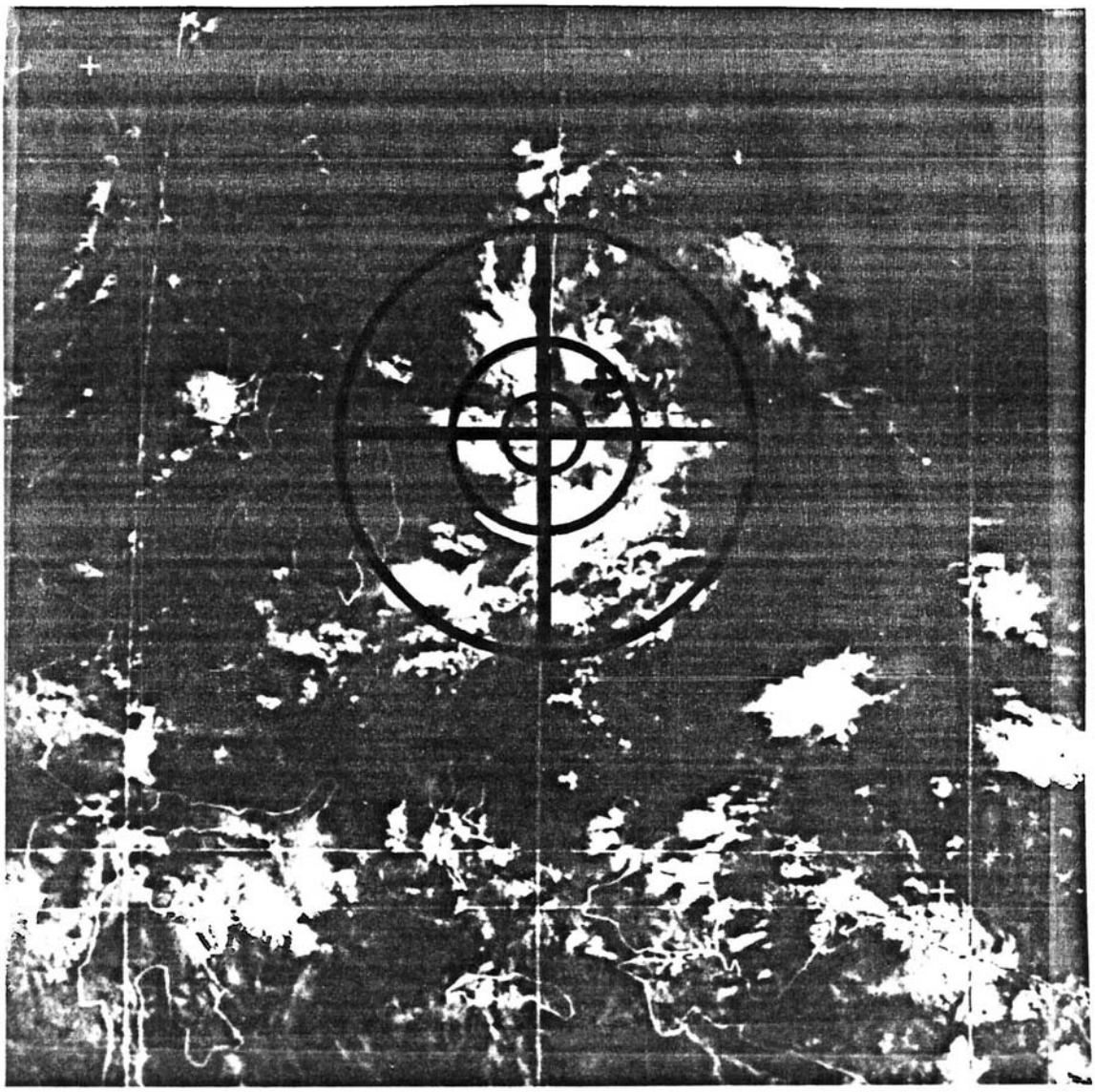

Figure 4.1: An example of GMS visual imagery available on microfilm. The resolution of the picture is adequate to determine the areas of deep convection. The concentric circles are at radii of 1°, 2.5°, 5.0°. The "+" designates the aircraft-located low-level circulation center (LLCC). This image is of a developing tropical depression (V_{max} $\sim$15 ms^{-1}) (to become named-storm Vera) on 12 July 1983, 00Z.

4.2 Cloud Cluster and LLCC Relative Locations

The first step involved the plotting of the LLCC positions on the satellite photographs. Care was taken so that no more than 1.5 hrs separated the image time from the invest flight time.

A grid with 2.5° and 5° radius circles and 1° radius inner circle was placed over the satellite picture with the grid center located at the center of the deep convection, as shown in Fig. 4.2. The choice of the above radii was based on Arnold's (1977) use of radii at 1.4° and 4.2° to define inner and outer limits of disturbance convection. The inner 1° approximates the area Arnold used for center location. If the aircraft-located position fell into the inner 1°, this was considered a cloud cluster "center" LLCC position. If the low-level circulation center was located more than 1° to one side of the cloud cluster center position, this was considered a quadrant LLCC position. The 2.5° radius circle was placed so that the most prominent convection associated with the disturbance, was enclosed by the circle. The 5° radius circle was used to estimate the net deep convection outside the 2.5° radius. The quadrant that the already plotted center lay in was recorded, as was the convection type as specified by the nomenclature of Dvorak (1975, 1984), eg.: CDO, BAND; and size of convective features, etc.

Table 4.1 shows the location distribution of LLCC vortex centers relative to the disturbance's cloud cluster convection.

Values in Table 4.1 are graphically portrayed in Fig. 4.3. The sustained winds of all systems were generally less than 25 kts.

Note the general lack of LLCC's within one degree (latitude) radius of the main convective center of both developing and non-developing systems. Low-level circulation centers are not typically located in the center of the disturbance convection. The typical cloud cluster signatures which are required by JTWC for the tasking of an invest flight are solid convection of 3-5° in diameter that is persistent in time (> 12 hours). Invest flights were not generally tasked for broad-scale convective areas on the scale of the monsoon trough (tens of degrees latitude).

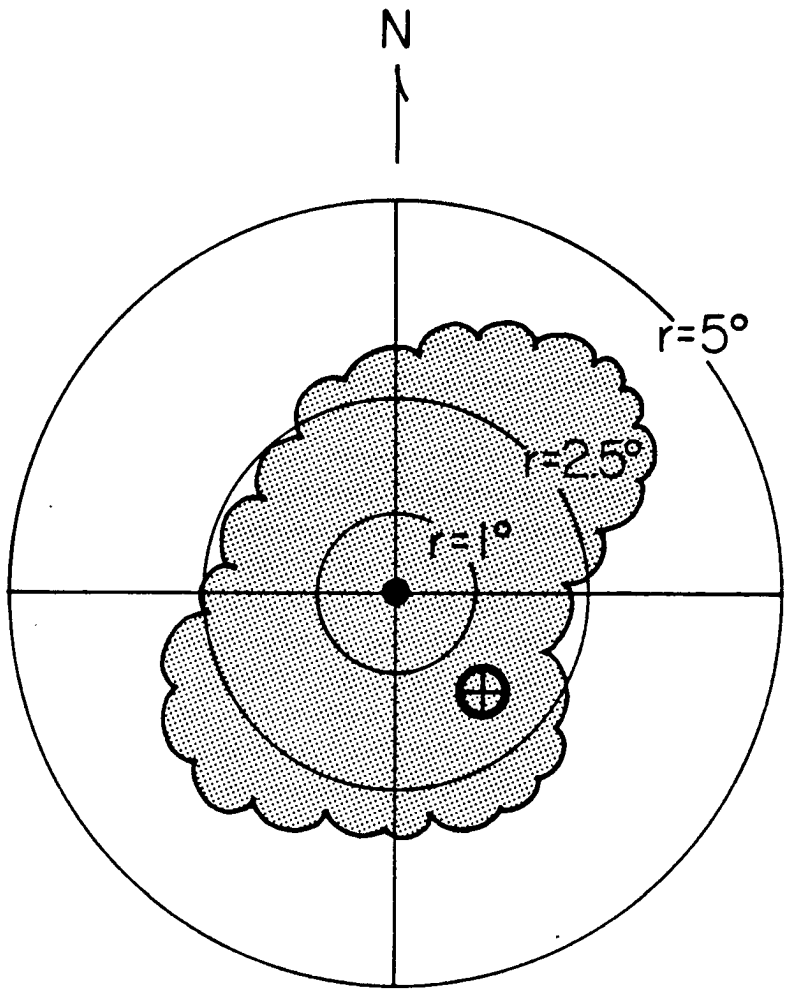

Figure 4.2: Example of the grid used to overlay the GMS imagery in order to classify the Low-level Circulation Centers (LLCC) in relation to the cloud cluster disturbance center. In this case the LLCC was located to the southeast of the cloud cluster center.

Table 4.1: Number and percentage of total cases of LLCC's located in each quadrant or center of the D1 or NON-DEV disturbance's cloud cluster convection.

	Northeast	Southeast	Southwest	Northwest	Center
Early-Stage Developers (94 cases)	5 (5%)	27 (29%)	24 (25%)	28 (31%)	10 (10%)
Non-Developers (110 cases)	28 (26%)	31 (28%)	31 (28%)	17 (15%)	3 (3%)

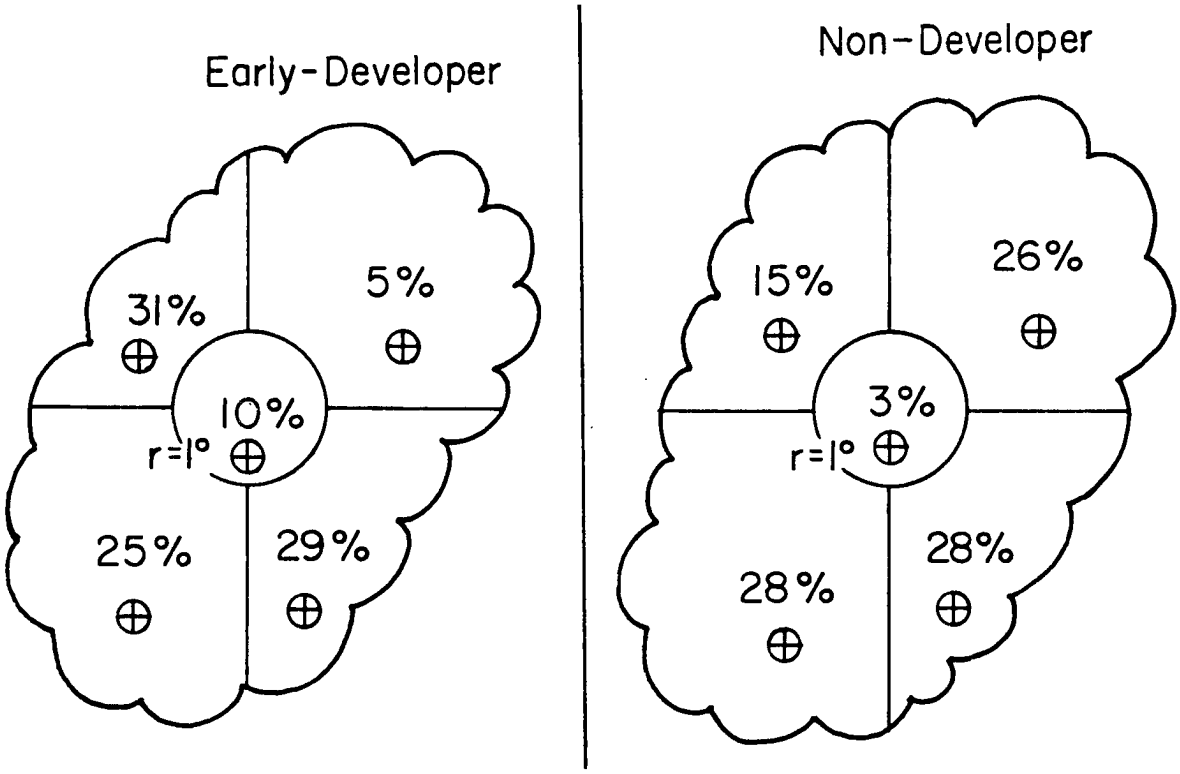

Figure 4.3: Percentage occurrence of Low-Level Circulation Centers (LLCC) in the respective quadrants (or center) relative to the associated cloud cluster convection. D1 sample has 94 cases (Left) and NON-DEV sample has 110 cases (Right).

The LLCC center positions also were rarely beneath the center of the heaviest cloud cluster convection. Often the centers were found fully or partially exposed to the side of the disturbance's cloud cluster convection. At this early stage of development, cloud clusters were often less organized than the typical BAND or CDO cloud patterns (Dvorak, 1975, 1984) commonly discussed by Dvorak in his ideal case analysis. This relates well to Arnold's (1977) results that showed over 50% of his circulation centers could be identified with a relative minimum in deep convection. Arnold (op.cit) goes on to say that, "had more of the clusters been based on aircraft reconnaissance, it is expected that the cloud free regions would have more frequently coincided with the circulation centers". These earlier findings of Arnold (1977) are in general agreement with the results of this research.

The presence of dynamically forced subsidence and its relationship to the low-level center, as described by Arnold (op.cit.) may indeed be created by convergence of outflow. This results in subsidence, upper-level warming, and lower pressures at the surface (see

Fig. 4.4) in response to the formation of a low-level circulation center or where circulating initiating deep convection may have already died off. This topic needs much further study.

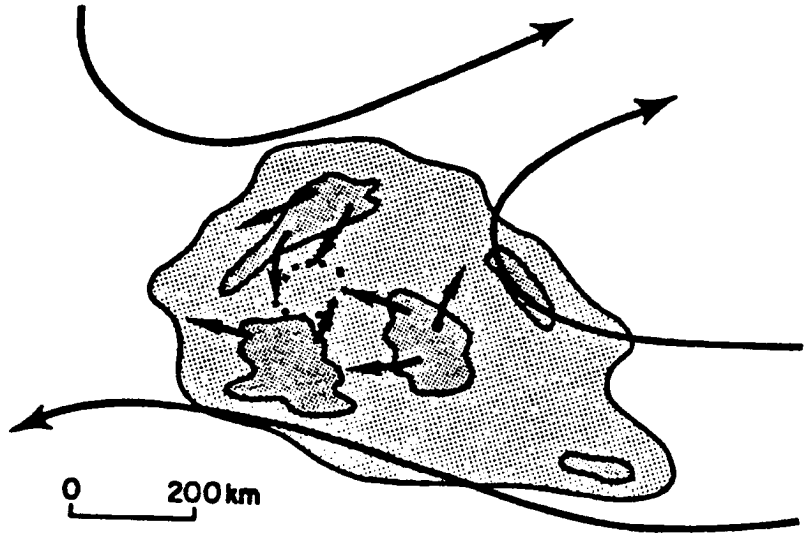

Figure 4.4: Conditions where dynamically-forced subsidence occurs within the disturbance cirrus shield (light shading) and between active convective elements (heavy shading). The cirrus level outflow from the deep convective areas is indicated by the dotted circle region. (From Gray, 1979.)

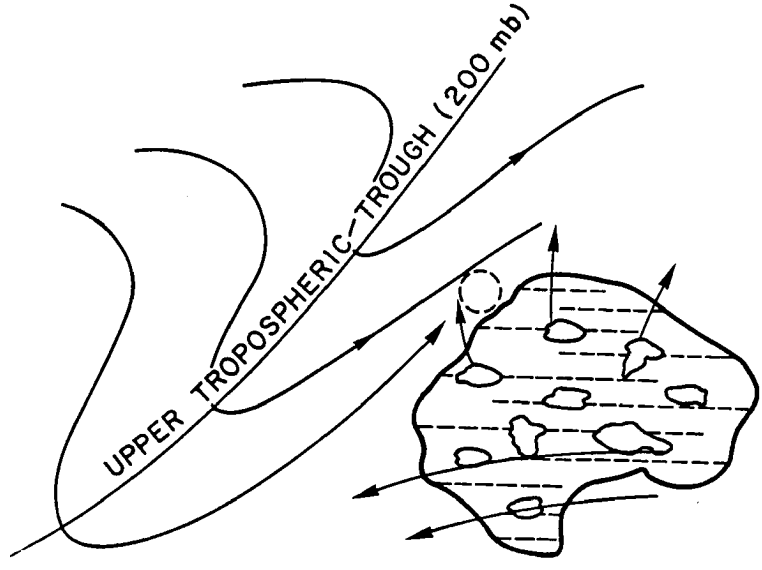

Figure 4.5: Similar to Fig. 4.4 except dynamically forced subsidence occurring in an exposed clear region surrounding the cluster. Dashed circle represents the area of maximum convergence between outflow from convective elements and southwesterly flow from the upper-level trough (from Arnold, 1977).

Another interesting observation derived from Fig. 4.3 is the lack of LLCC's in the northeastern quadrant of the developing systems in comparison with the many centers which occurred in the northeastern quadrant of the non-developers. This effect is probably closely related to the more dominant mean relative easterly wind flow across the non-developers and the opposite or relative westerly flow for the developers (as discussed in Chapter 3). It would logically follow that with more prevalent mean westerly flow in developers, the occurrence of LLCC's in the northwest quadrant would be greater. As shown in Fig. 4.3, that is the case. Experienced JTWC forecasters have noted that a disturbance's LLCC is typically located on the up-wind side of the cloud cluster's relative upper-tropospheric wind flow (see Fig. 4.5).

Later stages of development, e.g., Middlebrooke and Gray's D2 ($1002 \geq$ MSLP $\geq$ 997 mb) or middle stage developers show more convection surrounding the LLCC. Of the 116 cases of middle-stage developers, the percentage of LLCC's occurring within one degree of the center of the cloud cluster increased to 25 percent. It is common that deep convection more uniformly develops around the LLCC as it intensifies toward tropical storm classification.

4.3 Association of Upper-Tropospheric Relative Wind Flow in Relation to the Position of LLCC Within the Cloud Cluster Convection

By compositing the relative (or MOT) 250 mb winds for cases that coincided with LLCC positions in the various cloud cluster quadrants, the mean upper-tropospheric flow associated with the various LLCC quadrant positions could be determined. A summary of the results for all D1 cases is shown in Fig. 4.6. This figure shows the mean 250 mb relative (or MOT) wind vectors at 6 degrees for LLCC positions in the various quadrants of the cluster convection.

Developing and non-developing wind vectors are very similar. When upper-tropospheric flow relative to the LLCC has an easterly component the LLCC is usually located on the eastern side of the cloud cluster convection irrespective of whether the system develops or not. The same upwind location is evident for relative westerly component flow. In this

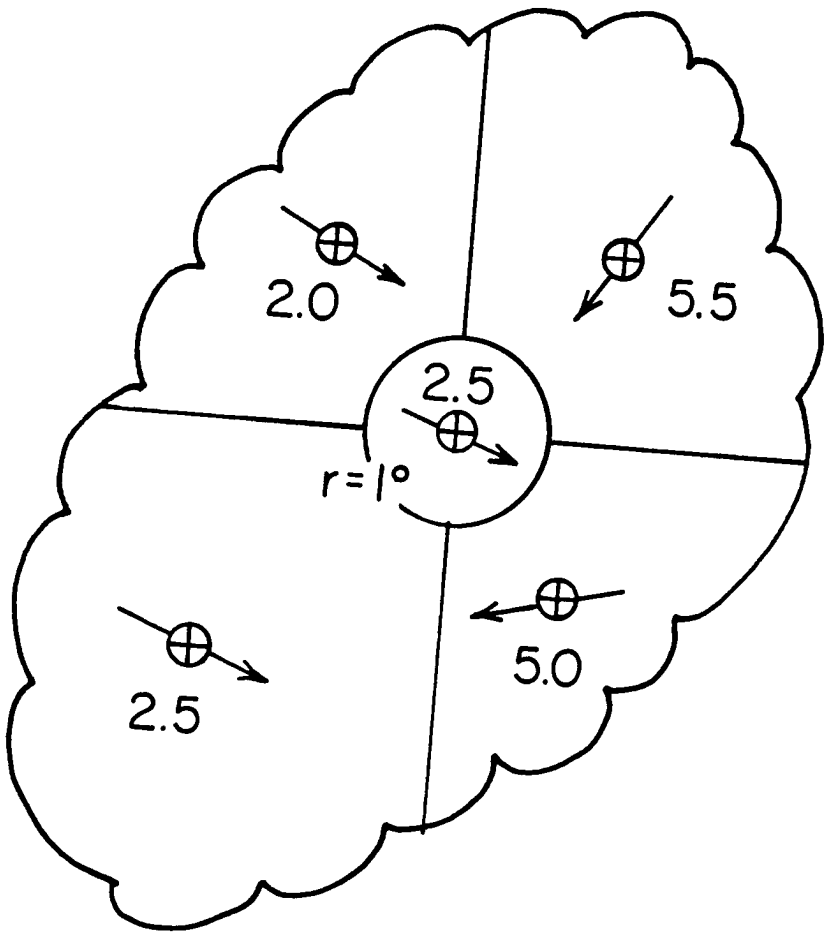

Figure 4.6: Depiction of the mean 250 mb (6° radius and center) wind vector (in ms^{-1}) for early-stage developing disturbances when the LLCC is located in various cloud cluster quadrants.

case the LLCC will generally be found on the western side of the cluster convection (as shown in Table 4.2).

For mature cyclone systems undergoing strong baroclinic shearing influences, the observation of a low-level center existing on the upwind side of the sheared off convection is quite common. However, in early stage low latitude and summer conditions, as discussed here, this documentation of a relative upwind location of the LLCC may provide some beneficial guidance to the forecaster as to the location of a LLCC or to the flight officer as to where to direct his reconnaissance aircraft.

Figures 4.7a-d and 4.8a-d are the plotted 3° and 6° composite 250 mb relative (or MOT) Darwin/200 mb ECMWF winds, for the D1 and NON-DEV classifications. Each chart represents a particular quadrant in which the LLCC was found. The charts for LLCC center locations were omitted due to lack of data. The center of the grid is the location of the LLCC, not the convective center as shown in Fig. 4.9.

Table 4.2: Mean relative (or MOT) 250 mb wind vectors in ms^{-1} for LLCC located in the various quadrants (or center) of the cloud cluster convection.

MEAN VECTOR WIND FOR RESPECTIVE LLCC LOCATION					
	NE	SE	SW	NW	Center
Early-Developing (D1) (134 cases)	*021/5.5	083/5.0	292/2.5	301/2.0	289/2.5
Non-Developing (NON-DEV) (148 cases)	035/2.4	052/2.7	347/2.6	354/2.5	*312/7.5
* denotes less than 10 cases.					

Note that in six of these eight 250 mb wind composites the area of main cloud cluster convection is associated with an upper-level ridge or anticyclone. Diagrams 4.7b and 4.7c are the exceptions. In all cases the 250 mb relative winds over the LLCC are very weak. This helps assure that the vertical structure of the LLCC can be more easily maintained through the troposphere and not develop strong vertical slope and become sheared off.

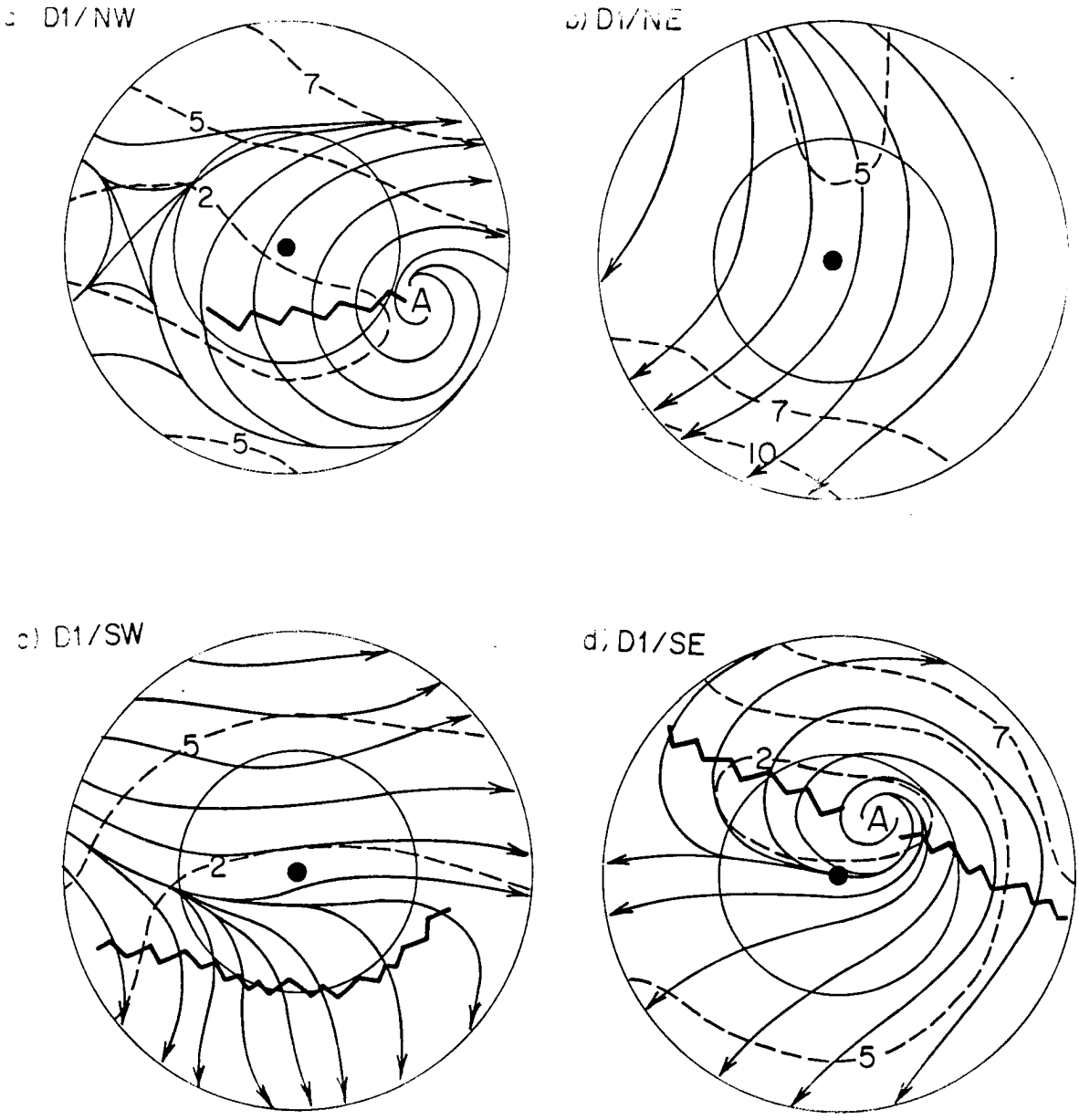

Figure 4.7: a-d. Composite 250 mb wind analyses of the upper tropospheric flow (MOT coordinate system) across the D1 disturbances with LLCC's in the: a) NW quadrant, b) NE quadrant, c) SW quadrant, d) SE quadrant. Streamline analysis based on center, 3° and 6° radii MOT winds (in ms^{-1}).

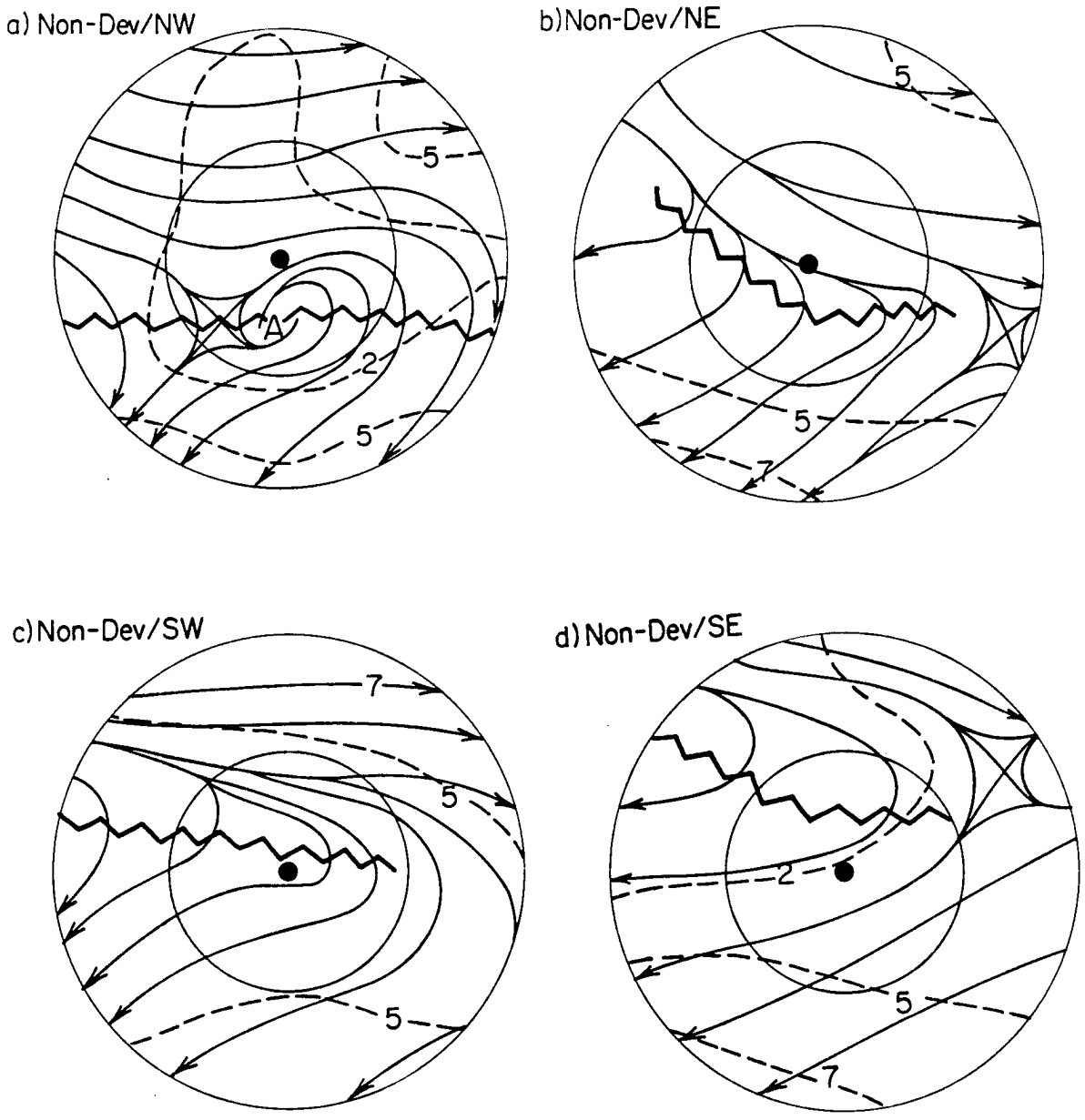

Figure 4.8: a-d. Same as for Fig. 4.7a-d, except for NON-DEV disturbance composites.

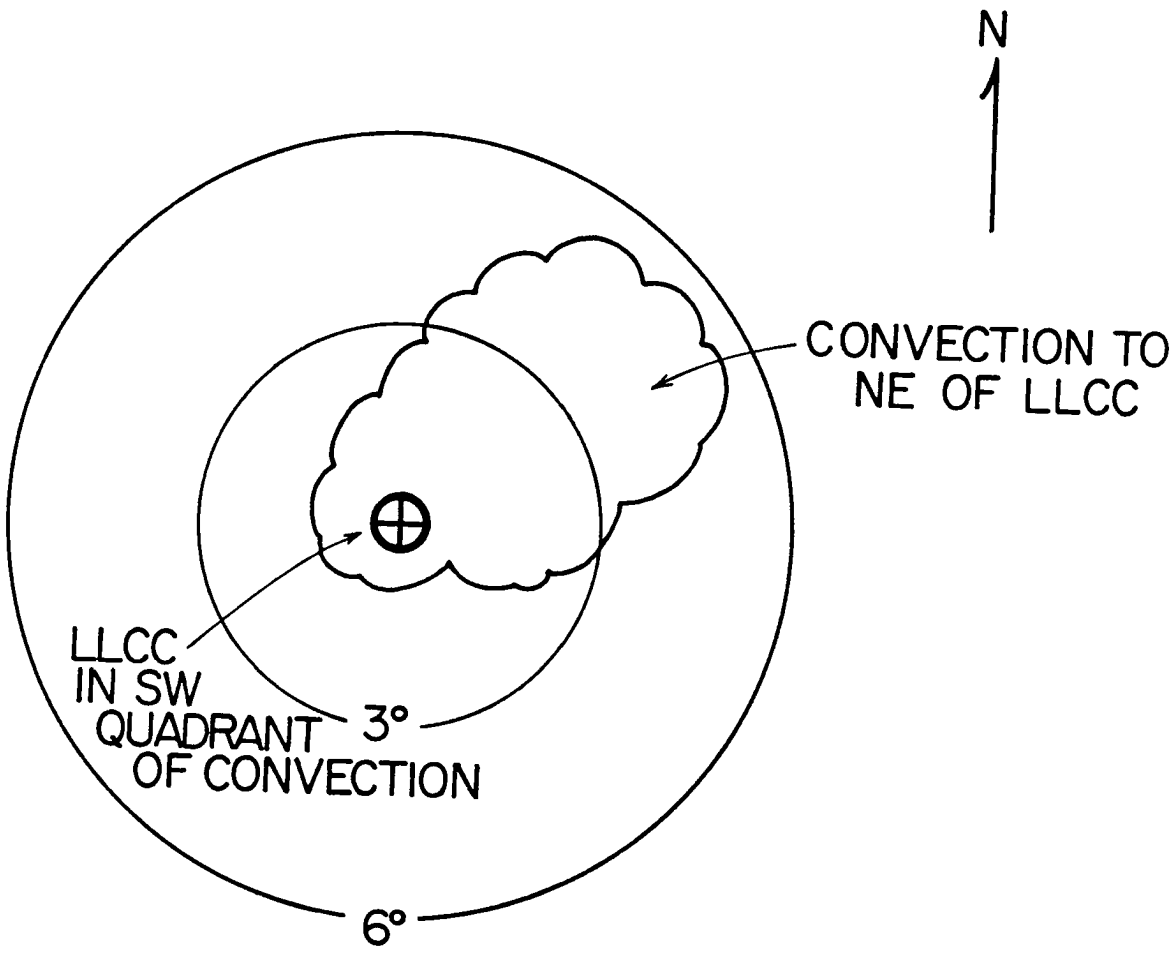

Figure 4.9: Typical example of the cloud cluster's main convection (MC) location relative to the Low-Level Circulation Center (LLCC) from a LLCC in the southwest quadrant of the cluster convection. This type of center would be considered a "SW", with the majority of the disturbance convection to the northeast.

To help illustrate this relationship two cases will now be shown. The NAT coordinate system is used since this is the one which the forecaster would employ.

Example 1—A disturbance that was destined to become Tropical Storm Thelma two days hence (see Fig. 4.10a) has its LLCC to the southwest of the main cloud cluster convection. The corresponding 250 mb NAT composite wind field for all disturbances with southwest centers is shown in Fig. 4.10b. Note the proximity of the convection relative to the ridge. Also note that the motion of the system is to the west-northwest at 5 ms^{-1} and that the relative or MOT wind over the LLCC would be weakly from the west.

Example 2—The satellite image (Fig. 4.11a) of future Tropical Storm Orchid is shown with the associated LLCC to the northwest of the main convection. This is two days prior to this disturbance attaining tropical storm strength. Figure 4.11b shows the corresponding composite flow for all centers in the northwest and the superimposed convective region. As this system was moving towards the northwest at about 5 ms^{-1} note that the relative or MOT wind over the LLCC would be weakly from the northwest.

Thus, general relationships between the relative positions of the LLCC and cloud cluster convection and the motion of the upper-level flow across the LLCC and cloud cluster appear to be verified.

4.4 Concentration of Deep Convection Near the LLCC

To investigate differences in the concentration of deep convection near the LLCC's centers in developing vs. non-developing cases, the higher resolution polar orbiting DMSP visual satellite (0.6 km resolution) imagery has been employed in lieu of the lower resolution, deep cell resolving GMS satellite pictures. Arnold (1977) had previously pointed out how developing TC's had a significantly higher concentration of deep convection within their inner core. A determination was made of the magnitude of this deep convection concentration for the developing and non-developing disturbances. The author's previous experience as an officer in charge of the tropical forecast section at Air Force Global

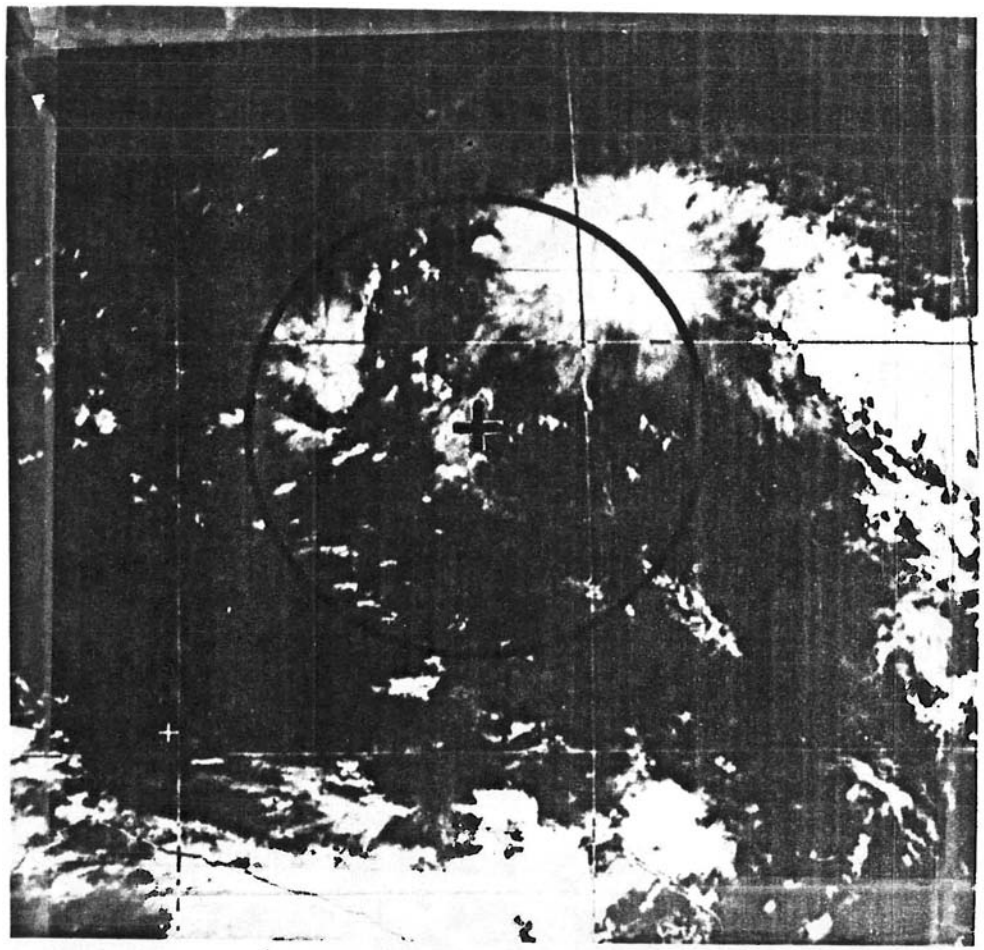

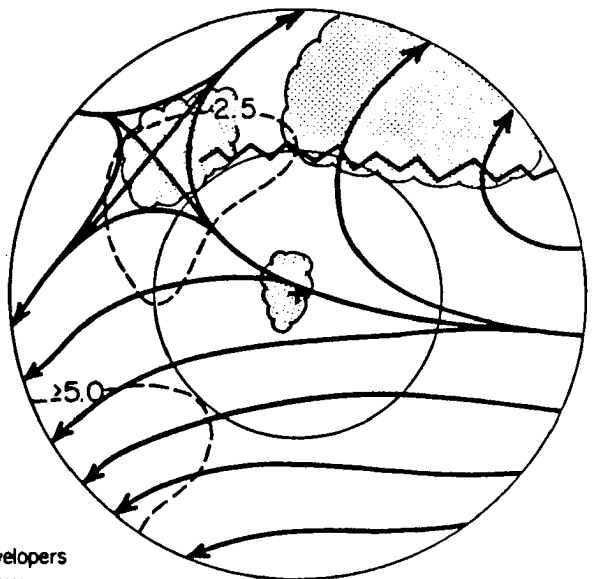

Early Developers
Center - SW
NAT System

Figure 4.10:a-b. Depiction of the GMS satellite image of the convection and associated LLCC in a disturbance (TC24W) that would become Tropical Storm Thelma (1983) (left diagram). Composite 250 mb flow (NAT coordinate) for systems with LLCCs in the southwest region of the cluster convection (right diagram). Shading is the cloud pattern represented in the satellite image. As this system was moving WNW at about 5 ms^{-1}, the 250 mb relative or MOT flow relative to the LLCC would be from the SW.

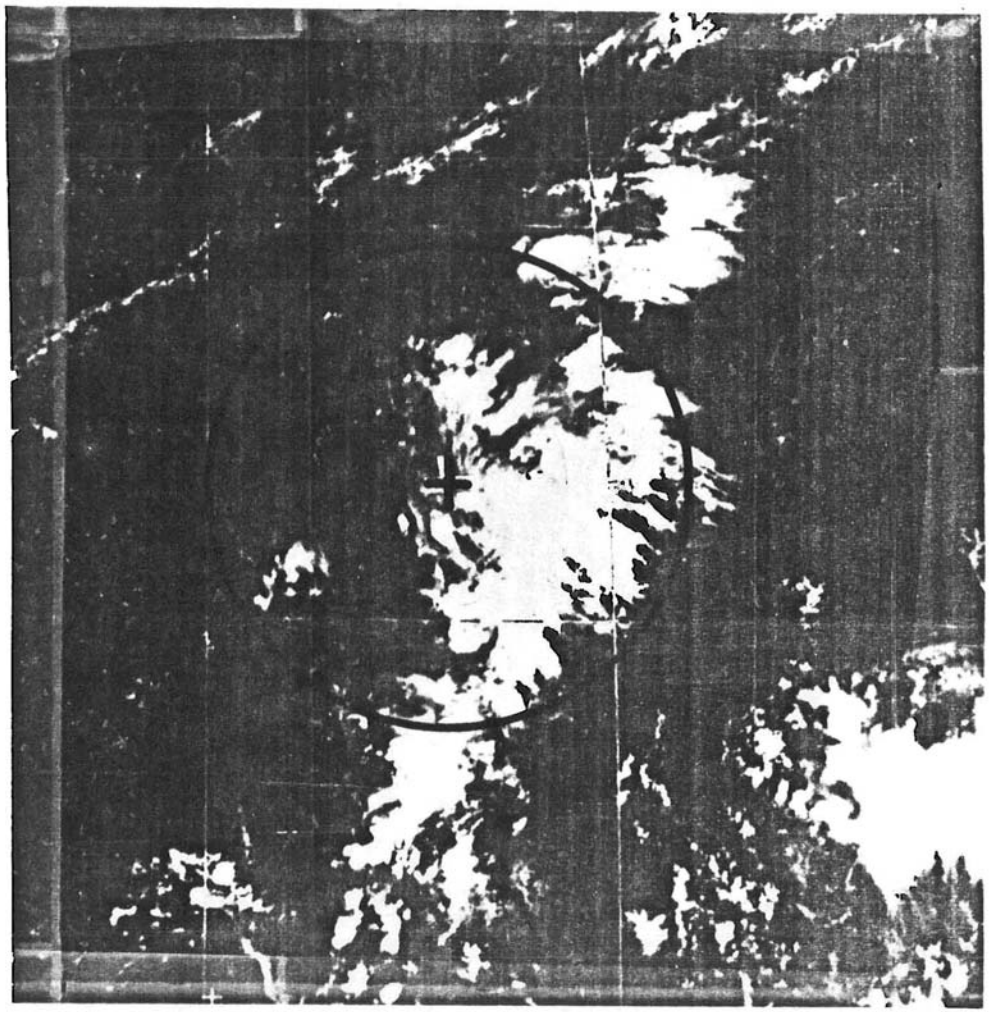

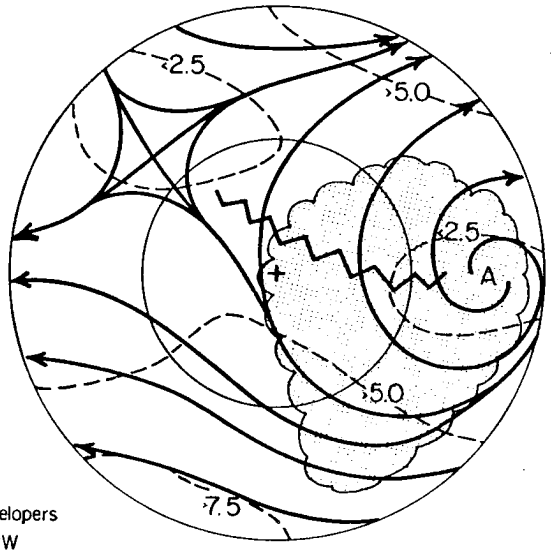

Early Developers
Center - NW
NAT System

Figure 4.11:a-b. Similar to Fig. 4.10a-b, except for TC20W (to become Typhoon Orchid 1983). The flow pattern is for centers located in the northwest region of the disturbance convection. As this system was moving NW at about 5 ms^{-1}, the 250 mb relative or MOT flow relative to the LLCC would be from the NW.

Weather Central (AFGWC), Offutt AFB, NE, greatly aided in making a number of necessary subjective decisions concerning the use of the DMSP data for this purpose.

DMSP visible imagery was obtained for the years 1977-1979, 1983 and 1984. 1980-1982 had limited or non-existent data due to satellite problems during that period. Image quality was best in 1983 and 1984.

Even in 1983 and 1984 the DMSP imagery was sometimes poor. Since the satellite orbits at a low altitude (approximately 850 km), the swath that it covers is approximately 2500 km wide (Fig. 4.12). This occasionally leaves disturbances cut in half or in the "terminator" area where there is a line at which point darkness ends and the brightness of the early morning sun begins. This often makes part of the picture unusable.

The combination of missing data and simultaneity problems between the reconnaissance time and the flight mission time reduced the over-200 images down to 19 good DMSP visual pictures for developing systems and 19 similar pictures for non-developing disturbances.

After selecting, matching and gridding the satellite imagery, analysis was carried out to detect and record the number of deep convective elements (cumulonimbus, or Cb tops) or Basic Convective Elements (BCE's) as defined by Arnold (1977). The BCEs are the primary components of the deep convection. They are also known as multi-cellular complexes or meso-convective elements. The area taken up by penetrative cells in the BCE's within 2° radius of the center was integrated and then compared to the area of BCE's or penetrative cells in the 2-4° surrounding ring.

It was determined that the best time to detect these convective cells was during the morning hours following sunrise. The shadows cast to the west of the "overshooting tops" provided easy identification of these elements, as shown in Fig. 4.13. Also, there was less cirrus "debris" and anvil cirrus surrounding the disturbance in the morning hours as compared with the evening hours.

An acetate overlay with 2° and 4° radius circles was used in the analysis. A simple count was made of the convective elements in each radial band for each of the 19 developing

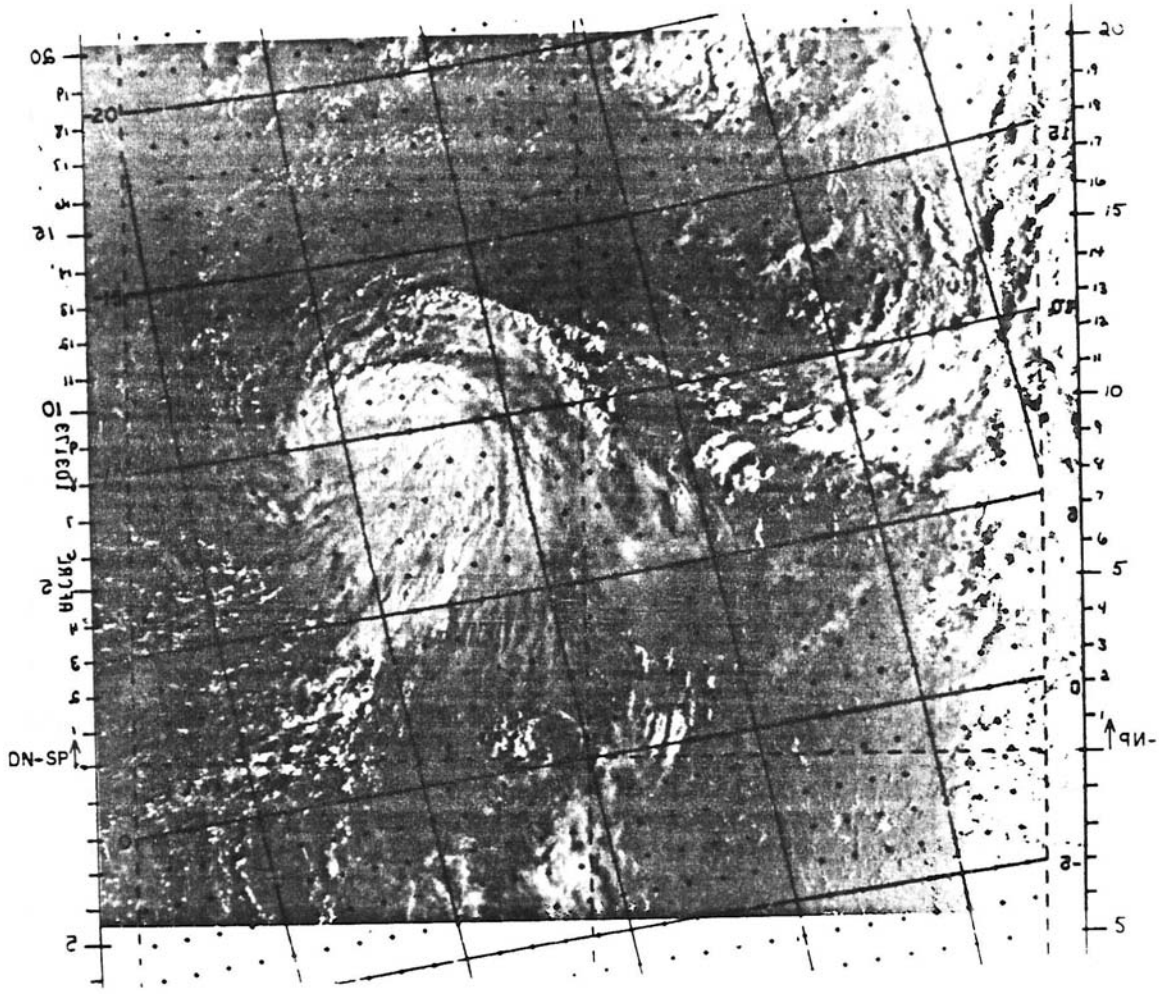

Figure 4.12: Example of a DMSP visible image (.6 km resolution at sub-point) with navigational grid overlay used to accurately locate the position of the disturbance relative to land features or ephemeris data.

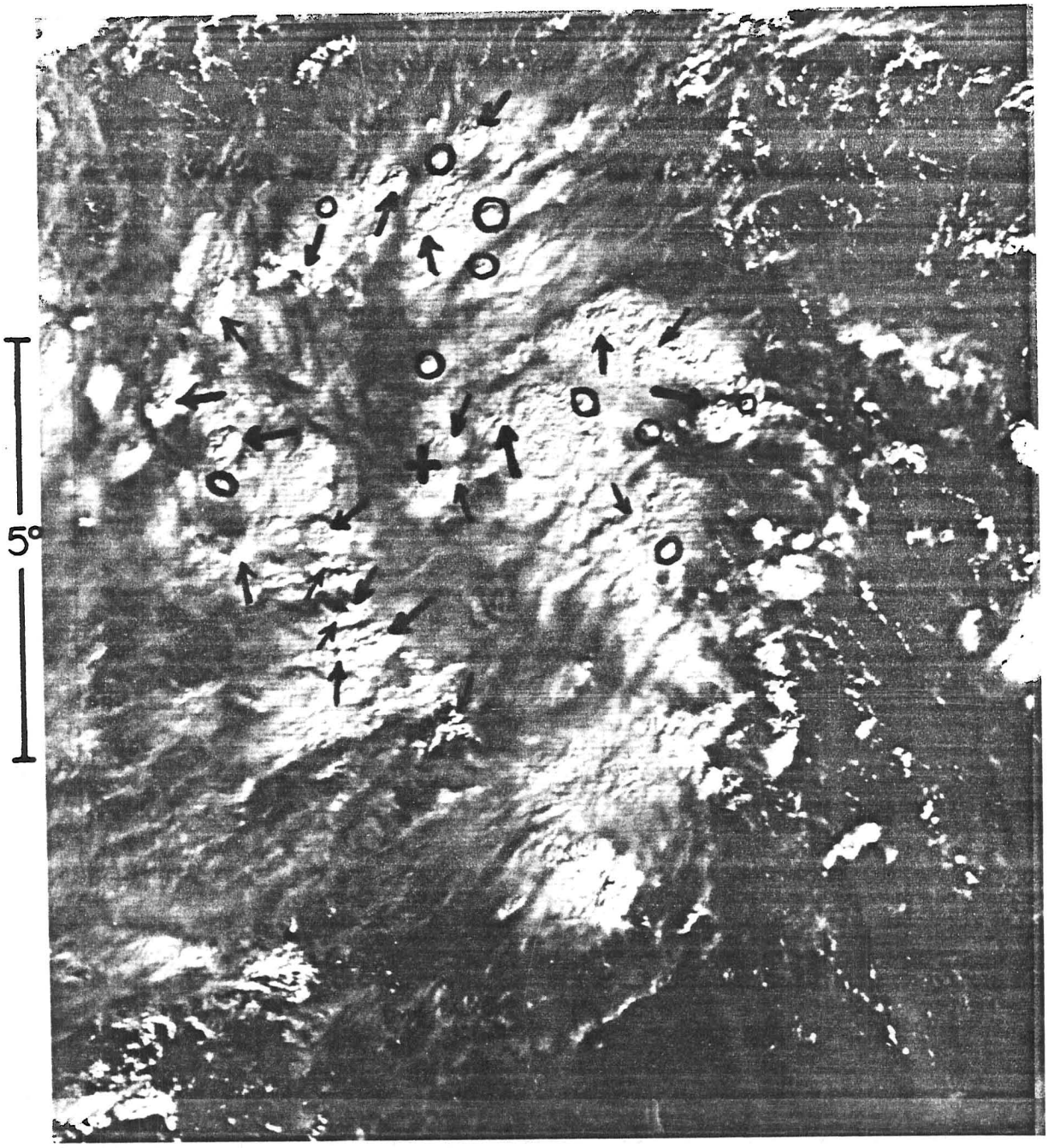

Figure 4.13: A DMSP visible image of a developing disturbance (TC24W —to become TS Thelma 1983). Arrows indicate multicell complexes (BCEs) and circles designate individual penetrative cells.

and non- developing systems. Figure 4.14 depicts the types of analyses that were made. Small circles represent individual or components of multiple deep convective cells.

4.5 D1 vs. NON-DEV Inner-Core Penetrative Differences

Concentration of inner-core convection, as evidenced by the convective burst, has been shown by Lee (1986) and others to be present frequently in early stage TC development. This brings up the question of how different are the amounts of inner-core deep convection relative to the centers of the LLCC of the early-stage developing (D1) and non- developing (NON-DEV) systems?

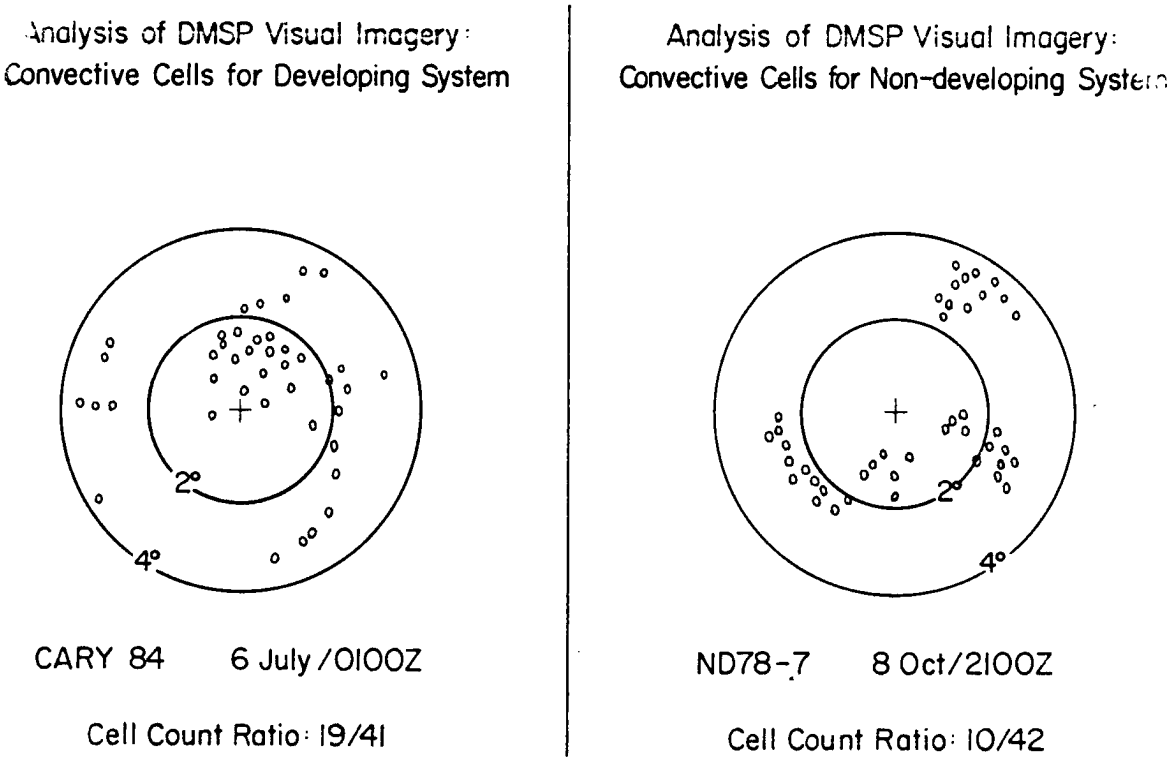

Figure 4.14: Typical cases of D1 and NON-DEV disturbances showing the amount of deep convective cells in the inner 0-2° and outer 2-4° annulus. The cell number ratio is for the 0-2° area (e.g., 19 in Cary 1984) divided by the total number of cells in the 0-4° area (e.g., 41 in Cary 1984).

Because it was necessary to select images that lacked obscuring cirrus, there was a definite bias toward early morning images rather than later morning or afternoon images. The diurnal influence here would be a generally greater upper-tropospheric divergence/lower-tropospheric convergence at 0000 GMT ($\sim$ 10 LT) time as compared

to 1200 GMT (~ 22 LT) for the northwest Pacific, as shown by Ruprecht and Gray (1976) and Gray and Jacobson (1977) in Fig. 4.15. This diurnal factor may influence the amount of convection in these disturbances. Cases were chosen so that this bias occurred for both developing and non-developing disturbances.

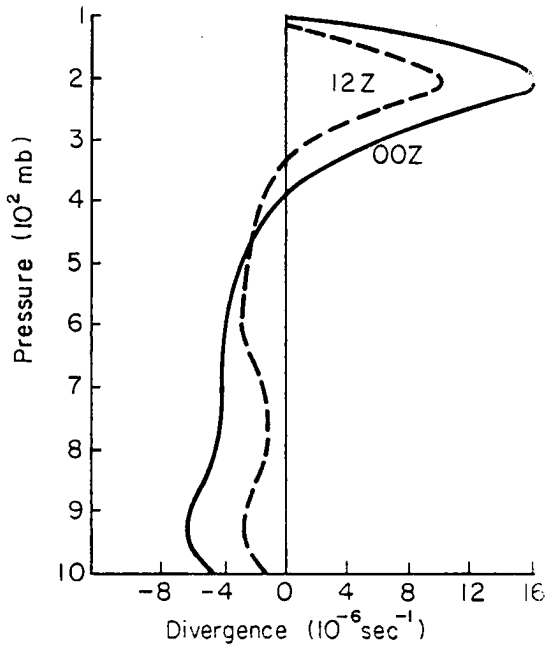

Figure 4.15: Evidence of diurnal character of diurnal variation in cloud cluster divergence. The nearly two-to-one differences are hypothesized to produce a significant modulation in cloudiness (from Gray and Jacobson, 1977). 00Z corresponds to about 09 to 10 Local Time.

Of the 19 cases of each classification (D1, NON-DEV) approximately one-third, or six of nineteen cases, were considered "late" in the day while the other two-thirds were considered "early" in the day. Early and late are defined here as before or after local noon time (approximately 03 GMT). The average time of the satellite image for the early classification was 2300 GMT (0800 LT). The average time for the late classification was 0500 GMT (1400 LT).

Individual cell counts for the inner 0-2° radius area were compared to the overall 0-4° radius. Table 4.3 shows a comparison of the mean areas of deep convection for the inner 0-2° radius circle and the 2-4° circular area which is three times greater in size. If the convection was presumed to be evenly distributed within the 4° radius circle, then one

would expect three times the amount of convection in the 2-4° annulus as compared to the 2° radius circle. The analysis, however, shows about the same amount of deep convection in the 0-4° area. The 19 NON-DEV systems showed about 17% more 0-4° deep convection than the 19 D1 cases. There was on average nearly twice the area of concentrated deep convection (.46 vs. .24) within the inner 2° radius of the developing systems.

Table 4.3: Ratio of mean areas of 0-2° radius deep convection to mean area of 0-4° radius deep convection for D1 and NON-DEV cases.

	Ratio of (0-2°) cell count to (0-4°) cell count	Total (0-4°) Area of Deep Convection
Early-Developing (19 cases)	.46	737
Non-Developing (19 cases)	.24	865

This calculation agrees with Arnold's (1977) research which concluded that there was a concentration of deep convection about the circulation center of the developing tropical disturbance. Arnold also noted a significant decrease in deep convection in the outer region (approximately 1.5°-4.0°) during the initial period of early-stage development. Non-developing systems typically lack this inner region deep convection concentration, but have ample amount of overall cloud cluster convection. This analysis agrees quite well with Arnold's results.

It is likely that some type of low-level wind surge action is responsible for these differences in inner-core concentration of deep convection.

Chapter 5

PRESENCE AND LIKELY ROLE OF LOW-LEVEL MOMENTUM SURGES

The higher values of mean radial inflow in the early-stage developing systems as compared to non-developing systems (as shown in Fig. 1.4) lead to the need for a more detailed investigation of the wind and pressure fields of the individual invest flights. If a mechanism is available to cause a higher radial inflow and a more concentrated deep convection within the LLCC where relative vorticity is already high (2-5 times the Coriolis parameter), one would anticipate the possibility of a more efficient conversion of latent heat to warming and more rapid vortex spin-up (Hack and Schubert, 1986). With the relative vorticity of the 1-2° diameter LLCC being substantially higher than the Coriolis parameter and the radius of deformation consequently much reduced over general tropical conditions, it is possible for the wind fields to begin to adjust to changes in the pressure field.

We now turn to an analysis of the invest flight individual case wind fields to see the degree to which they are able to detect concentrated packets of low-level wind surge which penetrate to near the disturbances' centers.

5.1 Calculations Performed Using the Gridded Aircraft Data Set

To detect and more objectively describe the low-level invest wind fields, each invest flight wind report was separated into radial wind (V_R), tangential wind (V_T), relative angular momentum (V_R x V_T) components which were specified relative to the LLCC centers and printed out in NATural (NAT) and MOTion (MOT) coordinates on the cylindrical grid as shown in Fig. 2.3. The pressure field was also specified on this grid. Each of

the two stratification files of D1 and NON-DEV were also averaged in order to have mean stratification values with which the individual invest mission cases could be compared. This allowed a sub-stratification for high wind surge vs. low wind surge. By comparing the belts and octants of each invest mission where strong radial inflow (large negative values of V_R) or strong surge (negative values of V_R x V_T) existed, a determination could be made as to whether each case was a "High" or a "Low" wind surge case.

Tables 5.1, 5.2 and 5.3 give typical examples of the tabular printout displays developed for this wind surge analysis. Table 5.1 displays the radial and tangential winds for, in this example, all early-stage developers. The calculations were performed in the MOT (storm relative) system for each octant (1 through 8) and for each of the eleven 0.25° radial belts. Means were calculated for each octant/belt as well as the mean for all observations in each radial belt. A tally was kept for the number of observations in each octant and belt for all wind reports. This is recorded in Table 5.2. Table 5.3 displayed the averages of the various lowest (mostly negative) values of V_R and V_R x V_T as well as the average of the highest values of V_T, etc.

5.2 Surge Definition and Stratification

As an example of surge definition, suppose a wind surge was defined by five observations or more which were taken between the second and fifth radial belts (radius 15-135 n mi or 28 to 250 km). The average of these five or more V_R, V_T and V_R x V_T values for this case were compared to the display of the average five lowest (or highest) V_R, V_R x V_T (or V_T) for all early-developers in the same 15-135 n mi belt. This allowed the stratification of the D1 and NON-DEV classes into high or low wind surge. Belt 1 (0-15 n mi) was not used for any calculations except the pressure average.

For example, the individual case display for developing disturbance, TC- 11, in 1983 is shown in Table 5.4. This disturbance developed into Supertyphoon Forrest. The six observations chosen to define the surge are circled. An attempt was made to define the wind surge as a cohesive unit of observations, not just isolated high values of -V_R x V_T. Average 15-135 n mi radius values of -V_R, V_T, and V_R x V_T (for 6 observations) for all

cases were respectively, 7 kts, 15 kts, and 43 kts^2. The key measurement in defining surge was the radial wind. In most instances, high values of -V_R correspond with high values of -V_R x V_T.

In comparison to these average values the -V_R for Forrest far exceeds the -V_R for all cases and the -V_R x V_T for Forrest slightly exceeded the -V_R x V_T for all D1 cases. From this analysis and comparison, Forrest was classified as a high surge case.

Detailed analysis was accomplished to determine the characteristics of the "Hi Surge/Developer", "Low Surge/Developer" as well as the high and low surge non-developing cases.

Plan view displays of each of the -V_R, V_T, -V_R x V_T, and pressure fields were then generated in order to perform a full analysis of this surge information.

5.3 Surge Analysis

The most notable difference between the D1 and NON-DEV systems was the greater magnitude of radial inflow penetration to inner radii for the developing systems. This greater inflow is evidence of special mesoscale momentum surges.

In the D1 class, the average regions where a surge existed and the typical pattern of the surge flow is shown in Fig. 5.1. The apparent spiral pattern was determined by calculating the octant/belt averages of highest frequency of high surge occurrence for each of the D1 and NON- DEV cases. As shown in Table 5.5, the average surges of the D1 cases covered a radial distance of about 4 belts or two degrees. The average surge moves through approximately three azimuthal octants. The average surge penetrates to 1.1° radius for the D1 cases and to only 1.8° radius for the NON-DEV cases.

It is not just the presence of the surge itself which is important but also the degree of inward penetration by the surge. Note that the surge penetration of D1 cases is one-half degree or more closer to the disturbance center than for the NON-DEV cases. Few non-developing systems had surge penetration inside of the third radial belt (45-75 n mi), while many D1 systems exhibited surge penetration to within the third radial belt. Surges are thus classified as "penetrative" if they extend inside 1.25° radius (approximately 140 km from the center). Table 5.6 summarizes these findings for penetrative surges.

Table 5.1: Example of the composite output for all early-stage developers (D1). Values shown here are for MOT radial and tangential winds winds (knots) for each of the 8 octants in each of the 11 belts. Avg. mean is defined as the average of the 8 octant means; mean is the average of all belt observations (belt total of observations in next to last row in each section indicated by arrow).

RADIAL WIND (KNOTS) (MOT)

	0-15	15-45	45-75	75-105	105-135	135-165	165-195	195-225	225-255	255-285	285-315	AVG MEAN	MEAN
1	5.	-1.	-4.	-5.	-9.	0.	-8.	-7.	-8.	1.	-15.	-5.	-5.
2	0.	-6.	-7.	-7.	-6.	-12.	-12.	-5.	-9.	-25.	******	-9.	-7.
3	-10.	-6.	-12.	-8.	-12.	-9.	-11.	-8.	-10.	-16.	-9.	-10.	-10.
4	-10.	-9.	-10.	-7.	-11.	-9.	-10.	-6.	-7.	******	******	-9.	-9.
5	-4.	-2.	-3.	-1.	-2.	0.	0.	4.	14.	3.	1.	1.	-1.
6	6.	5.	5.	1.	5.	3.	5.	5.	4.	11.	-4.	4.	4.
7	-1.	5.	7.	5.	8.	6.	4.	5.	2.	3.	3.	4.	5.
8	2.	2.	1.	2.	2.	-2.	-3.	-7.	-3.	-4.	-8.	-2.	0.
AVG MEAN													
	8	8	8	8	8	8	8	8	8	7	6		
	-2.	-2.	-3.	-3.	-3.	-3.	-4.	-2.	-2.	-4.	-5.		
MEAN													
	77	189	250	235	202	145	92	64	57	36	25		
	-5.	-2.	-3.	-2.	-3.	-2.	-3.	-2.	-3.	-4.	-7.		

TANGENTIAL WIND (KNOTS) (MOT)

	0-15	15-45	45-75	75-105	105-135	135-165	165-195	195-225	225-255	255-285	285-315	AVG MEAN	MEAN
1	6.	7.	8.	5.	5.	12.	11.	9.	12.	7.	10.	8.	8.
2	-4.	5.	9.	10.	12.	8.	4.	14.	7.	4.	******	7.	8.
3	3.	10.	10.	11.	13.	11.	11.	5.	6.	8.	10.	9.	9.
4	-2.	15.	14.	16.	13.	11.	17.	15.	16.	******	******	13.	14.
5	20.	16.	16.	17.	13.	11.	13.	13.	16.	16.	13.	15.	15.
6	9.	16.	13.	12.	13.	8.	11.	16.	9.	8.	12.	12.	13.
7	4.	11.	12.	11.	9.	8.	6.	11.	6.	4.	7.	8.	9.
8	-2.	9.	5.	6.	6.	11.	9.	11.	13.	-2.	8.	7.	7.
AVG MEAN													
	8	8	8	8	8	8	8	8	8	7	6		
	4.	11.	11.	11.	10.	10.	10.	12.	11.	7.	10.		
MEAN													
	77	189	250	235	202	145	92	64	57	36	25		
	3.	12.	11.	11.	10.	10.	9.	12.	9.	6.	8.		

Table 5.2: Similar to Table 5.1, except for $V_R x V_T$ (surge in knots^2) and pressure (mb). Counter for winds is a tally of aircraft observations in each octant.

VR * VT (KNOTS^2) (MGT)

	0-15	15-45	45-75	75-105	105-135	135-165	165-195	195-225	225-255	255-285	285-315	AVG MEAN	MEAN
1	111.	76.	-56.	-32.	-39.	19.	-82.	-46.	-64.	-1.	-153.	-24.	-21.
2	3.	-15.	-56.	-75.	-60.	-85.	-24.	-32.	-20.	-102.	******	-47.	-52.
3	-23.	-42.	-105.	-99.	-153.	-99.	-117.	-3.	-49.	-133.	-74.	-82.	-85.
4	23.	-139.	-172.	-88.	-113.	-82.	-169.	-100.	-90.	******	******	-103.	-123.
5	-91.	-40.	-21.	1.	-12.	-1.	38.	66.	210.	56.	14.	20.	-7.
6	54.	79.	60.	31.	42.	-10.	51.	43.	-1.	61.	-100.	28.	41.
7	33.	56.	76.	57.	73.	58.	5.	32.	11.	6.	-80.	30.	40.
8	-11.	29.	-15.	-7.	-36.	-106.	6.	-107.	-60.	11.	-59.	-32.	-25.
AVG MEAN													
	3	8	8	8	8	8	8	8	8	7	6		
	12.	0.	-36.	-26.	-27.	-39.	-37.	-19.	-8.	-15.	-75.		
MEAN													
	77	189	250	235	202	145	92	64	57	36	25		
	-5.	-5.	-37.	-24.	-40.	-32.	-29.	-12.	-16.	-19.	-76.		

COUNTER FOR WINDS

	0-15	15-45	45-75	75-105	105-135	135-165	165-195	195-225	225-255	255-285	285-315
1	5	19	34	32	30	20	11	6	5	6	2
2	7	23	33	26	29	16	5	6	4	2	0
3	42	15	31	29	31	18	11	6	8	7	2
4	1	33	31	30	17	17	8	7	4	0	0
5	4	26	25	30	14	19	5	5	2	3	2
6	2	30	29	22	29	19	12	7	8	3	3
7	10	23	31	39	21	27	26	19	19	10	11
8	6	20	36	27	31	16	14	8	7	5	5

PRESSURE (mb)

	0-15	15-45	45-75	75-105	105-135	135-165	165-195	195-225	225-255	255-285	285-315	AVG MEAN	MEAN
1	1006.	1006.	1006.	1007.	1007.	1007.	1007.	1008.	1008.	1007.	1006.	1007.	1007.
2	1005.	1006.	1006.	1006.	1006.	1006.	1006.	1007.	1007.	1008.	******	1006.	1006.
3	1005.	1007.	1007.	1007.	1007.	1007.	1005.	1007.	1006.	1006.	1007.	1006.	1006.
4	1005.	1006.	1006.	1007.	1007.	1007.	1008.	1007.	1009.	******	******	1007.	1006.
5	1006.	1005.	1007.	1006.	1008.	1007.	1007.	1007.	1003.	1005.	1011.	1007.	1006.
6	1005.	1006.	1006.	1007.	1007.	1007.	1006.	1009.	1007.	1006.	1008.	1007.	1007.
7	1004.	1007.	1007.	1007.	1007.	1007.	1009.	1008.	1009.	1009.	1009.	1008.	1008.
8	1005.	1006.	1007.	1006.	1006.	1006.	1009.	1009.	1009.	1009.	1007.	1007.	1007.
AVG MEAN													
	8	8	8	8	8	8	8	8	8	7	6		
	1005.	1006.	1006.	1007.	1007.	1007.	1007.	1008.	1007.	1007.	1006.		
MEAN													
	72	162	216	198	168	128	76	51	46	30	21		
	1005.	1006.	1006.	1006.	1007.	1007.	1007.	1008.	1007.	1007.	1004.		

Table 5.3: Tabular display of strongest (most negative) V_R and $V_R x V_T$ and strongest (most positive) V_T values. The average of the maximum 1 through 8 occurrences of the values in individual cases and in the composite sense were compared to help stratify surge cases.

TOTAL VR CASES FOR EARLY DEVELOPERS.

	15-45	45-75	15-135	135-225	15-255
AVG LOWEST 1:	-7.	-9.	-16.	-10.	-17.
AVG LOWEST 2:	-5.	-7.	-13.	-7.	-15.
AVG LOWEST 3:	-3.	-6.	-11.	-5.	-13.
AVG LOWEST 4:	-3.	-5.	-9.	-5.	-12.
AVG LOWEST 5:	-4.	-3.	-8.	-4.	-11.
AVG LOWEST 6:	-5.	-2.	-7.	-4.	-10.
AVG LOWEST 7:	-4.	****	-7.	-8.	-8.
AVG LOWEST 8:	****	****	-6.	-5.	-7.
AVG ALL VRS:	-1.	-3.	-2.	-2.	-2.
NUMBER OF OBS:	173	220	756	310	1066

TOTAL VT CASES FOR EARLY DEVELOPERS.

	15-45	45-75	15-135	135-225	15-255
AVG HIGHEST 1:	16.	16.	22.	15.	23.
AVG HIGHEST 2:	15.	13.	20.	14.	21.
AVG HIGHEST 3:	14.	14.	18.	14.	19.
AVG HIGHEST 4:	11.	12.	17.	12.	19.
AVG HIGHEST 5:	13.	11.	16.	11.	18.
AVG HIGHEST 6:	8.	10.	15.	11.	16.
AVG HIGHEST 7:	9.	****	15.	11.	15.
AVG HIGHEST 8:	****	****	14.	10.	15.
AVG ALL VTS:	12.	11.	11.	10.	14.
NUMBER OF OBS:	173	220	756	310	1066

TOTAL VRVT CASES FOR EARLY DEVELOPERS.

	15-45	45-75	15-135	135-225	15-255
AVG LOWEST 1:	-95.	-127.	-227.	-118.	-259.
AVG LOWEST 2:	-43.	-93.	-182.	-83.	-217.
AVG LOWEST 3:	-26.	-92.	-150.	-67.	-180.
AVG LOWEST 4:	-37.	-75.	-127.	-62.	-159.
AVG LOWEST 5:	-45.	-50.	-107.	-53.	-137.
AVG LOWEST 6:	-64.	9.	-93.	-52.	-121.
AVG LOWEST 7:	-18.	******	-86.	-120.	-105.
AVG LOWEST 8:	******	******	-74.	-115.	-93.
AVG ALL VRVTS:	0.	-39.	-27.	-30.	-28.
NUMBER OF OBS:	173	220	756	310	1066

Table 5.4: Partial display of individual case printout (like Tables 5.1 and 5.2) for a developing disturbance (to become STY Forrest). The circled values are those values analyzed that define a wind surge in this disturbance. The averages of these values were compared to the average D1 case in order to classify this disturbance as a high or low surge case.

STORM: FORREST NO: 11 YR: 83 MIS: 2 EARLY DEVELOPERS

RADIAL WIND (KNOTS) (MOT)

	0-15	15-45	45-75	75-105	105-135	135-165
1	******	******	******	******	******	******
2	0.	******	-12.	-4.	******	10.
3	******	******	-16.	-17.	-17.	-26.
4	******	-19.	******	******	-29.	******
5	******	******	******	******	******	******
6	******	15.	******	******	******	******
7	******	7.	******	34.	******	19.
8	******	******	******	******	******	******

TANGENTIAL WIND (KNOTS) (MOT)

	0-15	15-45	45-75	75-105	105-135	135-165
1	******	******	******	******	******	******
2	-35.	******	12.	7.	******	13.
3	******	******	1.	3.	9.	1.
4	******	4.	******	******	5.	******
5	******	******	******	******	******	******
6	******	23.	******	******	******	******
7	******	21.	******	17.	******	11.
8	******	******	******	******	******	******

RAD WIND * TANG WIND (KNOTS**2) (MOT)

	0-15	15-45	45-75	75-105	105-135	135-165
1	******	******	******	******	******	******
2	0.	******	-145.	-26.	******	123.
3	******	******	-8.	-49.	-166.	-39.
4	******	-81.	******	******	-134.	******
5	******	******	******	******	******	******
6	******	340.	******	******	******	******
7	******	139.	******	591.	******	189.
8	******	******	******	******	******	******

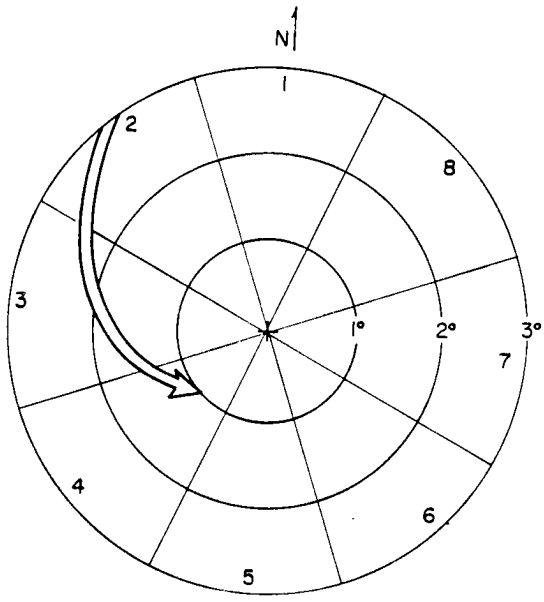

Figure 5.1: Schematic portrayal of mean location of occurrence of the typical surge in the developing disturbances. The spiral nature of the pattern was determined through analysis of 52 (D1) different surges associated with early-stage cyclone development.

Table 5.5: Average surge dimensions and average number of octants and belts in which the surge is located.

	No. of Octants	No. of Belts	Mean Radial Penetration of Surge
Developing (D1)	3.2 (octants 2 to 5)	3.6 (belts 2 to 5)	to 1.1° radius
Non-developing (NON-DEV)	2.7 (octants 2 to 4)	3.5 (belts 3 to 6)	to 1.8° radius

Table 5.6: Number of wind surge cases and percentage of surges which are classified as high surge, penetrative, or weak. MOT coordinate.

	High Surge	High and Penetrative	Weak Surge
Early Developers D1 (52 Cases)	35, (67%) of total D1 cases	27 (52%)	17 (33%)
Non-developers NON-DEV(49 Cases)	19 (39%) of total NON-DEV Cases	9 (18%)	30 (61%)

Differences in D1 vs. NON-DEV surge should not be surprising given the nearly two-to-one difference in inner-core radial wind between developing and non-developing systems as shown in Fig. 1.4. D1 vs. NON-DEV radial wind differences are strongest in the west and southwest portions of the disturbance. Figure 5.2 shows a plan view plot of mean high surge values for both D1 and NON-DEV stratifications. Higher values of radial wind are in octant 4. Greater inner-radial penetration occurs with the early-stage developers. Another important factor is the stronger low-level relative flow across the non-developing cases. The overall area of positive V_R (outward flow) on the east side of the disturbance is greater than 5 ms^{-1} for the NON-DEV cases. This is more than twice the outflow of the average D1 cases. Zehr (1976) also found tropical disturbance ventilation in non-developing systems to be highest in the lower and middle troposphere in agreement with these results.

Some examples of the strong inward radial winds which can exist with these asymmetric wind surges are shown in Table 5.7. These are twenty of the most prominent surge cases available in the D1 data set. They help to better identify and portray this phenomenon.

Column two of this Table gives the maximum radial inflow (in ms^{-1}) exhibited by one observation for each disturbance. Most values occurred within 135 n mi ($\sim 2.25°$ radius) of the disturbance center. The next column gives the mean V_R for the entire 15-135 n

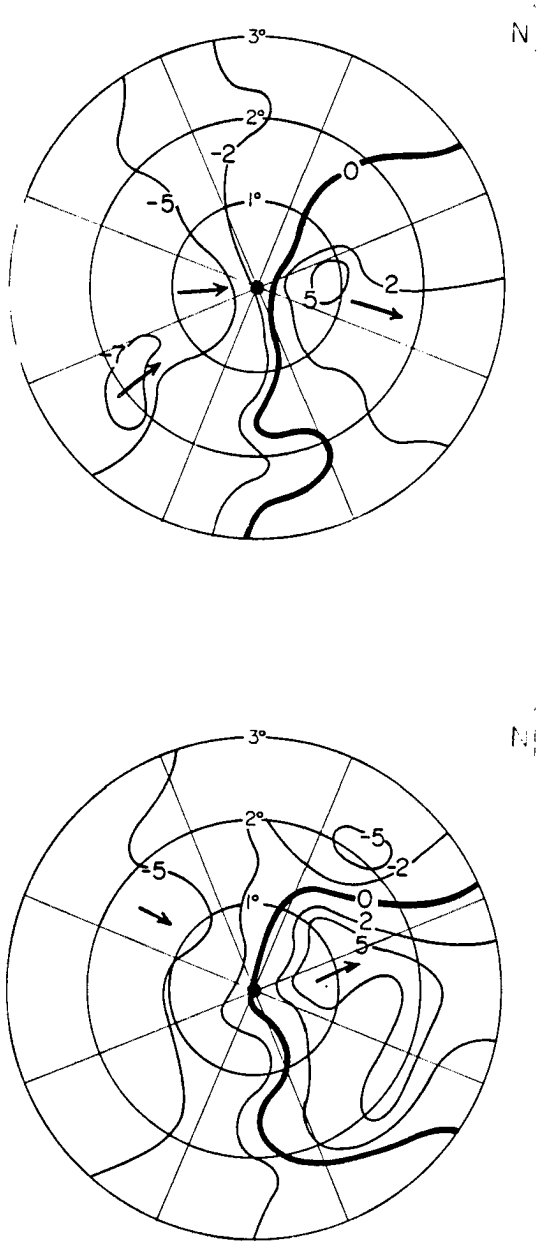

Figure 5.2: Composite radial wind (ms^{-1}) for 52 high surge cases in developing systems (D1) in the MOT system (top diagram) vs. 49 high surge events in NON-DEV cases (bottom diagram).

Table 5.7: Radial inflow (in relative or MOT coordinate) for 20 of the highest surge cases of the developing systems. Value in ms^{-1}.

Name/Year/Mission	Maximum Radial Wind (V_R)	Mean V_R (~15-135 n mi)	No. of Obs. Defining Mean V_R Value with 15-135 n mi.
1. Dom 80-3	-7	-4	4
2. Joe 80-1	-11	-8	5
3. Joe 80-2	-8	-6	9
4. Alex 81-1	-11	-5	5
5. Lynn 81-1	-17	-12	4
6. Agnes 81-1	-17	-10	5
7. Pat 82-3	-15	-7	7
8. Owen 82-1	-10	-8	4
9. Vera 83-1	-12	-7	4
10. Vera 83-2	-13	-10	5
11. Wayne 83-1	-11	-6	9
12. Abby 83-1	-6	-4	6
13. Abby 83-1	-8	-7	7
14. Forrest 83-2	-15	-10	6
15. Forrest 83-3	-11	-7	10
16. Lex 83-2	-9	-7	6
17. Marge 83-1	-8	-5	8
18. Sperry 83-1	-11	-6	7
19. Cary 84-1	-6	-5	6
20. Freda 84-2	-20	-11	8

mi surge. The number of observations that made up the average surge is given in the last column. These multiple observation averages show that it is not just one extremely high radial wind value which is responsible for the surge, but that the surge is composed of a number of associated inflow values. Surge appears to be made up of a "packet" of high inflow momentum. Such individual surge information allows for the classification of individual case "strong" or "weak" surge events.

Figure 5.3 compares the relative magnitudes of the (-V_R x V_T) surge for high surge cases of both D1 and NON-DEV. The magnitude of the surge is obviously less for the NON-DEV class as shown in the bottom diagram. The top diagram of this figure shows a maximum of -125 m^2/s^2 that occurs near one degree radius, while the -100 m^2/s^2

maximum in the NON-DEV class appears at a greater radius of 2°. On a larger scale, the -50 m^2/s^2 area of the D1 systems covers nearly twice the area covered by the NON-DEV systems. These measurements show more overall surge action in the D1 than the NON-DEV classes. This is the optimum situation for inward penetrating surges.

The difference in the surge action between D1 and NON-DEV cases results primarily from the magnitude of penetrative radial inflow. The tangential wind fields for both cases are quite similar, especially in the western portions of the disturbance where the surge action is most prevalent (Fig. 5.4). The developing or D1 case V_T wind field shows a generally stronger tangential wind at a large radius and a slightly more symmetric wind pattern than the NON-DEV cases.

Surges depend primarily on the strength of the radial wind, rather than the tangential wind. Table 5.8 shows how 44 surge cases of D1 systems and 42 surge cases of NON-DEV systems were broken down by dominant -V_R or V_T surge component. As shown in this table the D1 cases displayed a clear dominance for -V_R over V_T in the high surge cases. V_R is the major contributor to the surge. In the NON-DEV cases it is not as clear but there was also evidence of - V_R dominance in the high surge cases. The low surge cases in both D1 and NON-DEV showed an equal or greater contribution by the V_T wind toward total surge strength. A dominant surge component could not be chosen in some surge cases which had both average V_R and V_T values. This situation eliminated eight D1 cases and seven NON-DEV cases.

For D1 and NON-DEV cases of low surge, similar diagrams have also been prepared. Figure 5.5 shows D1 class low surge cases (top diagram) having higher surge values over a larger area compared to low surge NON- DEV systems (bottom diagram), but most inflow occurs at a radius greater than 2-3°. Figure 5.6 shows that low surge classes are of similar magnitude (maximum of about -50 m^2/s^2) but developers (top) have their surge closer to the center. The radial outflow for the NON-DEV systems on the east side was concentrated near the inner core as in the high surge NON-DEV cases. Figure 5.7 shows that the V_T fields for the low surge cases differ between D1 and NON-DEV only slightly.

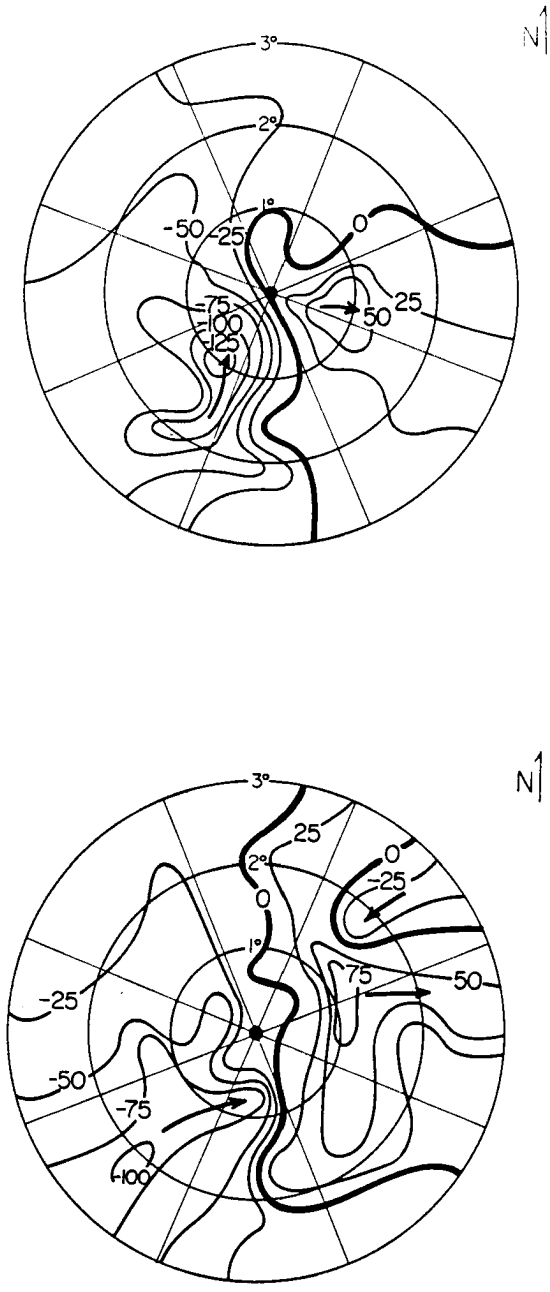

Figure 5.3: Composite relative angular momentum import (V_R x V_T) for 52 high surge in D1 cases in the MOT system (top diagram) vs. 49 high surge NON-DEV cases (bottom diagram) (units $m^2 s^{-2}$).

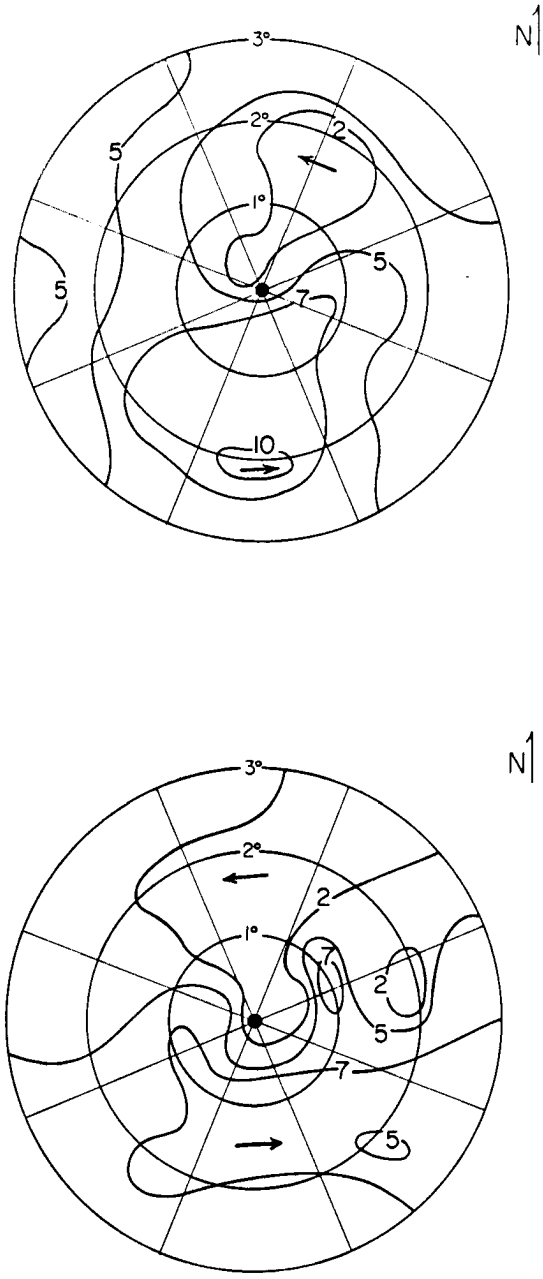

Figure 5.4: Composite tangential wind (ms^{-1}) for 52 high surge D1 (top diagram) cases in MOT system vs. 49 high surge NON-DEV cases (bottom diagram).

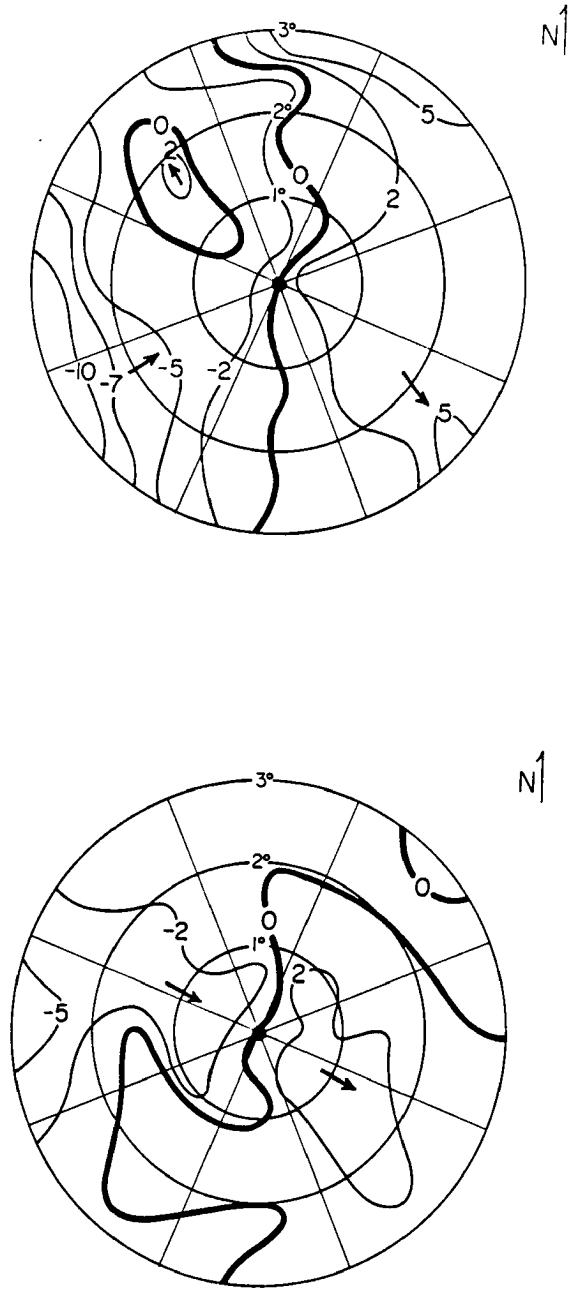

Figure 5.5: Comparison of V_R (ms^{-1} for MOT system) in low surge cases for D1 (top diagram) vs. NON-DEV (bottom diagram).

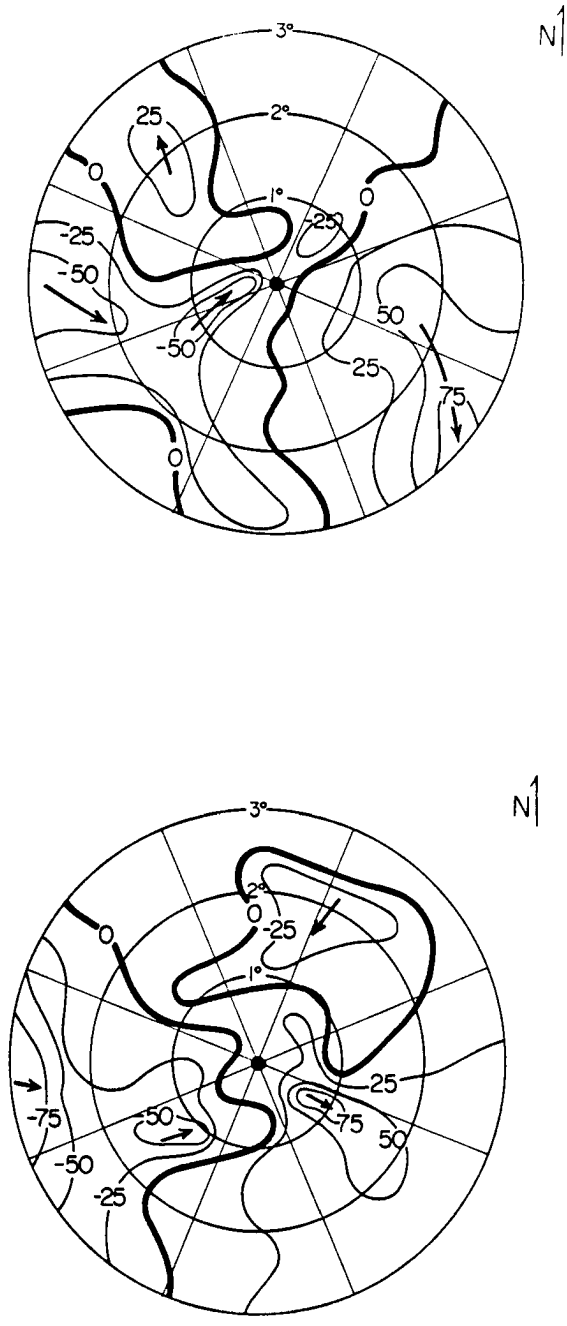

Figure 5.6: Same as Fig. 5.5, except for V_R x V_T (in m^2s^{-2} for MOT system) in low surge cases.

Table 5.8: Number of surge cases where V_R or V_T is the dominant surge component. Column (1) denotes total D1 and NON-DEV surge cases, Column (2) denotes D1 or NON-DEV cases with high surge, and Column (3) denotes D1 and NON-DEV cases with low surge. For example, in 29 of 44 surge cases of D1 disturbances $-V_R$ exceeded the mean V_R value by a greater percentage than the individual case V_T exceeded the mean V_T.

(1) ALL EARLY DEVELOPERS 44 CASES		(2) EARLY DEVELOPERS WITH HIGH SURGE 32 CASES		(3) EARLY DEVELOPERS WITH LOW SURGE 12 CASES	
$-V_R$ dominant	V_T dominant	$-V_R$ dominant	V_T dominant	$-V_R$ dominant	V_T dominant
29	15	23	9	6	6
ALL NON-DEVELOPERS 42 CASES		NON-DEVELOPERS WITH HIGH SURGE 19 CASES		NON-DEVELOPERS WITH LOW SURGE 23 CASES	
$-V_R$ dominant	V_T dominant	$-V_R$ dominant	V_T dominant	$-V_R$ dominant	V_T dominant
23	19	14	5	9	14

Even though surge values are substantially lower in a number of the low surge developing cases, the degree of penetration of the radial winds and surge action is still greater for the developing than the non- developing systems.

Surge Pressure Gradients. An analysis of the radial gradient of pressure associated with the twenty highest surge cases of Table 5.7 show very weak inward pressure gradients. If pressure gradient was responsible for these high radial wind surge values, it should be detectable in these cases. The average pressure for the inner three radial belts (0-1.25°) was subtracted from the pressure in belts four through six (1.25°-2.75°). Belt averaging assured better accuracy. The resulting difference in surface pressure was:

- (Outer Belts (4-6°) pressure = 1007.7)
- (Inner Belts (1-3°) pressure = 1006.6), Difference 1.1 mb.

This is a very small inner to outer pressure difference. Individual cases also showed very small inner vs. outer-core pressure differences.

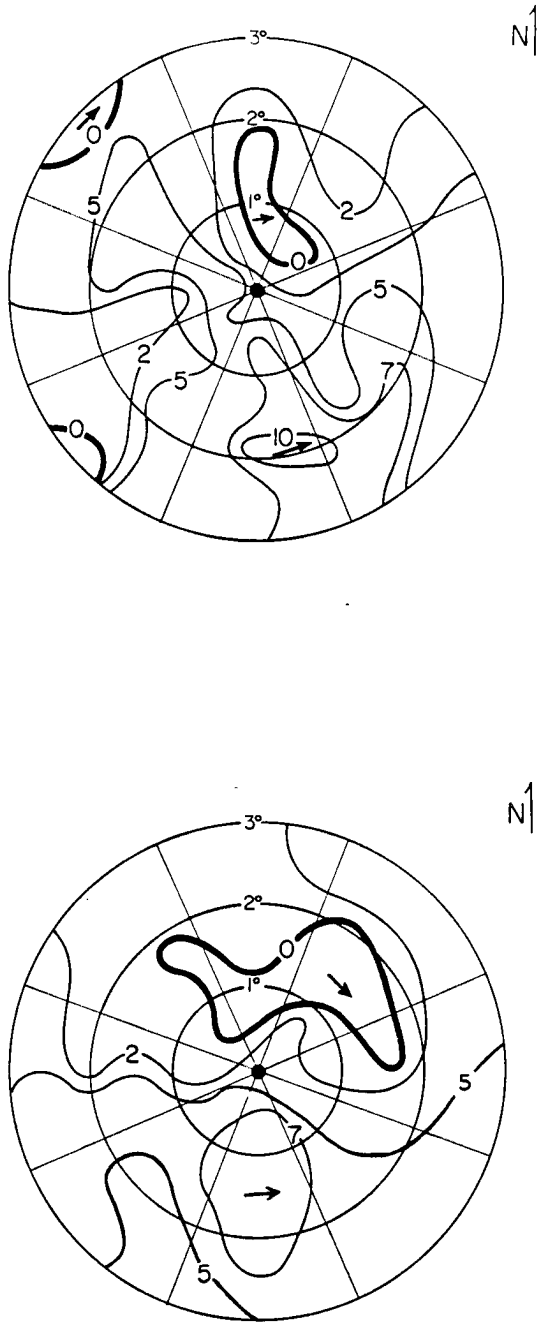

Figure 5.7: Same as Fig. 5.5 and Fig. 5.6, except for tangential wind (V_T) fields (in ms^{-1}) in low surge cases.

These results should discourage any ideas that the wind is being drawn into the LLCC through pressure acceleration. The evidence of this research points to the surge winds being driven towards the LLCC by some type of outside environmental momentum-forcing mechanism. The wind surge appears to be channeled into packets of momentum by the disturbance's surrounding environmental wind. It appears to be driven rather than being pulled toward the disturbance's inner core.

5.4 Case Analysis—Vera 1983

To show a representative surge case of the aforementioned parameters of -V_R, V_T, V_R x V_T and pressure, a typical early-stage developer was chosen. Vera was flown by reconnaissance for two missions prior to being upgraded to tropical storm status. The second mission depicted here, in Fig. 5.8a-d is in the early stages of formation of this sytem.

Figure 5.8a depicts very strong radial inflow in the typical regions that other high surge cases experience strong -V_R. The flow through the system is slightly greater than normally shown in high surge developers. Figure 5.8b depicts an inner-core maximum in V_T. The strength of the V_T within one degree radius is another indication of a strong vortex. The V_R x V_T field (Fig. 5.8c) is exceptional in its magnitude and consistent with the mean of the high surge cases in its area of occurrence. The relatively weak inner-core pressure gradient field (Fig. 5.8d) is to be noted.

5.5 Effect of the Surge on Convective Patterns

The effect of the inward momentum of the surge is to bring about increased vertical motion as low-level mass accumulates near the inner vortex center. This vertical motion generates enhanced deep convection. This can result in a convective burst as is often detected when wind surge reaches the vicinity of a disturbance system (Lee, 1986). The surges Lee (op. cit.) referred to were on a larger scale than those detected here. It is possible that there is a connection between these two size scales of surge.

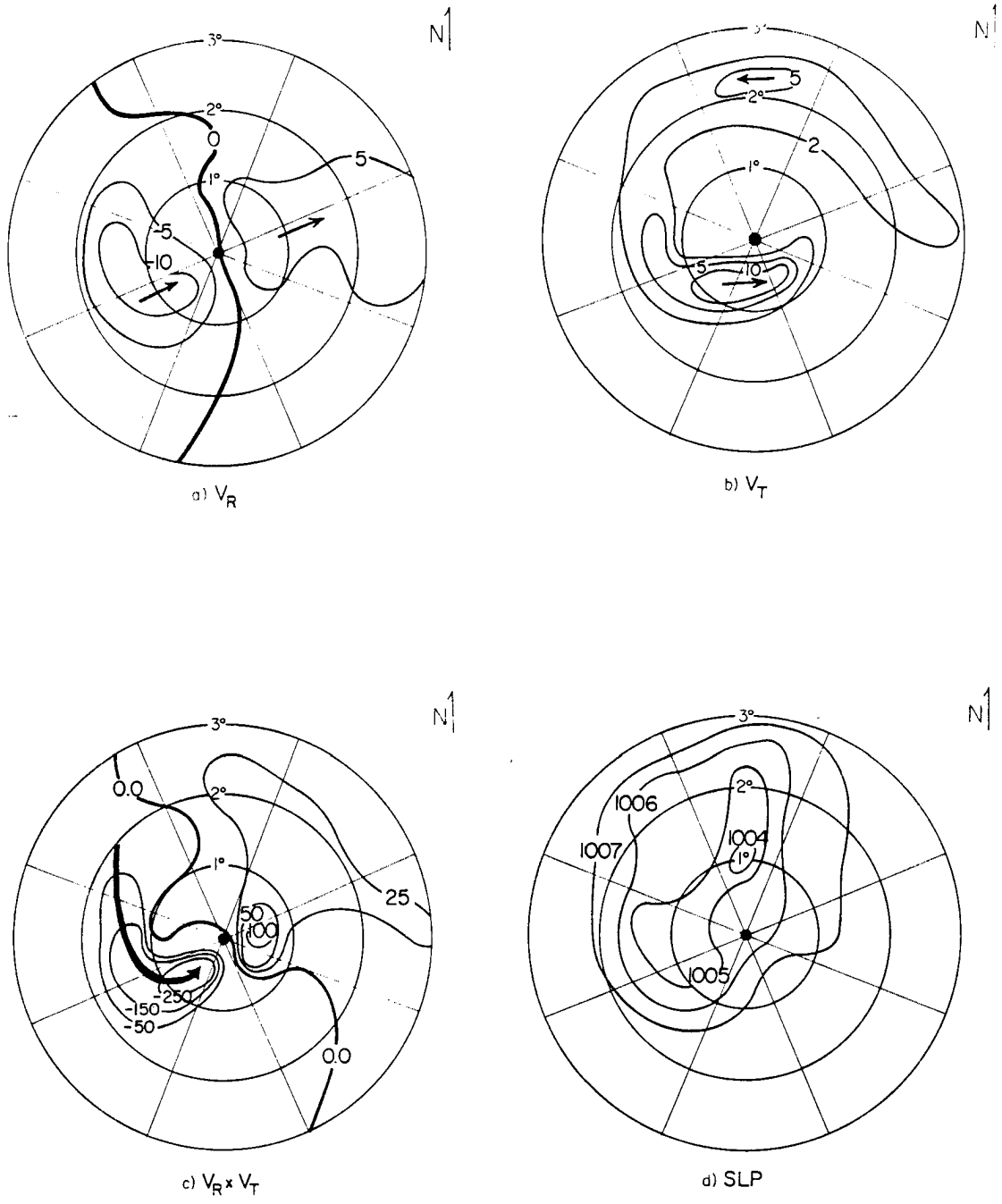

Figure 5.8: An example of an invest flight observed high surge (D1) case for a tropical disturbance ($V_{max} \sim 15\ ms^{-1}$, MSLP $\sim$ 1004 mb) which later became Typhoon Vera. Data portrayed in MOT coordinate system. Units ms^{-1} or m^2s^{-2}.

Surge-induced deep convection may be in evidence on the high resolution DMSP images. Figure 5.9 shows three examples.

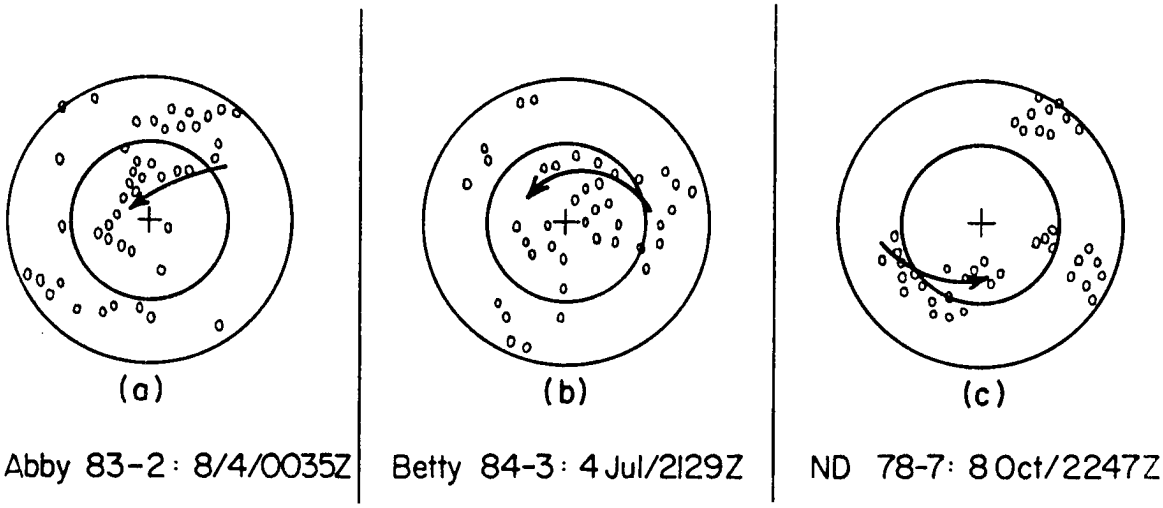

Figure 5.9: a-c. Relationship of aircraft determined wind surge (arrow) to penetrative convective cells (small circles) for 3 disturbances with $V_{max} < 15\ ms^{-1}$. Two of these disturbances developed into typhoon (Abby) and tropical storm (Betty) intensity. ND78-7 did not develop into a named storm.

Examples a) and b) are for early-stage developing cases prior to becoming named storms while c) is for a non-developing system.

The surges for the D1 cases appear to be aligned or surrounded by enhanced convection. Although this may be a chance alignment, the possibilities for surge detection from satellites appear to show some promise. The occurrence of high surge in the non-developing case relates well to the convective pattern. But, as was shown previously, the surge and enhanced convection fail to concentrate in this non-developing case, suggesting the reason for the lack of development.

5.6 Inner-Core Surge in Relation to Environmental Wind Field

The bridging of momentum packets of the environmental flow to near the disturbance center which we denote as surge has been extensively discussed by (Lee, 1986) from synoptic-scale data. Following Lee the author has chosen to investigate this relationship using ECMWF tropical belt 850 mb flow analysis.

An attempt was made to use the Darwin surface and 850 mb charts but lack of consistent low-level data around these disturbance systems precluded their use. Instead the ECMWF objective analyses for a number of cases were studied at the 1200 GMT period. One D1 case and one NON-DEV case were chosen. The attempt here is to try to demonstrate the possibility that these momentum surges to inner radii may originate and may at times be observationally traced to the surrounding environmental flow.

- Case 1—1st Period: Vera 1983—position from ATCR; 2.5 days prior to tropical storm strength (7/10/83), $V_{max} \sim 10\ ms^{-1}$—see Fig. 5.10a.

Important points to note are the maximum in the trade winds ($> 10ms^{-1}$) and occurrence of the cold outbreak near Australia of which Love (1985a,b) has indicated is frequently an important factor. This cold front appeared to strengthen the Southern Hemisphere trades.

- Case 1—2nd Period: Vera 1983—invest mission 1; derived low-level center; 1.5 days prior to tropical storm strength (7/11/83), $V_{max} \sim 12\ ms^{-1}$, MSLP $\sim$ 1009 mb—see Fig. 5.10b.

Increased gradient near equator doubled the strength of the Southern Hemisphere trades and a cross-equatorial flow was initiated. Analysis of aircraft data indicated high surge near two degrees radius in southwest portion of disturbance.

- Case 1—3rd Period: Vera 1983—invest mission 2; LLCC fixed by ARWO; 0.5 days prior to tropical storm strength (7/12/83), $V_{max} \sim 15\ ms^{-1}$, MSLP $\sim$ 1003 mb—see Fig. 5.10c.

Low-level center aligned with region of northward progressing cross- equatorial flow. High surge values were evident within one degree of the center in the southwest portion of the developing depression.

Both invest missions flown into Vera indicated high surge values. The initial outer vortex circulation was only moderate (8-10 ms^{-1}) at best. Vera's high surge values appear

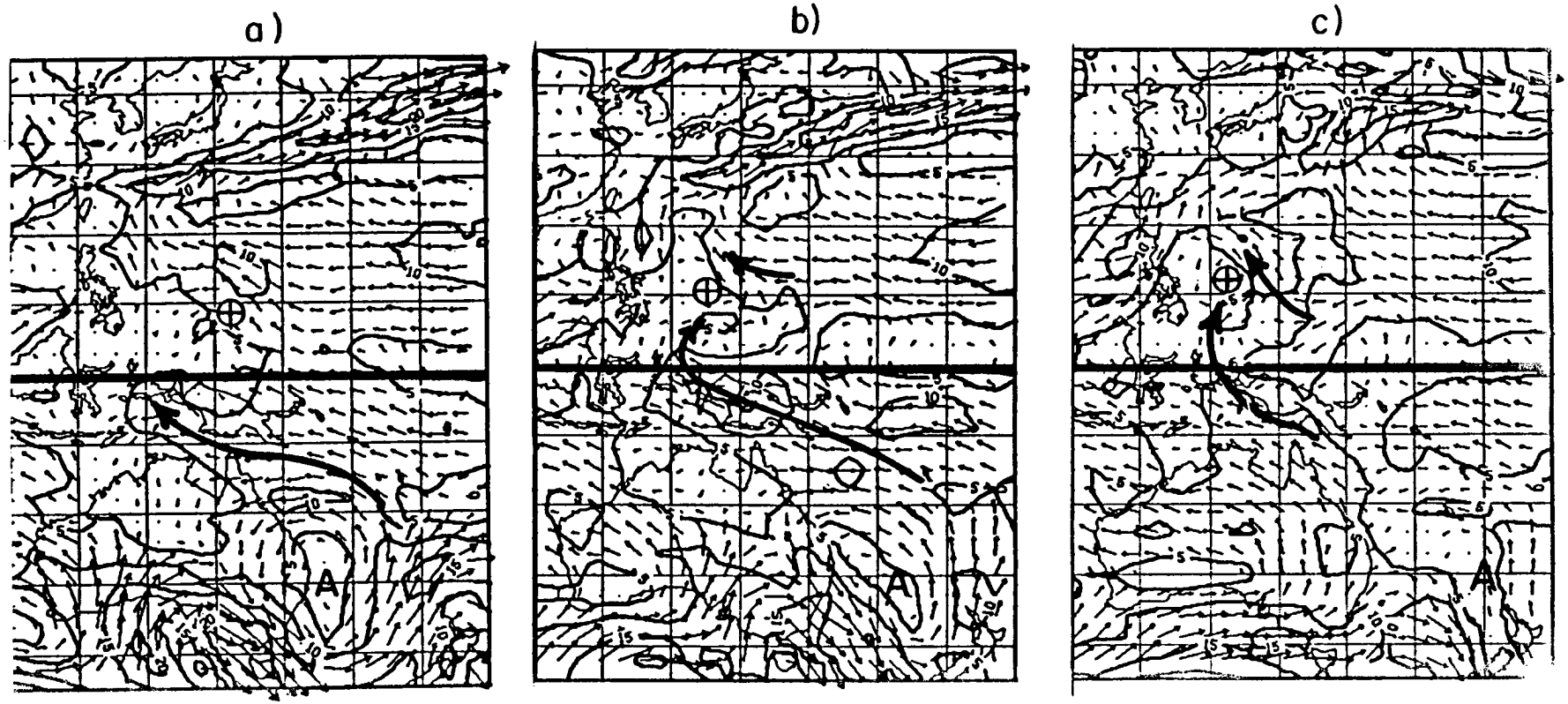

Figure 5.10:a-c. Three 850 mb analyses of successive 24-hour periods for a developing disturbance which became Typhoon Vera, 1983. a) 10 July 1983 ($V_{max} \sim 10ms^{-1}$) - 850 mb flow, 2.5 days prior to named-storm development. Low-level position ⊗ from ATCR, 1983. b) 11 July 1983 (($V_{max} \sim 12ms^{-1}$, MSLP$\sim$ 1009 mb) first invest flight into disturbance indicates high surge values. Center derived from surrounding data. c) 12 July 1983 ($V_{max} \sim 15ms^{-1}$, MSLP 1003 mb)— second invest mission fixed a low-level center and detected high surge values.

to be more likely a combination of the converging Northern Hemisphere trade and cross-equatorial flow components.

- Case 2—1st Period: Non-developer 82-7; mission 1, derived LLCC position from aircraft data (9/14/82); $V_{max} \sim 10\ ms^{-1}$, MSLP $\sim$ 1006 mb—see Fig. 5.11a.

Broad-scale trough with strong surrounding flow. Appeared to be a cold outbreak in Southern Hemisphere but lacked cross-equatorial flow. High surge from aircraft data detected at outer radii was due primarily to tangential rather than radial wind. No penetration of surge to the inner region was evident.

- Case 2—2nd Period: ND 82-7; mission 2, aircraft fix position (9/15/82); $V_{max} \sim 10\ ms^{-1}$, MSLP $\sim$ 1002 mb—see Fig. 5.11b.

Some indications of broad-scale (10° diameter) vortex developing but flow near LLCC dominated by tangential wind on both sides. No noticeable approach of cross-equatorial maximum. Aircraft data indicated low surge with radial flow away from LLCC on south side.

Summary. When compared to the previous development examples of D1 cases, the apparent differences in the non-formation cases were: 1) the lack of low-level penetrative inflow in the direction near the disturbance's LLCC, and 2) a generally broader and stronger tangential wind. The first difference may coincide with the lack of radial inflow for the NON-DEV system. The second difference may create excessive inertial stability, thereby providing resistance to radial displacements (Schubert and Hack, 1982).

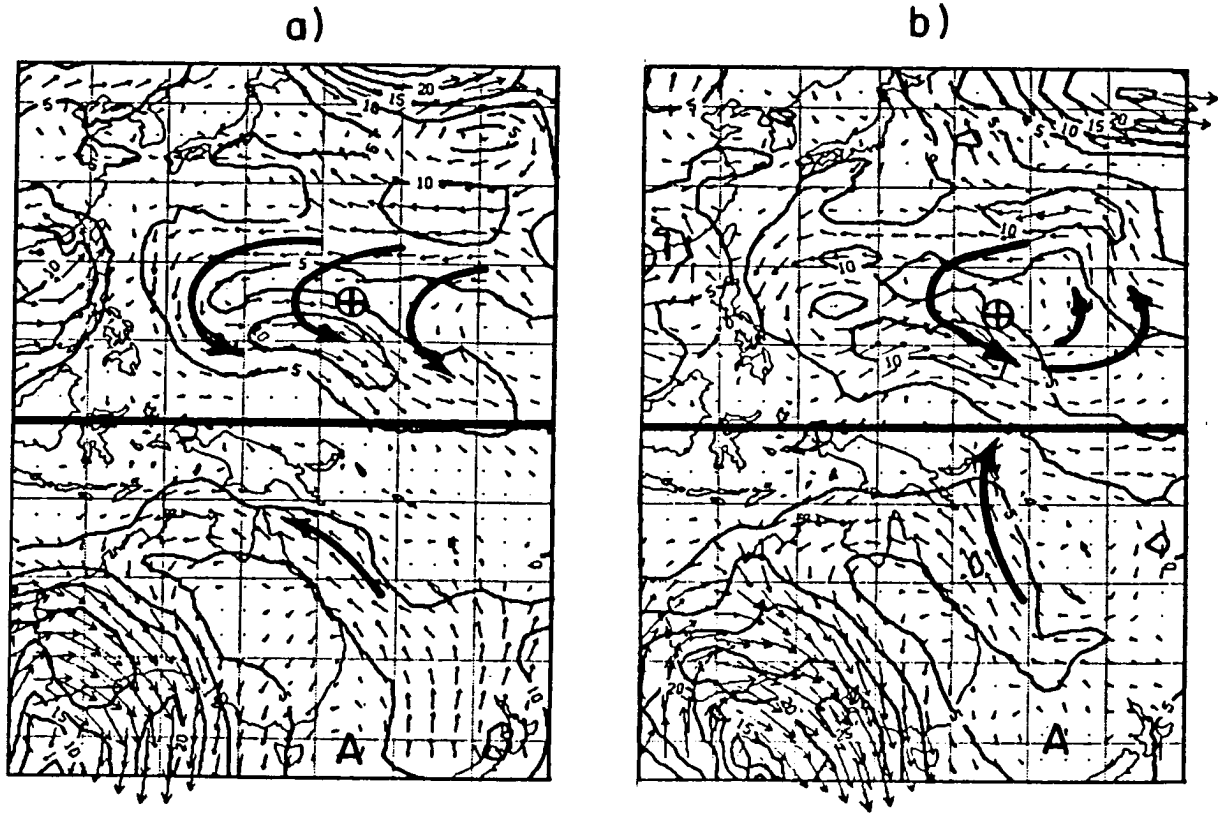

Figure 5.11:a-b. a) 850 mb analysis surrounding the first invest flight (14 September 1982) into a non-developing disturbance ($V_{max} \sim 10ms^{-1}$, MSLP $\sim$ 1006 mb), (ND7-82) displaying a high surge value at outer radii. Analysis shows derived center and broad-scale circulation evident in the synoptic field (ms^{-1}). b) The second invest flight of 15 September 1982 formed a closed-off a low-level center ($V_{max} \sim 10ms^{-1}$, MSLP $\sim$ 1002 mb), but aircraft data analysis indicated lack of inner- region surge due to weak radial inflow.

Chapter 6

COMBINING BLOWTHROUGH AND SURGE—PREDICTIVE POTENTIAL

The inhibiting effect of upper-tropospheric wind blowthrough across the incipient disturbance combined with the positive effects of low-level momentum surges are now investigated for high and low combinations of both influences.

6.1 Blowthrough Values For the Invest Flight Cases

The blowthrough statistics given earlier in this report, Table 3.3, were for all 250 mb Darwin wind cases (134-D1, 148-NON-DEV). The cases presented in Table 6.1 are only for those situations which most closely matched the invest flight times. Some interpolation of 0000 GMT and 1200 GMT blowthrough values was performed to get representative high/low values for particular missions. Blowthrough calculations were performed on maps at time periods that bracketed the aircraft flights. The ratio of the two classes indicates, on the average, high blowthrough only slightly favors non-development, low blowthrough slightly favors development. Both D1 and NON-DEV classes had approximately the same total number of high ($V_{BT} > 5\ ms^{-1}$) and low ($V_{BT} < 5\ ms^{-1}$) blowthrough cases. The comparison of combined D1/NON-DEV high blowthrough cases indicates that slightly less than half of these cases develop. For the combined low blowthrough cases, slightly more than half of these cases also develop. Thus, as previously stated, average blowthrough by itself did not offer any significant help in distinguishing the average developing cases from the average non-developing cases.

Table 6.1: Number of cases and percentage of total cases of high or low blowthrough for D1 and NON-DEV classes. The ratio of the two classes indicates high blowthrough only slightly favors non-development, low blowthrough slightly favors development.

	Blowthrough: Predictive Capability	
	High Blowthrough $V_{BT} > 5\ ms^{-1}$	Low Blowthrough $V_{BT} < 5\ ms^{-1}$
Early-developers (52)	23 (42%)	32 (58%)
Non-developers (49)	27 (51%)	26 (49%)
Ratio of: D1/NON-DEV	0.9/1	1.2/1
A few (three D1, four NON-DEV) cases were eliminated from the initial surge data set because data was insufficient to determine if a surge existed.		

6.2 Surge Values for the Invest Flight Cases

High surge statistics for both classes (D1 and NON-DEV) are portrayed in Table 6.2. D1 and NON-DEV cases are distinguished by their wind surge values, particularly the degree of surge which goes to the inner core. Thirty-five of fifty-four (or 65%) of those cases exhibiting high surge developed into tropical storms or typhoons. This is a ratio of nearly 2 to 1. When the surge was classified further as a "penetrative" surge, the percent of cases developing increased from 65% to 75%, as shown in Table 6.3. Of those cases lacking high surge (or exhibiting low surge), 30 of 47 (or 64%) of the cases did not develop. Note also that D1 cases have 3 times the number of penetrative surge cases as NON-DEV systems.

6.3 Different Combinations of High/Low Blowthrough (BT) and High/Low Surge

By classifying disturbances by High/Low Blowthrough and High/Low Surge, a greater statistical predictability of genesis is obtained. Tables 6.4 and 6.5 show the number of cases and percentages in this 4-class scheme for D1 and NON-DEV cases.

The first comparisons to make are the optimum ones in developing and non-developing situations. Low BT/High Surge (bottom/left-hand box in Tables 6.4 and 6.5) are optimum

Table 6.2: The number of surge cases and percentage of the total number of surge cases in each category of D1 and NON-DEV. The ratios indicate that high surge is most prevalent in developing D1 cases. Low surge is more prevalent in non-developing cases.

	High Surge	Low Surge
Early-developers (D1) (52)	35 (67%) of total D1 Cases	17 (33%)
Non-developers (NON-DEV) (49)	19 (39%) of total NON-DEV Cases	30 (61%)
Ratio of: D1/NON-DEV	1.8/1	0.6/1

Table 6.3: The number of high surge cases and percentage of the total number of surge cases in which radial penetration of the surge was detected inside 1.25° radius. High penetrative surge was most prevalent in D1 cases.

	High Penetrative Surge
Early-developers (D1) (52)	27 (52%)
Non-developers (NON-DEV) (49)	9 (18%)
Ratio of: D1/NON-DEV	3/1

conditions for development. When this set of circumstances occurs, the combined statistics for D1 and NON-DEV indicate that 22 of 31 (or 71%) of the cases develop.

The optimum non-development case is High BT/Low Surge (upper/right-hand box in Tables 6.4 and 6.5). The combined cases for D1 and NON-DEV with these conditions show 14 of 21 (or 67%) of the cases do not develop. Apparently restrictive upper flow cannot be compensated for due to a lack of low level surge in the NON-DEV cases.

Table 6.6 presents further evidence of the conditions most favorable for disturbance development. Many more cases of development occur when the high surge cases are further stratified by the degree of radial penetration of the surge. The bottom row of

Table 6.4: Number of cases and percentage of the total number of cases of the combinations of High/Low (Hi/Low) Surge and High/Low 250 mb wind blowthrough (Hi/Low BT).

Early-stage Developers (D1)—52 cases	
Hi BT/Hi Surge	Hi BT/Low Surge
13/52 (25%)	7/52 (14%)
Low BT/Hi Surge	Low BT/Low Surge
22/52 (42%)	10/52 (19%)

Table 6.5: Similar to Table 6.4, except for the NON-DEV class of disturbances.

Non-Developers (NON-DEV)—49 Cases	
Hi BT/Hi Surge	Hi BT/Low Surge
10/49 (20%)	14/49 (29%)
Low BT/Hi Surge	Low BT/Low Surge
9/49 (18%)	16/49 (33%)

data in Table 6.6 shows 18 of 20 cases (or 90%) that exhibit less restrictive low values of upper-tropospheric blowthrough and strong, inward radially penetrating momentum surge do in fact develop to become named storms. A much higher percentage of cases that eventually develop exhibit these characteristics.

Table 6.6: Number of Hi/Low BT and Hi penetrative surge cases and percentage of the total number of cases for each class of disturbance. The optimum conditions for development are most prevalent in the disturbances that become named storms.

Early-stage Developers (D1) (52 Cases)	Non-Developers (NON-DEV) (49 Cases)	Ratio D1/NON-DEV
Hi BT/Hi Penetrative Surge	Hi BT/Hi Penetrative Surge	
9/52 (17%)	7/49 (14%)	1.3/1
Low BT/Hi Penetrative Surge	Low BT/Hi Penetrative Surge	
18/52 (35%)	2/49 (4%)	9/1

The idea of compensation by the surge, where the surge acts to supply momentum until a less restrictive upper-troposphere pattern evolves was discussed by Lee (1986), who described the upper-level pattern as more of a hindering mechanism if strong mid-to upper-

level shearing is present. Lee also indicated that a weak upper-level anticyclonic circulation was favorable for formation and that even under unfavorable upper-level conditions, the low-level cyclonic circulation can still maintain itself if the low-level vorticity is large enough. Once the unfavorable condition disappears the convection can reorganize itself and the system can develop again.

Surge appears to be the key, or more dominant factor in these cases. Under conditions of High BT/High Surge (upper-left box in Tables 6.4 and 6.5), 57% of the cases develop despite the restrictive upper flow. In 16 of 26 (or 62%) of the cases with Low BT/Low Surge (bottom/right box in Tables 6.4 and 6.5), even though the restriction was not present in the upper troposphere, the systems failed to develop. The surge, or the momentum "trigger", was not present to stimulate development.

6.4 Differences in Low-level Equivalent Potential Temperature Between D1 and NON-DEV Cases

Some individuals may feel that a significant portion of the differences between developing and non-developing cases may be associated with higher values of low-level temperature and/or moisture values occurring in the formation cases. This analysis did not find any such temperature/moisture difference. An analysis of the equivalent potential temperature (θ_e) normalized to the 950 mb level (see Table 6.7) showed no appreciable differences. This is not surprising in that little daily and regional differences of sea surface temperature (SST) and boundary layer temperature and moisture occur in the low latitude summer and autumn environment of the northwest tropical Pacific where these flights were made. This well fits forecaster experience in this region.

Table 6.7: Aircraft measured mean radial values of equivalent potential temperature (θ_e) normalized to 950 mb for 52 early-developing (D1) and 49 non-developing (NON-DEV) cases.

	Radius (° Latitude)					
	0-.5	.5-1.0	1.0-1.5	1.5-2.0	2.0-2.5	2.5-3.0
D1 (52 Cases)	385.3	385.5	386.0	385.9	385.9	386.2
NON-DEV (49 Cases)	385.5	386.5	385.7	386.6	385.3	385.6
Difference (D1-NON-DEV)	-0.2	-1.0	0.3	-0.7	0.6	0.6

Chapter 7

SUMMARY AND DISCUSSION

It has been established that tropical cyclone formation requires the presence of certain climatological and synoptic factors, such as the proper formation region, the right season, high sea-surface temperature, small vertical wind shear, the high vorticity of a monsoon trough, etc. (Gray, 1979). However, such favorable climatology and synoptic-scale factors do not assure individual case formation. One also needs a meso-scale deep convective cloud cluster to organize the tropical disturbance throughout the troposphere. But even if a good cloud cluster exists in a favorable climatological and synoptic environment (McBride, 1981a, 1981b; McBride and Zehr, 1981) with low tropospheric blowthrough or ventilation, formation is still not certain. An additional missing ingredient may be, in many cases, an environmentally-induced lower-level wind surge.

This research has followed the work of Lee (1986, 1987), Lee and Gray (1985) and Love (1985a, 1985b) in which all found that environmentally induced wind surges can be a fundamental ingredient of the TC development process. This appears to be a result of the surge's ability to bring about low-level mass penetration into the tropical disturbance's inner-core region where a small scale circulation center is often present with its accompanying high relative vorticity. Strong inward radial penetration does not typically take place without such surge action. This is evident in many developing cases of this study. It appears that two wind surges are frequently associated with the formation process, one to establish a LLCC and a second surge occurring 1-3 days later which initiates the more rapid early intensification.

The surge process is hypothesized to facilitate the establishment of an enhanced inner-core region of deep convection. This inner-core deep convection exists for a sufficient time

($\sim$ 6-12 hours) so as to stimulate the establishment of a non-linear and unstable inner-core intensification cycle. Inner-core moist-instability processes (such as CISK) are then able to become activated to the extent that they can continue the inner-core intensification after the surge which initiated this unstable growth has dissipated. It appears that such low-level momentum surges can act as the necessary short-term trigger mechanism to force the establishment of the disturbance's inner-core unstable growth. Molinari and Skubis (1985) have documented a case of low-level wind surge initiation of tropical cyclone formation in the Atlantic.

It is crucial that the nature of the LLCC (1-2° diameter) formation be better understood. Such LLCC vortex formation may be the result of special surge action or the result of the intense deep convection associated with multiple cell deep convective elements, or a combination of such surge action into areas where deep convection is already underway.

Once established the LLCC vortex has relative vorticity 2-5 times that of the earth's vorticity. The radius of deformation is much reduced over that normally present in the large-scale disturbance circulation. New deep convection which is set off within this small LLCC vortex will be a much more efficient warming mechanism. This facilitates the establishment of the needed early-stage unstable growth process which would not be possible for deep convection occurring where the ratio of relative to earth vorticity is less than one.

It thus appears that the presence or lack of a mechanism to enhance deep convection within a disturbance's LLCC is a fundamental factor in specifying whether TC intensification will or will not occur. Our project's other research on TC formation supports this view. Lee (1986) states that the most significant result of his extensive observational analysis of northwest Pacific tropical cyclone genesis was the observation that there were often large-scale low-level momentum surges acting upon pre-cyclone cloud clusters right before they began to intensify into named storms. Such surge influences were generally not present in the systems which did not develop. Lee's analysis of all FGGE year cases of cyclone development in the northwest Pacific showed that there were at least three types of low-level surge action which could act upon the pre-cyclone disturbance: cross-equatorial

monsoon wind surges on the equatorial side of the disturbance, trade wind surges on its poleward side, and southwest monsoon surges which originated over the North Indian Ocean. Lee and Gray (1985) found similar large-scale surges during cyclogenesis in the North Indian Ocean. Love (1985a,b) has also shown that a cold outbreak in the opposite hemisphere can cause lower tropospheric cross-equatorial wind surges which appear to be associated with cyclogenesis in the western Pacific and in the Australian region.

The upper-tropospheric analysis method of wind blowthrough, by itself, had little predictive capability in that there was little blowthrough difference, in the average sense, between developing and non-developing disturbances. The analysis of the location of the LLCC as influenced by the mean upper-tropospheric flow exhibited good potential in specifying the position of the LLCC relative to the area of convection. This could be a helpful aid in diagnosing the region of the disturbance where surge activity and enhanced convection could have the maximum influence on the formation and development of the LLCC. The angle of the approaching surge flow may be an important factor in providing the proper forcing to the inner-core regions of the disturbance's unstable growth.

Further studies are needed to better understand the conditions associated with the small-scale 1-2° diameter LLCC vortex formation.

Chapter 8

DEVELOPMENT VS. NON-DEVELOPMENT FORECAST RULES

1. If invest reconnaissance missions of the satellite is able to detect a small Low-Level Circulation Center (LLCC), development there is a three times greater likelihood that a named tropical cyclone will develop than when a LLCC is not found.

2. Development is nearly assured if a LLCC is found together with both high penetrative wind surge values and low values of upper tropospheric wind blowthrough or ventilation.

3. There is a better than 50 percent chance of TC development without a LLCC if high wind surge and low values of upper tropospheric wind ventilation are present.

4. Non-development is virtually assured if a LLCC is not present and low values of wind surge and high ventilation are present.

ACKNOWLEDGEMENTS

Many thanks go to Professor William M. Gray for his suggestion of this research topic and his guidance and encouragement in the completion of this investigation. The painstaking work done by Captain Michael Middlebrooke made possible the use of the aircraft flight data. Others that provided invaluable support: Bill Thorson and Todd Massey for their programming assistance; Patti Nimmo, Jerry Brumit, and Lisa Paone for their help in assembling the extensive wind and satellite data sets; Judy Sorbie for her excellent drafting skills. Special thanks go to Barbara Brumit for her organization and extreme patience in the preparation of this manuscript.

The support and encouragement of the author's wife, Andrea, children, Elissa and Grant, and parents is greatly appreciated.

This paper has been financially supported by the National Science Foundation/National Oceanic and Atmospheric Administration ATM-8419116 and the AF Grant through DEO306 DOD-NAVY-ONR Grant No. N00014-87-K-0203 PO2. Finally, the sponsorship by the US Air Force of the author is gratefully acknowledged.

REFERENCES

Anthes, R. A., 1972: The development of asymmetries in a three- dimensional numerical model of the tropical cyclone. *Mon. Wea. Rev.*, 100, 461-476.

Anthes, R. A., 1982: Tropical cyclones, their evolution, structure and effects. *Meteor. Monographs*, Vol. *19*, AMS, 45 Beacon Street, Boston, MA, 02108, 208 pp.

Arnold, C. P., 1977: Tropical cyclone cloud and intensity relation- ships. Dept. of Atmos. Sci. Paper No. 277, Colo. State Univ. Fort Collins, CO, 154 pp.

Bauer, K. G., 1976: A comparison of cloud motion winds with coinciding radiosonde winds. *Mon. Wea. Rev.*, 104, 922-931.

Black, P. G. and R. A. Anthes, 1971: On the asymmetric structure of the tropical cyclone outflow layer. *J. Atmos. Sci.*, 28, 1348-1366.

Chen, L. and W. M. Gray, 1984: Global view of the upper level outflow patterns associated with tropical cyclone intensity changes during FGGE. Postprints, 15th Technical Conference on Hurricanes and Tropical Meteorology, AMS, January 9-13, Miami, FL, 224-231.

Chen, L. and W. M. Gray, 1985: Global view of the upper level outflow patterns associated with tropical cyclone intensity changes during FGGE. Dept. of Atmos. Sci. Paper No. 392, Colo. State Univ., Fort Collins, CO, 126 pp.

Dvorak, V. F., 1975: Tropical cyclone intensity analysis and forecasting from satellite imagery. *Mon. Wea. Rev.*, 103, 420-430.

Dvorak, V. F., 1984: Tropical cyclone intensity analysis using satellite data. NOAA Tech. Rept. NESO15 11, 47 pp.

Erickson, S. L., 1977: Comparison of developing vs. non-developing tropical disturbances. Dept. of Atmos. Sci. Paper No. 274, Colo. State Univ., Fort Collins, CO, 81 pp.

European Centre for Medium Range Weather Forecasts (ECMWF), 1981-1984: Daily Global Analyses, Reading, Berkshire RG29AX, England.

Fingerhut, W. A., 1978: A numerical model of a diurnally varying tropical cloud cluster disturbance. *Mon. Wea. Rev.*, 106, 255-264.

Frank, W. M., 1977a: The structure and energetics of the tropical cyclone, I: Storm structure. *Mon. Wea. Rev.*, *105*, 9, 1119-1135.

Frank, W. M., 1977b: The structure and energetics of the tropical cyclone, II: Dynamics and energetics. *Mon. Wea. Rev.*, *105*, 9, 1136-1150.

Frank, W. M., 1977c: Momentum and kinetic energy processes in the tropical cyclone. Volume of Conf. Papers, 11th Technical Conf. on Hurricanes and Tropical Meteorology, Dec. 13-16, Miami, FL, Published by the AMS, Boston, MA, 535-542.

Gentry, R. C., E. Rodgers, J. Steranka, and W. Shenk, 1980: Predicting tropical cyclone intensity using satellite measured equivalent blackbody temperature of cloud tops. *Mon. Wea. Rev.*, 108, 445-455.

Gray, W. M., 1968: Global view of the origin of tropical disturbances and storms. *Mon. Wea. Rev.*, 96, 669-700.

Gray, W. M., 1975: Tropical cyclone genesis. Dept. of Atmos. Sci. Paper No. 234, Colo. State Univ., Fort Collins, CO, 119 pp.

Gray, W. M. and R. Jacobson, Jr., 1977: Diurnal variation of deep cumulus convection. *Mon. Wea. Rev.*, 105, 1171-1188.

Gray, W. M., 1979: Hurricanes: their formation, structure, and likely role in the tropical cyclone. Meteorology over the Tropical Oceans. D. B. Shaw, Ed., *Roy. Meteor. Soc.*, 155-218.

Gray, W. M., 1981: Recent advances in tropical cyclone research from rawinsonde composite analysis. Paper prepared for the WMO Committee of Atmospheric Science, Geneve, Switzerland, 407 pp.

Hack, J. J., and W. H. Schubert, 1986: On the nonlinear response of atmospheric vortices to heating by organized cumulus convection. *J. Atmos. Sci.*, 43, 1559-1573.

Henderson, R. S., 1978: USAF aerial weather reconnaissance using the Lockheed WC-130 aircraft. *Bull. Amer. Meteor. Soc.*, 59, 1136-1143.

Holland, G. J., 1983: Angular momentum transports in tropical cyclones. *Quart. J. Roy. Meteor. Soc.*, 109, 187-209.

Holland, G. J. and R. T. Merrill, 1984: On the dynamics of tropical cyclone structural changes. *Quart. J. Roy. Meteor. Soc.*, 110, 723-745.

Holliday, C. R. and A. H. Thompson, 1979: Climatological characteristics of rapidly intensifying typhoons. *Mon. Wea. Rev.*, 107, 1022-1034.

Joint Typhoon Warning Center (JTWC), 1980: Annual tropical cyclone report. US Naval Oceanography Command Center, Joint Typhoon Warning Center, COMNAVMARIANAS Box 17, FPO San Francisco, 96630, NTIS AD A094668, 185 pp.

Joint Typhoon Warning Center (JTWC), 1981: Annual tropical cyclone report. US Naval Oceanography Command Center, Joint Typhoon Warning Center, COMNAVMARIANAS Box 17, FPO San Francisco, 96630, NTIS AD A112002, 194 pp.

Joint Typhoon Warning Center (JTWC), 1982: Annual tropical cyclone report. US Naval Oceanography Command Center, Joint Typhoon Warning Center, COMNAVMARIANAS Box 17, FPO San Francisco, 96630, NTIS AD A124860, 236 pp.

Joint Typhoon Warning Center (JTWC), 1983: Annual tropical cyclone report. US Naval Oceanography Command Center, Joint Typhoon Warning Center, COMNAVMARIANAS Box 17, FPO San Francisco, 96630, 195 pp.

Joint Typhoon Warning Center (JTWC), 1984: Annual tropical cyclone report. US Naval Oceanography Command Center, Joint Typhoon Warning Center, COMNAVMARIANAS Box 17, FPO San Francisco, 96630, 219 pp.

Lee, C.-S., 1986: An observational study of tropical cloud cluster evolution and cyclogenesis in the western North Pacific. Dept. of Atmos. Sci. Paper No. 403, Colo. State Univ., Fort Collins, CO, 250 pp.

Lee, C.-S., 1987: An observational study of tropical cyclone formation in the western North Pacific. Proceedings of 17th AMS Conference on Hurricanes and Tropical Meteorology, Miami, FL, April, 4 pp.

Lee, C.-S. and W. M. Gray, 1985: Characteristics of North Indian Ocean tropical cyclone activity. US Navy Environmental Prediction Research Facility Rept. No. CR 84-11, 108 pp. Available from the US Navy, Monterey, CA. (To appear in *Mon. Wea. Rev.*).

Lopez, R. E., 1968: Investigation of the importance of cumulus convection and ventilation in early tropical storm development. Dept. of Atmos. Sci. Paper No. 124, Colo. State Univ., Fort Collins, CO, 86 pp.

Lopez, R. E., 1973: Cumulus convection and larger-scale circulations, I: Broadscale and mesoscale considerations, II: Cumulus and mesoscale interactions. *Mon. Wea. Rev.*, 101, 839-870.

Love, G., 1982: The role of the general circulation in western Pacific tropical cyclone genesis. Dept. of Atmos. Sci. Paper No. 340, Colo. State Univ., Fort Collins, CO, 215 pp.

Love, G., 1985a: Cross-equatorial influence of winter hemisphere subtropical cold surges. *Mon. Wea. Rev.*, 113, 1487-1498.

Love, G., 1985b: Cross-equatorial interactions during tropical cyclone genesis. *Mon. Wea. Rev.*, 113, 1499-1509.

McBride, J. L., 1979: Observational analysis of tropical cyclone formation. Dept. of Atmos. Sci. Paper No. 308, Colo. State Univ., Fort Collins, CO, 230 pp.

McBride, J. L., 1981a: Observational analysis of tropical cyclone formation, Part I: Basic description of data sets. *J. Atmos. Sci.*, 1117-1131.

McBride, J. L., 1981b: Observational analysis of tropical cyclone formation, Part III: Budget analysis. *J. Atmos. Sci.*, 1152-1166.

McBride, J. L. and R. Zehr, 1981: Observational analysis of tropical cyclone formation. Part II: Comparison of non-developing versus developing systems. *J. Atmos. Sci.*, 38, 1132-1151.

Merrill, R. T., 1985: Environmental influences on hurricane intensification. Dept. of Atmos. Sci. Paper No. 394, Colo. State Univ., Fort Collins, CO, 156 pp.

Middlebrooke, M. G., 1988: Investigation of tropical cyclone genesis and development using low-level aircraft flight data. Dept. of Atmos. Sci. Paper No. 429, Colo. State Univ., Ft. Collins, CO, 94 pp.

Middlebrooke, M. and W. M. Gray, 1987: Comparison of low-level aircraft observations between early stage developing and non-developing tropical disturbances in the northwest Pacific. Proceedings of the 17th AMS Conference on Hurricanes and Tropical Meteorology, Miami, FL, April, 4 pp.

Molinari, J. and S. Skubis, 1985: Evolution of the surface wind field in an intensifying tropical cyclone. *J. Atmos. Sci.*, 42, 2856- 2864.

Nunez, E., 1981: Tropical cyclone structure and intensity change. Dept. of Atmos. Sci. Ph. D. Thesis, Colo. State Univ., Fort Collins, CO, 192 pp.

Rodgers, E. B. and R. C. Gentry, 1983: Monitoring tropical cyclone intensity using environmental wind fields derived from short-interval satellite images. *Mon. Wea. Rev.*, 111, 976-996.

Rodgers, E. B., R. C. Gentry, W. Shenk and V. Oliver, 1979: The benefits of using short-interval satellite images to derive winds for tropical cyclones. *Mon. Wea. Rev.*, 107, 575-584.

Ruprecht, E. and W. M. Gray, 1976: Analysis of satellite-observed tropical cloud clusters, I: Wind and dynamic fields. *Tellus*, 28, 391-413.

Sadler, J. C., 1976: A role of the tropical upper tropospheric trough in early season typhoon development. *Mon. Wea. Rev.*, 104, 1266- 1278.

Sadler, J. C., 1978: Mid-season typhoon development and intensity changes and the tropical upper tropospheric trough. *Mon. Wea. Rev.*, 106, 1137-1152.

Schubert, W. H. and J. J. Hack, 1982: Inertial stability and tropical cyclone development. *J. Atmos. Sci.*, 39, 1687-1697.

Tuleya, R. E., 1986: The simulation of the genesis of tropical storms using the FGGE III-b data set. Preprints, National Conference on Scientific Results of the First GARP Global Experiment, AMS, January 14-17, Miami, FL, 78-81.

Tuleya, R. E. and Y. Kurihara, 1981: A numerical study on the effects of environmental flow on tropical storm genesis. *Mon. Wea. Rev.*, 109, 2487-2506.

Vonder Haar, T. H. and D. W. Hillger, 1984: WMO Compendium of Lecture Notes on Meteorological Satellites, Education and Training Directorate World Meteorological Organization, Geneve, Switzerland, 500 pp.

Weatherford, C. L., 1985: Typhoon structural variability. Dept. of Atmos. Sci. Paper No. 391, Colo. State Univ., Fort Collins, CO, 75 pp.

Weatherford, C. L. and W. M. Gray, 1984: Relating typhoon intensity to outer 1-3° radius circulation as measured by reconnaissance aircraft. Postprints, 15th Technical Conference on Hurricanes and Tropical Meteorology, AMS, January 9-13, Miami, FL, 238-242.

Williams, K., 1970: Statistical analysis of trade wind cloud clusters in the western North Pacific. Dept. of Atmos. Sci. Paper No. 161, Colo. State Univ., Fort Collins, CO, 80 pp.

Williams, K. and W. M. Gray, 1973: A statistical analysis of satellite-observed trade wind cloud clusters in the western North Pacific. *Tellus*, 21, 313-336.

Zehr, R., 1976: Tropical disturbance intensification. Dept. of Atmos. Sci. Paper No. 259, Colo. State Univ., Fort Collins, CO, 91 pp.

Appendix A

W. M. GRAY'S FEDERALLY SUPPORTED RESEARCH PROJECT REPORTS SINCE 1967

CSU Dept. of Atmos. Sci. Report No.	Report Title, Author, Date, Agency Support
104	The Mutual Variation of Wind, Shear and Baroclinicity in the Cumulus Convective Atmosphere of the Hurricane (69 pp.). W. M. Gray. February 1967. NSF Support.
114	Global View of the Origin of Tropical Disturbances and Storms (105 pp.). W. M. Gray. October 1967. NSF Support.
116	A Statistical Study of the Frictional Wind Veering in the Planetary Boundary Layer (57 pp.). B. Mendenhall. December 1967. NSF and ESSA Support.
124	Investigation of the Importance of Cumulus Convection and ventilation in Early Tropical Storm Development (88 pp.). R. Lopez. June 1968. ESSA Satellite Lab. Support.
Unnumbered	Role of Angular Momentum Transports in Tropical Storm Dissipation over Tropical Oceans (46 pp.). R. F. Wachtmann. December 1968. NSF and ESSA Support.
Unnumbered	Monthly Climatological Wind Fields Associated with Tropical Storm Genesis in the West Indies (34 pp.). J. W. Sartor. December 1968. NSF Support.
140	Characteristics of the Tornado Environment as Deduced from Proximity Soundings (55 pp.). T. G. Wills. June 1969. NOAA and NSF Support.
161	Statistical Analysis of Trade Wind Cloud Clusters in the Western North Pacific (80 pp.). K. Williams. June 1970. ESSA Satellite Lab. Support.
—	A Climatology of Tropical Cyclones and Disturbances of the Western Pacific with a Suggested Theory for Their Genesis/Maintenance (225 pp.). W. M. Gray. NAVWEARSCHFAC Tech. Paper No. 19-70. November 1970. (Available from US Navy, Monterey, CA). US Navy Support.

CSU Dept. of Atmos. Sci. Report No.	Report Title, Author, Date, Agency Support
179	A diagnostic Study of the Planetary Boundary Layer over the Oceans (95 pp.). W. M. Gray. February 1972. Navy and NSF Support.
182	The Structure and Dynamics of the Hurricane's Inner Core Area (105 pp.). D. J. Shea. April 1972. NOAA and NSF Support.
188	Cumulus Convection and Larger-scale Circulations, Part I: A Parametric Model of Cumulus Convection (100 pp.). R. E. Lopez. June 1972. NSF Support.
189	Cumulus Convection and Larger-scale Circulations, Part II: Cumulus and Meso-scale Interactions (63 pp.). R. E. Lopez. June 1972. NSF Support.
190	Cumulus Convection and Larger-scale Circulations, Part III: Broadscale and Meso-scale Considerations (80 pp.). W. M. Gray. July 1972. NOAA-NESS Support.
195	Characteristics of Carbon Black Dust as a Tropospheric Heat Source for Weather Modification (55 pp.). W. M. Frank. January 1973. NSF Support.
196	Feasibility of Beneficial Hurricane Modification by Carbon Black Seeding (130 pp.). W. M. Gray. April 1973. NOAA Support.
199	Variability of Planetary Boundary Layer Winds (157 pp.). L. R. Hoxit. May 1973. NSF Support.
200	Hurricane Spawned Tornadoes (57 pp.). D. J. Novlan. May 1973. NOAA and NSF Support.
212	A Study of Tornado Proximity Data and an Observationally Derived Model of Tornado Genesis (101 pp.). R. Maddox. November 1973. NOAA Support.
219	Analysis of Satellite Observed Tropical Cloud Clusters (91 pp.). E. Ruprecht and W. M. Gray. May 1974. NOAA/NESS Support.
224	Precipitation Characteristics in the Northeast Brazil Dry Region (56 pp.). R. P. L. Ramos. May 1974. NSF Support.
225	Weather Modification through Carbon Dust Absorption of Solar Energy (190 pp.). W. M. Gray, W. M. Frank, M. L. Corrin, and C. A. Stokes. July 1974.
234	Tropical Cyclone Genesis (121 pp.). W. M. Gray. March 1975. NSF Support.

CSU Dept. of Atmos. Sci. Report No.	Report Title, Author, Date, Agency Support
—	Tropical Cyclone Genesis in the Western North Pacific (66 pp.). W. M. Gray. March 1975. US Navy Environmental Prediction Research Facility Report. Tech. Paper No. 16-75. (Available from the US Navy, Monterey, CA). Navy Support.
241	Tropical Cyclone Motion and Surrounding Parameter Relationships (105 pp.). J. E. George. December 1975. NOAA Support.
243	Diurnal Variation of Oceanic Deep Cumulus Convection. Paper I: Observational Evidence, Paper II: Physical Hypothesis (106 pp.). R. W. Jacobson, Jr. and W. M. Gray. February 1976. NOAA-NESS Support.
257	Data Summary of NOAA's Hurricanes Inner-Core Radial Leg Flight Penetrations 1957-1967, and 1969 (245 pp.). W. M. Gray and D. J. Shea. October 1976. NSF and NOAA Support.
258	The Structure and Energetics of the Tropical Cyclone (180 pp.). W. M. Frank. October 1976. NOAA-NHEML, NOAA-NESS and NSF Support.
259	Typhoon Genesis and Pre-typhoon Cloud Clusters (79 pp.). R. M. Zehr. November 1976. NSF Support.
Unnumbered	Severe Thunderstorm Wind Gusts (81 pp.). G. W. Walters. December 1976. NSF Support.
262	Diurnal Variation of the Tropospheric Energy Budget (141 pp.). G. S. Foltz. November 1976. NSF Support.
274	Comparison of Developing and Non-developing Tropical Disturbances (81 pp.). S. L. Erickson. July 1977. US Army Support.
—	Tropical Cyclone Research by Data Compositing (79 pp.). W. M. Gray and W. M. Frank. July 1977. US Navy Environmental Prediction Research Facility Report. Tech. Paper No. 77-01. (Available from the US Navy, Monterey, CA). Navy Support.
277	Tropical Cyclone Cloud and Intensity Relationships (154 pp.). C. P. Arnold. November 1977. US Army and NHEML Support.
297	Diagnostic Analyses of the GATE A/B-scale Area at Individual Time Periods (102 pp.). W. M. Frank. November 1978. NSF Support.
298	Diurnal Variability in the GATE Region (80 pp.). J. M. Dewart. November 1978. NSF Support.
299	Mass Divergence in Tropical Weather Systems, Paper I: Diurnal Variation; Paper II: Large-scale Controls on Convection (109 pp.). J. L. McBride and W. M. Gray. November 1978. NOAA-NHEML Support.

CSU Dept. of Atmos. Sci. Report No.	Report Title, Author, Date, Agency Support
—	New Results of Tropical Cyclone Research from Observational Analysis (108 pp.). W. M. Gray and W. M. Frank. June 1978. US Navy Environmental Prediction Research Facility Report. Tech. Paper No. 78-01. (Available from the US Navy, Monterey, CA). Navy Support.
305	Convection Induced Temperature Change in GATE (128 pp.). P. G. Grube. February 1979. NSF Support.
308	Observational Analysis of Tropical Cyclone Formation (230 pp.). J. L. McBride. April 1979. NOAA-NHEML, NSF and NEPRF Support.
—	Tropical Cyclone Origin, Movement and Intensity characteristics Based on Data Compositing Techniques (124 pp.). W. M. Gray. August 1979. US Navy Environmental Prediction Research Facility Report. Tech. Paper No. CR-79-06. (Available from the US Navy, Monterey, CA). Navy Support.
—	Further Analysis of Tropical Cyclone Characteristics from Rawinsonde Compositing Techniques (129 pp.). W. M. Gray. March 1981. US Navy Environmental Prediction Research Facility Report. Tech. Paper No. CR-81-02. (Available from the US Navy, Monterey, CA). Navy Support.
333	Tropical Cyclone Intensity Change—A Quantitative Forecasting Scheme. K. M. Dropco. May 1981. NOAA Support.
—	Recent Advances in Tropical Cyclone Research from Rawinsonde Composite Analysis (407 pp.). WMO Publication. W. M. Gray. 1981.
340	The Role of the General Circulation in Tropical Cyclone Genesis (230 pp.). G. Love. April 1982. NSF Support.
341	Cumulus Momentum Transports in Tropical Cyclones (78 pp.). C. S. Lee. May 1982. ONR Support.
343	Tropical Cyclone Movement and Surrounding Flow Relationships (68 pp.). J. C. L. Chan and W. M. Gray. May 1982. ONR Support.
346	Environmental Circulations Associated with Tropical Cyclones Experiencing Fast, Slow and Looping Motions (273 pp.). J. Xu and W. M. Gray. May 1982. NOAA and NSF Support.
348	Tropical Cyclone Motion: Environmental Interaction Plus a Beta Effect (47 pp.). G. J. Holland. May 1982. ONR Support.
—	Tropical Cyclone and Related Meteorological Data Sets Available at CSU and Their Utilization (186 pp.). W. M. Gray, E. Buzzell, G. Burton and Other Project Personnel. February 1982. NSF, ONR, NOAA, and NEPRF Support.

CSU Dept. of Atmos. Sci. Report No.	Report Title, Author, Date, Agency Support
352	A Comparison of Large and Small Tropical Cyclones (75 pp.). R. T. Merrill. July 1982. NOAA and NSF Support.
358	On the Physical Processes Responsible for Tropical Cyclone Motion (200 pp.). Johnny C. L. Chan. November 1982. NSF, NOAA/NHRL and NEPRF Support.
363	Tropical Cyclones in the Australian/Southwest Pacific Region (264 pp.). Greg J. Holland. March 1983. NSF, NOAA/NHRL and Australian Government Support.
370	Atlantic Seasonal Hurricane Frequency, Part I: El Nino and 30 mb QBO Influences; Part II: Forecasting Its Variability (105 pp.). W. M. Gray. July 1983. NSF Support.
379	A Statistical Method for One- to Three-Day Tropical Cyclone Track Prediction (201 pp). Clifford R. Matsumoto. December, 1984. NSF/NOAA and NEPRF support.
—	Varying Structure and Intensity Change Characteristics of Four Western North Pacific Tropical Cyclones. (100 pp.). Cecilia A. Askue and W. M. Gray. October 1984. US Navy Environmental Prediction Research Facility Report No. CR 84-08. (Available from the US Navy, Monterey, CA). Navy Support.
—	Characteristics of North Indian Ocean Tropical Cyclone Activity. (108 pp.). Cheng-Shang Lee and W. M. Gray. December 1984. US Navy Environmental Prediction Research Facility Report No. CR 84-11. (Available from the US Navy, Monterey, CA). Navy Support.
391	Typhoon Structural Variability. (77 pp.). Candis L. Weatherford. October, 1985. NSF/NOAA Support.
392	Global View of the Upper Level Outflow Patterns Associated with Tropical Cyclone Intensity Change During FGGE. (126 pp.). L. Chen and W. Gray. October, 1985. NASA support.
394	Environmental Influences on Hurricane Intensification. (156 pp.). Robert T. Merrill. December, 1985. NSF/NOAA Support.
403	An Observational Study of Tropical Cloud Cluster Evolution and Cyclogenesis in the Western North Pacific. (250 pp.). Cheng-Shang Lee. September, 1986. NSF/NOAA support.
—	Factors Influencing Tropical Cyclone Genesis as Determined from Aircraft Investigative Flights into Developing and Non-Developing Tropical Disturbances in the Western North Pacific. Michael Middlebrooke. October, 1986 (70 pp.). NSF/NOAA support.

CSU Dept. of Atmos. Sci. Report No.	Report Title, Author, Date, Agency Support
—	Recent Colorado State University Tropical Cyclone Research of Interest to Forecasters. (115 pp.). William M. Gray. June, 1987. US Navy Environmental Prediction Research Facility Contractor Report CR 87-10. Available from US Navy, Monterey, CA. Navy support.
428	Tropical Cyclone Observation and Forecasting With and With and Without Aircraft Reconnaissance. (105 pp.) Joel D. Martin. May, 1988. USAF, NWS, ONR support.
429	Investigation of Tropical Cyclone Genesis and Development Using Low-level Aircraft Flight Data. (94 pp.) Michael G. Middlebrooke. May, 1988. USAF, NSF support.
—	Typhoon structural evolution. Candis Weatherford. December, 1988.